
**ONONDAGA LAKE CAPPING, DREDGING,
HABITAT AND PROFUNDAL ZONE (SMU 8)
FINAL DESIGN**

APPENDIX B – CAP MODELING

Prepared for:

Honeywell

301 Plainfield Road, Suite 330
Syracuse, NY 13212

Prepared by:

PARSONS

301 Plainfield Road, Suite 350
Syracuse, NY 13212



290 Elwood Davis Road, Suite 318
Liverpool, NY 13088
Phone: (315) 451-1905

MARCH 2012

PARSONS

TABLE OF CONTENTS

	<u>PAGE</u>
1.0 EXECUTIVE SUMMARY	1
2.0 MODELING OBJECTIVES	3
3.0 DESIGN MODELS	3
3.1 Analytical Steady State Model	3
3.2 Numerical Model	4
3.3 Model Conservatism.....	5
4.0 MODELING AREAS	7
5.0 MODEL INPUTS	9
6.0 DESIGN OPTIMIZATION CONSIDERING VARIABILITY IN SITE CONDITIONS	9
6.1 Extensive Data Collection and Bench Testing	10
6.2 Small Model Areas to Minimize Spatial Variability	10
6.3 Initial Conservative Modeling Used Maximum Porewater Concentrations	10
6.4 Model Conservatism Offset Potential Impacts of Variability.....	10
6.5 Mean Values Used as Best Estimate	11
6.6 Conservative Probabilistic Modeling Used to Evaluate Robustness of Design	11
7.0 MODELING APPROACH AND RESULTS.....	11
7.1 Mercury	14
7.2 VOCs and Phenol	15
7.3 PAHs/PCBs	16
7.4 Cap in 6-9 Meter Zone of Remediation Areas A and E	18
7.5 Sub-area Modeling	19
7.6 Sources of Uncertainty in Model Results	21
8.0 CONCLUSIONS	22
9.0 REFERENCES	23

TABLE OF CONTENTS (CONTINUED)**LIST OF TABLES**

- Table 1 Summary of Compounds Meeting Performance Criteria Assuming Initial Conservative Analytical Steady State and Transient Model Evaluations
- Table 2 Carbon Application Rate Evaluation
- Table 3 Monte Carlo Modeling Results at Final GAC Application Rates
- Table 4 Summary of Compounds Meeting Performance Criteria using Initial Conservative Analytical Steady State and Transient Model Evaluations of 6-9 M Zones and Sub-areas Modeling
- Table 5 Carbon Application Rate for 6-9 M Zones and Sub-areas Modeling

LIST OF FIGURES

- Figure B-1 Remediation and Model Areas Location Map
- Figure B-2 Remediation Area A Porewater Sample Locations
- Figure B-3 Remediation Area B Porewater Sample Locations
- Figure B-4 Remediation Area C Porewater Sample Locations
- Figure B-5 Remediation Area D Porewater Sample Locations
- Figure B-6 Remediation Area E Porewater Sample Locations
- Figure B-7 Remediation Area A Sediment Sample Locations
- Figure B-8 Remediation Area B & Wastebeds 1-8 Connected Wetlands Sediment Sample Locations
- Figure B-9 Remediation Area C Sediment Sample Locations
- Figure B-10 Remediation Area D & Wastebed B/Outboard Area Sediment Sample Locations
- Figure B-11 Remediation Area E Sediment Sample Locations
- Figure B-12 Remediation Area A Mercury Concentration
- Figure B-13 Remediation Area A Benzene Concentration
- Figure B-14 Remediation Area A Toluene Concentration
- Figure B-15 Remediation Area A Ethylbenzene Concentration
- Figure B-16 Remediation Area A Total Xylene Concentration
- Figure B-17 Remediation Area A Chlorobenzene Concentration
- Figure B-18 Remediation Area A Total DCB Concentration
- Figure B-19 Remediation Area A Total TCB Concentration

TABLE OF CONTENTS (CONTINUED)**LIST OF FIGURES**

- Figure B-20 Remediation Area A Naphthalene Concentration
- Figure B-21 Remediation Area A Calculated Phenol Concentration
- Figure B-22 Remediation Area A Sediment pH
- Figure B-23 Remediation Area B & Wastebeds 1-8 Connected Wetland Mercury Concentration
- Figure B-24 Remediation Area B & Wastebeds 1-8 Connected Wetland Benzene Concentration
- Figure B-25 Remediation Area B & Wastebeds 1-8 Connected Wetland Toluene Concentration
- Figure B-26 Remediation Area B & Wastebeds 1-8 Connected Wetland Ethylbenzene Concentration
- Figure B-27 Remediation Area B & Wastebeds 1-8 Connected Wetland Total Xylenes Concentration
- Figure B-28 Remediation Area B & Wastebeds 1-8 Connected Wetland Chlorobenzene Concentration
- Figure B-29 Remediation Area B & Wastebeds 1-8 Connected Wetland Total DCB Concentration
- Figure B-30 Remediation Area B & Wastebeds 1-8 Connected Wetland Total TCB Concentration
- Figure B-31 Remediation Area B & Wastebeds 1-8 Connected Wetland Naphthalene Concentration
- Figure B-32 Remediation Area B & Wastebeds 1-8 Connected Wetland Calculated Phenol Concentration
- Figure B-33 Remediation Area B & Wastebeds 1-8 Connected Wetland Sediment pH
- Figure B-34 Remediation Area C Mercury Concentration
- Figure B-35 Remediation Area C Benzene Concentration
- Figure B-36 Remediation Area C Toluene Concentration
- Figure B-37 Remediation Area C Ethylbenzene Concentration
- Figure B-38 Remediation Area C Total Xylene Concentration
- Figure B-39 Remediation Area C Chlorobenzene Concentration
- Figure B-40 Remediation Area C Total DCB Concentration
- Figure B-41 Remediation Area C Total TCB Concentrations
- Figure B-42 Remediation Area C Naphthalene Concentration
- Figure B-43 Remediation Area C Calculated Phenol Concentration

TABLE OF CONTENTS (CONTINUED)**LIST OF FIGURES**

- Figure B-44 Remediation Area C Sediment pH
- Figure B-45 RA-D & WBB/HB Outboard Area Mercury Concentration
- Figure B-46 RA-D & WBB/HB Outboard Area Benzene Concentration
- Figure B-47 RA-D & WBB/HB Outboard Area Toluene Concentration
- Figure B-48 RA-D & WBB/HB Outboard Area Ethylbenzene Concentration
- Figure B-49 RA-D & WBB/HB Outboard Area Total Xylenes Concentration
- Figure B-50 RA-D & WBB/HB Outboard Area Chlorobenzene Concentration
- Figure B-51 RA-D & WBB/HB Outboard Area Total DCB Concentration
- Figure B-52 RA-D & WBB/HB Outboard Area Total TCB Concentration
- Figure B-53 RA-D & WBB/HB Outboard Area Naphthalene Concentration
- Figure B-54 RA-D & WBB/HB Outboard Area Calculated Phenol Concentration
- Figure B-55 RA-D & WBB/HB Outboard Area Sediment pH
- Figure B-56 Remediation Area E Mercury Concentration
- Figure B-57 Remediation Area E Benzene Concentration
- Figure B-58 Remediation Area E Toluene Concentration
- Figure B-59 Remediation Area E Ethylbenzene Concentration
- Figure B-60 Remediation Area E Total Xylenes Concentration
- Figure B-61 Remediation Area E Chlorobenzene Concentration
- Figure B-62 Remediation Area E Total DCB Concentration
- Figure B-63 Remediation Area E Total TCB Concentration
- Figure B-64 Remediation Area E Naphthalene Concentration
- Figure B-65 Remediation Area E Calculated Phenol Concentration
- Figure B-66 Remediation Area E Sediment pH

TABLE OF CONTENTS (CONTINUED)**LIST OF ATTACHMENTS**

ATTACHMENT 1	MODEL INPUT
ATTACHMENT 2	PARTITIONING COEFFICIENTS AND SEDIMENT TO POREWATER CALCULATIONS
ATTACHMENT 3	MODEL VALIDATION
ATTACHMENT 4	MODEL FILES
ATTACHMENT 5	NINEMILE CREEK SPITS EVALUATION
ATTACHMENT 6	ADDITIONAL SENSITIVITY EVALUATIONS

1.0 EXECUTIVE SUMMARY

The Onondaga Lake cap will meet performance criteria established to be protective of human health and the environment for 1,000 years or longer. Design of the chemical isolation layer for the Onondaga Lake sediment cap was accomplished through a rigorous modeling effort. This appendix and its attachments summarize the objectives, application, inputs, results and recommendations from this modeling effort.

The models and modeling framework referenced in this appendix were developed by experts and have been published in peer-reviewed journals and publications such as the *Journal of Soil and Sediment Contamination* (Lampert and Reible, 2009) and “Guidance for In Situ Subaqueous Capping of Contaminated Sediments” (Palermo et al., 1998).

Design of the chemical isolation layer of the cap, which covers more than 450 acres over five remediation areas of the lake and three adjacent areas, was accomplished through an extensive series of model simulations. Two models were used for these evaluations: an analytical steady state model and a time-variable numerical model. Both deterministic and probabilistic model evaluations were used in developing the chemical isolation layer design, to ensure that the cap provides long-term protection of human health and the environment. The modeling approach described in this appendix was used to develop the chemical isolation layer design in each of the model areas by simulating the fate and transport within the cap of each of the 26 contaminants for which cap performance criteria have been established.

The chemical isolation layer will consist primarily of sand. Based on treatability testing, amendments will be incorporated into the chemical isolation layer in certain areas to ensure long-term effectiveness of the cap. These amendments will consist of siderite (a naturally occurring mineral) to neutralize elevated pH and maintain conditions conducive to long-term biological decay of key contaminants within the cap, and granular activated carbon (GAC) to improve sorption of contaminants within the cap and provide an added level of protectiveness. Amendments to the cap will be included in Remediation Areas B, C, D, the Wastebed B/Harbor Brook (WBB/HB) Outboard Area and the Wastebeds 1-8 connected wetlands, and in portions of Remediation Areas A (including the Ninemile Creek spits) and E. Modeling was conducted for both GAC-amended and non-amended caps.

An initial evaluation of the chemical isolation layer was completed based on the maximum concentrations for contaminant porewater measured (or estimated based on sediment concentrations and partitioning theory for those contaminants for which porewater data was not available) within each respective modeling area and best estimates (mean values) for all other model input parameters (model input parameters are described in Attachment 1 to this Appendix). Mercury, polychlorinated biphenyls (PCBs) and most polycyclic aromatic hydrocarbons (PAHs) are predicted to be below cap performance criteria everywhere for over 1,000 years based on the conservative initial model evaluations that were completed. Many VOCs are also predicted to be below their criteria for over 1,000 years in several of the model areas based on these conservative simulations. This initial evaluation was based on analytical steady state and transient numerical modeling of a 1-ft. thick chemical isolation layer.

Based on the results from the initial conservative modeling, an evaluation of GAC amendment performance and more rigorous modeling were required for select VOCs and PAHs in several model areas. The recommended design application rate of GAC to isolate these VOCs and PAHs in each model area was determined using a numerical model that simulated the effects of GAC, based on conservative upper bound (defined as 95th percentile) porewater concentrations and best estimates (mean values) for other model input parameters over a long-term (1,000 year) evaluation period.

As a final evaluation of the robustness of the cap design, probabilistic model simulations were completed to assess GAC performance over the full range of potential input parameter values and conditions specific to each model area. The probabilistic evaluation was performed over a long-term (1,000 years) evaluation period and incorporated the worst-case values for model input parameters as they pertain to predictions of cap performance. GAC application rates from these evaluations based on the 90th percentile of the model outputs were developed. In cases where these GAC application rates exceeded those determined from the prior model runs, the GAC application rate was increased accordingly, providing even greater assurance that the cap would provide complete chemical isolation throughout the 1,000-year model evaluation period and beyond.

This modeling approach is very conservative and as a result, underestimates the long-term effectiveness of the cap. There are natural processes and several engineering/constructability considerations that will significantly enhance the long-term performance of the cap, but are difficult to precisely quantify; however, once the cap is constructed in the field, they will contribute to enhanced performance and protectiveness. Specific natural processes and engineering/constructability considerations that were not incorporated into the model, but will result in an even higher level of long-term chemical isolation and protection of human health and the environment than predicted by the model include:

- Additional cap thickness beyond the design-specified minimum will be placed during construction to ensure that the minimum thickness is achieved everywhere. This material over-placement will result in increased contaminant sorption, biological decay, and amendment application, and will lower concentrations throughout the cap and extend its long-term performance. The amount of over-placement and resulting chemical isolation conservatism will vary over the area of the cap.
- Additional GAC beyond the design-specified minimum will be incorporated into the chemical isolation layer to account for potential unequal mixing of the GAC with the sand. A capping field demonstration was completed in late 2011 using full-scale capping equipment. The capping field demonstration confirmed that the hydraulic placement equipment proposed for the Onondaga Lake cap can consistently place GAC mixed throughout a sand layer at the specific water depths required for the Onondaga Lake project. The capping field demonstration provided information relative to determining the amount of extra GAC addition required. The final amount of additional GAC required will be determined during the capping start-up period, as detailed in the Construction Quality Assurance Plan (CQAP).

- Rapid aerobic biodegradation will occur within the upper portion of the cap's habitat layer. This will result in lower contaminant concentrations at the surface of the cap, where essentially all benthic activity occurs.
- Additional material will be placed to account for mixing of the bottom of the cap with the underlying sediment.

A complete list of model conservatisms is presented in Section 3.3.

2.0 MODELING OBJECTIVES

Contaminant transport modeling was conducted to design a chemical isolation layer for the cap that will meet the ROD requirements and ensure long-term effectiveness. Specifically, the chemical isolation layer performance criterion is to meet the individual probable effects concentrations (PECs) for the 23 contaminants that were linked to toxicity on a lake-wide basis and the New York State Department of Environmental Conservation (NYSDEC) sediment screening criteria (SSC) for benzene, toluene, and phenol¹ throughout the habitat layer.

As stated in the ROD, the compliance point for the cap is the bottom of the habitat restoration layer. To ensure protectiveness, the isolation layer has been designed to prevent concentrations of contaminants from exceeding their performance criteria (PEC or SSC) throughout the habitat restoration layer.

3.0 DESIGN MODELS

Design evaluations were conducted using two models: an analytical steady state model and a more complex numerical model, which allows for time-varying evaluations and simulation of GAC performance. Both models are described below. The method for applying these two models is provided in Section 7.

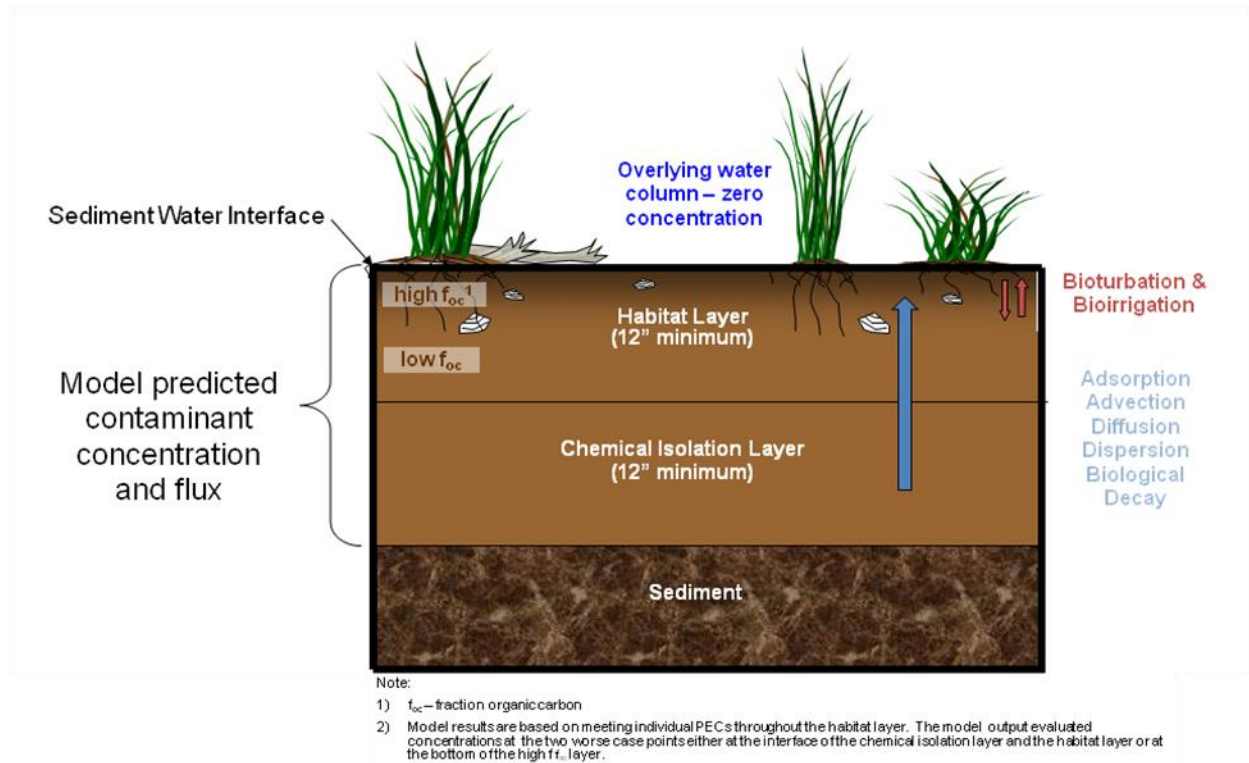
3.1 Analytical Steady State Model

The analytical steady state model was developed to simulate cap performance and develop an appropriate chemical isolation layer design for containment of contaminated sediments. Simulated transport processes within the typically homogeneous chemical isolation layer include porewater advection, diffusion and dispersion, reaction (where appropriate), and equilibrium partitioning between the dissolved and sorbed phases of the contaminant. Within the overlying habitat layer, the analytical steady state model includes these same processes, as well as sediment mixing and porewater pumping via bioturbation within the upper zone of that layer. The analytical steady state model thus allows the complexities of the biologically-active layer to be considered while maintaining an analytical form for convenient and rapid evaluation. The analytical steady state model evaluates a single material matrix in the chemical isolation layer and is not capable of modeling non-linear sorption processes, which is necessary for evaluating GAC adsorption. The schematic below indicates the general structure and processes included in the analytical steady state cap model.

¹ Benzene, toluene and phenol are not associated with lake-wide toxicity. Model results for benzene, toluene and phenol are compared to NYSDEC acute criteria. Comparison to acute criteria is consistent with comparison to PEC values which are based on acute toxicity.

FILE

**ILLUSTRATION OF CAP PROCESSES MODELED AND
STRUCTURE OF ANALYTICAL STEADY STATE MODEL**



The analytical steady state model was developed by experts in the field of contaminant transport modeling, and has been published in the peer-reviewed Journal of Soil and Sediment Contamination (Lampert and Reible, 2009). Validation of the analytical steady state model code was completed in accordance with Parsons standard procedures for software verification and validation. Model results for various test cases were also compared with calculations from well-documented 1-D solute transport equations by an independent reviewer; the model gave similar results using the same parameters and boundary conditions. A complete model validation report is included in Attachment 3.

3.2 Numerical Model

The general structure and processes included in the Onondaga Lake numerical cap model are consistent with those of the analytical steady state model. In addition, the numerical model simulates diffusional gradients in the underlying sediment, non-linear sorption within the isolation layer, porewater advection due to settlement-induced consolidation of the underlying sediment, and time-varying biodegradation rates through use of a lag period. The numerical solution scheme of this model also allows for time-variable simulations of the aforementioned processes. The USEPA guidance document entitled “Guidance for In Situ Subaqueous Capping

of Contaminated Sediments: Appendix B: Model for Chemical Containment by a Cap” describes the general modeling processes and basis for the numerical model (Palermo et al., 1998). The model code is the result of an extensive development process (fourth generation model) within the research group at the University of Texas (Go, J. et al, 2009 and Lampert and Reible, 2009). The University of Texas has developed and implemented the code within the MATLAB platform.

Both the analytical steady state and numerical modeling described herein assume an infinite source of contaminants is present in the underlying sediments. Upwelling velocities in the cap areas are relatively low, so transport from the underlying sediments upwards into the cap will be dominated by diffusion. This causes a concentration gradient to develop at the sediment/cap interface, which results in a decrease in chemical concentration in the sediments just below the sediment/cap interface over time. This, in turn, affects the overall rate of upward transport. In order to represent this process, the sediment underlying the cap is explicitly included as a layer in the numerical model. The sediment layer is modeled as 250 cm thick, with an infinite source boundary condition at the bottom of that layer. Model sensitivity analyses evaluating how alternate values for the thickness affect the cap design are documented in Attachment 6. The processes modeled in the underlying sediment layer include advective and diffusive transport and partitioning. Biological decay or other source depletion processes in the underlying sediment are conservatively not included in this modeling evaluation. This explicit representation of the underlying sediment is not included in the analytical steady state model, which is an additional conservatism of that model.

Validation of the numerical model was completed in accordance with Parsons standard procedures for software validation and verification. An independent validation of this model was performed by S.S. Papadopoulos and Associates. Multiple test scenarios were simulated with the numerical model and compared to results from MT3D (Zheng and Wang, 1998), a widely used groundwater transport model that has been extensively verified, as well as an analytical solution to the governing equation of the model (Neville, 2005). Additional validation was provided by Parsons and Anchor QEA, who found that the results of long-term simulations of the numerical model were consistent with the results of the analytical steady state model and with other solutions to the governing one dimensional contaminant transport equation. A complete model validation report is included in Attachment 3. Several updates were made to the model code to enhance its functionality during the course of the cap design; these updates are also documented in Attachment 3.

3.3 Model Conservatism

To ensure that the cap design is conservative and will provide long-term chemical isolation, the modeling used to develop the design of the chemical isolation layer does not incorporate numerous natural processes and engineering/constructability considerations that will significantly contribute to the long-term performance of the cap. Specific concepts and processes that were not incorporated into the model but will result in an even higher level of long-term chemical isolation than predicted by the model are listed below.

- Additional cap thickness beyond the design-specified minimum will be placed during construction to ensure that the minimum thickness is achieved everywhere. This

material over-placement will result in increased contaminant sorption, biological decay, and amendment application, and will lower concentrations throughout the cap and extend its long-term performance. The over-placement thickness is anticipated to average 3 in. or greater for each separate cap layer, which may result in the constructed thickness of the chemical isolation layer to be greater than the design thickness by 25 percent or more. The amount of over-placement and resulting chemical isolation conservatism will vary over the area of the cap.

- Additional GAC (amount to be specified in the Construction Quality Assurance Plan) beyond the design-specified minimum will be incorporated into the chemical isolation layer to account for potential unequal mixing of the GAC with the sand. A capping field demonstration was completed in late 2011 using full-scale capping equipment. The capping field demonstration confirmed that the hydraulic placement equipment proposed for the Onondaga Lake cap can consistently place GAC mixed throughout a sand layer at the specific water depths required for the Onondaga Lake project. The capping field demonstration provided information relative to determining the amount of extra GAC addition required. The final amount of additional GAC required will be determined during the capping start-up period, as detailed in the CQAP. .
- Additional material will be placed to account for mixing of the bottom of the cap with the underlying sediment. The bottom 3 in. of cap material placed is assumed to mix with the underlying sediment, and is not considered when meeting the minimum required isolation layer thickness. This material may mix with the underlying sediment and reduce contaminant concentrations in the zone immediately underlying the cap. It is also possible/likely that a portion of this dedicated mixing layer will not mix with the underlying sediment and therefore would provide even more protection as part of the cap.
- Rapid aerobic biodegradation will occur within the upper portion of the cap's habitat layer. This will result in lower contaminant concentrations at the surface of the cap, where essentially all benthic activity occurs.
- The analytical steady state model assumes a constant porewater concentration at the cap/sediment interface. However, as discussed above, mass conservation principles dictate that in order for diffusion to move contaminant mass out of the underlying sediment, a concentration gradient must be established at the sediment/cap interface. Mass transport out of the sediment, as well as any source depletion due to natural decay processes, are not considered in the analytical steady state model. Although the numerical model includes decreasing concentrations at the cap/sediment interface, the numerical model assumes an infinite source of constant concentration 2.5 meters below the sediment/cap interface.
- The numerical model considers diffusion/dispersion processes in the underlying sediment, which are in part dependant on sediment porosity. Porosity is set at a fixed value which does not change during the model run (the model input value is based on sediment samples collected in a given Remediation Area, as noted in Table A1.1 of Attachment 1). However, subsequent to cap placement, in those areas where significant dredging has not occurred prior to cap placement, consolidation of

underlying sediments will occur as a result of cap placement, which will reduce the porosity and permeability of the underlying sediments. The change will reduce the effective diffusion coefficient in the underlying sediments, which will result in a reduction in contaminant flux.

- In instances where multiple results exist for a given sampling location, maximum sample concentrations were selected from the analytical database. For example, if duplicate samples were collected at a particular location, the maximum value measured was used in the modeled dataset.

4.0 MODELING AREAS

The isolation cap will cover more than 450 acres of the lake bottom in Remediation Areas A, B, C, D, E, and F, as well as in the Wastebed 1-8 connected wetlands, WBB/HB Outboard Area and the Ninemile Creek spits. For cap design purposes, these remediation areas were subdivided into 17 model areas to account for the spatial variability observed in two of the key model input parameters: groundwater upwelling velocity and porewater contaminant concentrations. Each model area was evaluated independently. Cap design, including recommendations for isolation layer thickness and mass application rate of GAC, was based on the modeling results for each model area and is specific to the conditions present in each area. The 17 model areas are shown on Figure B-1. Supporting information such as figures showing contaminant porewater concentration and pH distributions in each area are provided in Figures B-2 through B-66, and the development of groundwater upwelling distributions for each model area is presented in Appendix C of this design report. The model areas are discussed below.

Remediation Area A was divided into two model areas due to the relatively elevated pH and porewater concentrations of VOCs observed at the mouth of Ninemile Creek and the higher measured groundwater upwelling in this area. The area at the mouth of Ninemile Creek has been designated as Model Area A2, and the remaining portion of the remediation area, where pH and VOCs are generally low, is designated as A1. There are isolated locations in Model Area A1 where pH exceeds 8.0, as shown on Figure B-22. However, these locations are not co-located in areas where phenol or other VOCs are present at levels that impact the design; therefore these locations did not factor into model area delineation. There are also some VOCs detected in Model Area A1 northwest of Model Area A-2, however, the concentrations are low and do not impact the design, and therefore Model Area A-2 does not include this area.

Model area delineation in Remediation Areas B and C was based on consideration of VOC and phenol concentrations and groundwater upwelling conditions (including identifying the portions of these areas that will be influenced by hydraulic barriers that have been or will be constructed and operated along the shoreline, as discussed in Appendix C). Based on this information, Remediation Area B was divided into two model areas (B1 and B2) and Remediation Area C was divided into three model areas (C1, C2, and C3). Model Areas B1 and C1 were then combined into a single model area (referred to hereafter as B1/C1) given the similar levels of concentrations of key compounds such as phenol and benzene and similarities in upwelling velocities.

Remediation Area D was divided into four sub-areas based on chemical concentrations and distributions. Appendix G presents the basis for development of these sub-areas, designated as the SMU 2, West, Center, and East sub-areas of Remediation Area D, as shown on Figure B-1. Due to the measured differences in contaminant concentrations and distributions as well as predicted groundwater upwelling velocities, each of these Remediation Area D sub-areas was modeled independently.

Remediation Area E was divided into three model areas due to the higher porewater concentrations of VOCs observed immediately adjacent to Remediation Area D (Model Area E2) and the elevated concentration of naphthalene offshore and at the mouth of Onondaga Creek (Model Area E3). Groundwater upwelling estimates are consistent throughout Remediation Area E and did not factor into model area delineation. There are isolated locations in Model Area E1 where pH exceeds 8.0, as shown on Figures B-66. However, these locations are not co-located with areas where phenol or other VOCs are present at levels that impact the design; therefore these locations did not factor into model area delineation.

Remediation Area F consists of two small areas totaling less than one acre. These areas were delineated based on sediment mercury concentrations that exceed the mercury PEC. Cap modeling was not conducted for these areas. These areas are not close to shore; therefore, groundwater upwelling velocities are expected to be low. Mercury concentrations are much lower in these areas than in other areas where modeling indicates that a 1-ft. chemical isolation layer will be sufficient. Therefore, the chemical isolation layer thickness in this area will be a minimum of 1 ft. consistent with the ROD. The pH in these areas is not elevated, so no amendments are necessary.

The Wastebed 1-8 connected wetland consists of 2.3 acres of connected wetlands that will be constructed adjacent to Remediation Area B. The Wastebeds 1-8 connected wetlands area (referred to hereafter as WB1-8) was evaluated as a single model area, as groundwater upwelling, pH, and contaminant concentrations do not exhibit significant variation across this small area.

The WBB/HB Outboard Area is a 16-acre area that lies between Onondaga Lake and the WBB/HB barrier wall alignment. It includes the mouth of Harbor Brook and areas of wetlands to be restored/constructed along the lake shoreline adjacent to Remediation Area D. The WBB/HB Outboard Area has been divided into three model areas for isolation cap design: east, center, and west (referred to hereafter as WBB-East, WBB-Center, and WBB-West, respectively). In general, elevated levels of VOCs and pH are observed throughout the WBB-West and WBB-Center model areas, and groundwater upwelling velocities are somewhat higher in these areas as well. The contaminant distributions are relatively similar between WBB-West and WBB-Center, while the upwelling increases going from WBB-Center to WBB-West, which formed the basis for modeling these two areas separately. The WBB-East area has lower levels of VOCs, generally low pH (with the exception of a few samples), and groundwater upwelling is lower in this area as well.

The spits of land that extend into Model Area A2 at the mouth of Ninemile Creek were incorporated into the cap design as part of Model Area A2. As documented in the Ninemile Creek OU-2 ROD (NYSDEC and USEPA, October 2009), remediation of the spits includes

sediment removal, placement of a cap/backfill material, and habitat restoration, consistent with the remediation of adjacent lake areas in Remediation Area A. Specific modeling considerations for this area are summarized in Section 7.5. Attachment 5 describes the data collected in the spits and provides additional detail on the inclusion of the spits in the Model Area A2 evaluation.

5.0 MODEL INPUTS

Accurate characterization of site conditions and cap material performance are critical to developing appropriate model input parameters. Model inputs for the cap were derived from extensive site sampling efforts, bench scale testing, and literature in some cases. Site-specific data have been collected in each model area to accurately characterize the underlying sediment and groundwater flow regime, assess cap material performance under model area specific conditions, and to inform input parameter selection on a model area basis.

Key model input parameters, including underlying porewater chemical concentrations and groundwater upwelling velocities, have been evaluated in each individual model area over the course of the seven year pre-design investigation (PDI). These data are supplemented by data from the remedial investigation, resulting in an extensive database that forms the basis for specifying the cap model inputs. Sorption parameters (including partitioning to sand cap materials and to GAC amendments) are also a key model input. Site specific data in model areas, as well as a multi-phase series of bench-scale evaluations were conducted between 2006 and 2011 to increase understanding and provide site-specific information for these key parameters. Model input parameters for which extensive site-specific field investigation and bench-scale laboratory studies have been performed include:

- Porewater chemical concentration
- Fraction of organic carbon (foc) in the isolation layer and at the cap surface (i.e., the bioturbation zone within the upper portion of the habitat layer)
- Groundwater upwelling velocity
- Organic carbon partitioning coefficient (Koc) for cap materials (as well as the underlying sediments)
- Parameters from the Freundlich isotherm equation to describe the non-linear sorption of VOCs and phenol to GAC
- Biological degradation rate
- Chemical isolation layer porosity

Attachment 1 contains details on the model input parameters, including the basis for specification of each input (i.e., applicable references and data sources), and a discussion of the statistical distributions used in probabilistic modeling evaluations.

6.0 DESIGN OPTIMIZATION CONSIDERING VARIABILITY IN SITE CONDITIONS

Understanding and accounting for variability in site conditions that constitute the basis for the model input parameters were critical components of completing the modeling to ensure it is truly predictive of future conditions. Variability in the data used to model cap performance

originated from two sources: 1) spatial variations due to natural and anthropogenic processes such as contaminant loadings to the lake and heterogeneity in permeability, deposition and erosion; and 2) measurement variability associated with sampling, processing and laboratory analysis, and data interpretation. Characterizing and accounting for these sources of variability to ensure that the cap is protective everywhere was a significant focus of the modeling effort described herein. Details are provided below.

6.1 Extensive Data Collection and Bench Testing

As discussed in Section 5, site-specific data were utilized in the model to maximize the accuracy and reliability of the results. An extensive site-specific database for the most important model input parameters was developed based on the RI and seven years of PDI data and laboratory studies. This database includes the analytical results from over 7,000 sediment samples and 5,500 porewater samples. In addition, site-specific measurements of groundwater upwelling velocity were taken at over 350 locations throughout the lake. Finally, extensive bench-scale testing was completed to accurately characterize important processes such as GAC adsorption and biological decay. As a result of this exhaustive data collection effort, uncertainty in input parameters has been minimized and variability can be accurately characterized and taken into consideration during modeling.

6.2 Small Model Areas to Minimize Spatial Variability

Remediation areas were developed to be reflective of localized conditions within the lake, such as contaminant sources and characteristics, water depth, and physical conditions. As discussed in Section 4, the five remediation areas of the lake were further divided into even smaller model areas to ensure that the cap would be designed specific to conditions in an area based on key model input parameters such as groundwater upwelling velocity and contaminant porewater concentrations. This same approach was taken in dividing up the WBB/HB Outboard Area into smaller model areas. By developing these smaller model areas, the spatial variability within each model area is significantly reduced, since zones of high/low concentration and/or upwelling velocity are modeled separately.

6.3 Initial Conservative Modeling Used Maximum Porewater Concentrations

To reduce the number and complexity of subsequent modeling simulations, the first phase of modeling conservatively used maximum porewater contaminant concentrations for analytical steady state simulations and for numerical simulations over a 1,000 year evaluation period. Porewater contaminant concentrations are one of the most significant model input parameters. As detailed in Section 7, the results from this initial conservative modeling indicated that cap performance criteria would be met for over 1,000 years for a majority of the contaminants in each area.

6.4 Model Conservatism Offset Potential Impacts of Variability

As discussed in Section 3.3, the model underestimates the effectiveness of the cap because it does not incorporate several natural processes and engineering/constructability considerations that will significantly contribute to the long-term performance of the cap, including over-placement of cap materials during construction. For example, in all amended cap areas except Model Areas E2, E3, and WBB-East, the minimum thickness of the GAC-amended isolation

layer is 9 in., which is the basis for the modeling and establishment of GAC application rates in these areas. Average over-placement of GAC-amended sand during construction is expected to be approximately 3 in. As a result, the carbon application rate and resulting cap performance in such areas will be approximately 33 percent greater than the design application rate determined from the modeling. In Model Areas E2, E3, and WBB-East, the GAC-amended isolation layer will be 12 in. (since pH amendments are not being used in these areas), for which a 3 in. over-placement would translate into a 25 percent increase in application rate.

6.5 Mean Values Used as Best Estimate

For modeling that used best estimates of parameters other than porewater concentration (Section 7), the mean rather than median values were used as the best estimate of each input parameter in a given model area. The mean values used were always greater than the median.

6.6 Conservative Probabilistic Modeling Used to Evaluate Robustness of Design

Probabilistic evaluations with the numerical model, which explicitly considered site-specific data on the variability of model inputs, were performed as part of the modeling used to determine GAC application rates. Probabilistic analysis is commonly used to account for input variability in models with multiple parameters (e.g., USEPA, 1997). The first step in performing a probabilistic analysis is to estimate a statistical distribution for each key input parameter, based on the data (for example, a normal distribution). Next, a model simulation is performed, selecting randomly from the distribution for each parameter. This represents one “realization,” and produces one possible outcome, in this case, one estimate of sorbed-phase and porewater concentrations within the cap. The model calculation is then repeated many times (5,000 realizations were used in this modeling evaluation), each time selecting a new value for each input parameter from its distribution. This produces a frequency distribution of computed concentrations. Management decisions can then be made using a chosen percentile of this distribution (e.g., 80th, 90th, or 95th percentile).

Probabilistic modeling based on the 90th percentile was used as a final conservative evaluation of the carbon application rates that were initially established by deterministic modeling with 95th percentile porewater concentrations and best estimate (mean) values for other input parameters (see Section 7 for discussion of the modeling approach). Distributions for the probabilistic analysis were developed for each key input parameter based on an analysis of the site data, in light of the underlying physical, chemical, and biological processes, as detailed in Attachment 1.

To ensure conservatism around two parameters that were not varied in probabilistic modeling (sediment consolidation in Remediation Area D and underlying sediment thickness) sensitivity analyses were conducted. These are included in Attachment 6, and demonstrate a negligible impact on model results.

7.0 MODELING APPROACH AND RESULTS

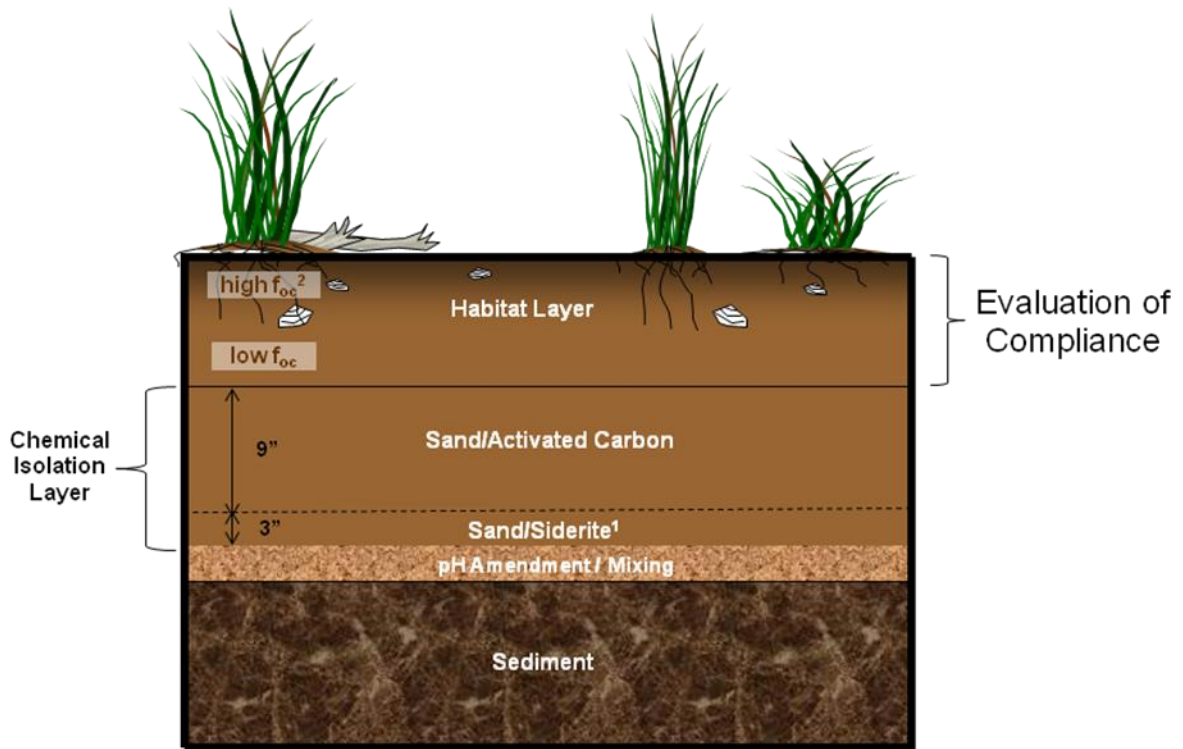
The modeling approach described below was used to develop the chemical isolation layer design in each of the 17 model areas described in Section 4, taking into consideration each of the 26 contaminants for which cap performance criteria were established, as listed below.

SUMMARY OF MODELED COMPOUNDS

Class	Compounds
Mercury	Mercury
VOCs and Phenol (9)	Benzene, Toluene, Ethylbenzene, Xylenes, Chlorobenzene, Dichlorobenzenes, Trichlorobenzenes, Naphthalene, Phenol
PCBs / PAHs (16)	Total PCBs, Fluorene, Phenanthrene, Acenaphthene, Acenaphthylene, Anthracene, Pyrene, Benzo(a)anthracene, Benzo(b)fluoranthene, Benzo(k)fluoranthene, Chrysene, Fluoranthene, Benzo(a)pyrene, Dibenz(a,h)anthracene, Indeno(1,2,3-cd)pyrene, Benzo(g,h,i)perylene

The cap modeling was generally based on a 12 in. isolation layer and a 12 in. habitat layer. As stated in the ROD, the compliance point for the cap is the bottom of the habitat restoration layer. To ensure protectiveness, the isolation layer has been designed to prevent concentrations of contaminants from exceeding their performance criteria (PEC or SSC) throughout the habitat restoration layer. Ensuring compliance throughout the habitat layer provides protection for benthic organisms in the actively mixed upper portion of the habitat layer as well as in the lower portion of the habitat layer (15-30 cm) where occasional deeper bioturbation may occur.

A general schematic of the amended cap is shown below; a schematic of the processes modeled is included in Section 3.1. In areas where amendments are not required to achieve long-term chemical isolation, the profile will be similar except that the chemical isolation layer will consist of a minimum of 12 in. of sand only.



1. In amended cap areas of Remediation Area E the chemical isolation layer will be 12" sand/carbon mix. Siderite will not be added to the cap as pH levels are at or close to neutral.

2. f_{oc} – fraction of organic carbon

Example Schematic of an Amended Cap

For contaminants and/or areas where the attenuation of contaminant flux is provided by the thickness of the sand cap material and not GAC, modeling was based on an 8 in. isolation layer, to allow for an additional level of conservatism in evaluating these cases. This model configuration was used for mercury in all areas and for all contaminants in Model Areas A1 and E1 (since initial modeling indicated that no GAC is needed in these two areas). For the remaining contaminants/areas, which include GAC to ensure long term effectiveness across all contaminants (except mercury as noted above), increasing the cap thickness would not have a significant impact on protectiveness (because the GAC application rate is the main determinant of its long-term performance). For those contaminants that rely on GAC to ensure long-term effectiveness, significant conservatism is already incorporated into the modeling and minimum compliance period of 1,000 years, as summarized in Section 3.3. The modeled thicknesses of each layer are detailed in the table below.

MODELED CAP LAYER THICKNESSES

Cap Model Layers	Sand Cap Areas	Amended Cap Areas	
		GAC and pH Amendment	GAC Only
	A1 and E1	A2, B1/C1, B2, C2, C3, D, WB1-8, WBB-West, and WBB-Center	E2, E3, and WBB-East
Habitat Layer	12 in.		
Chemical Isolation Layer	Start with 8 in. and increase if needed.	12 in. isolation layer including 9 in. sand/GAC and 3 in. sand/siderite layer. For mercury an 8 in. sand isolation layer was modeled.	12 in. sand/GAC amendment isolation layer. For mercury an 8 in. sand isolation layer was modeled.

For areas where the cap will include a pH amendment, the upper 3 in. of that sand/siderite layer was included in the chemical isolation layer, and is therefore represented in the model, including simulation of biological decay in this layer. To facilitate biodecay in this layer, the siderite layer was modeled/designed to ensure that the pH in this layer remains less than 8 for at least 1,000 years, following the initial period of higher porewater flux resulting from consolidation of underlying sediments (see Appendix I).

The modeling approach consisted of an initial highly-conservative evaluation based on analytical steady state modeling of a sand only chemical isolation layer, followed by more refined evaluations using the transient numerical model to simulate GAC performance (including probabilistic modeling in some cases) for chemicals/areas that did not meet the performance criteria based on the conservative set of input assumptions used during the initial steady state evaluation. The modeling approach differed slightly by chemical class and is described below along with a discussion of the results. Detailed model results are provided in Tables 1 through 5 and model input and output files are included in Attachment 4.

7.1 Mercury

Mercury was initially evaluated in each model area using the analytical steady state model. Deterministic simulations were performed using the following inputs:

- Maximum mercury concentration measured in porewater
- Best estimate (mean value) of all other parameters

Based on results from this modeling, if the maximum mercury concentration throughout the habitat layer was less than the PEC, then no further modeling of mercury was required for a given area. As shown on Table 1, mercury concentrations in Model Areas B2, C3, WB1-8, WBB-West, and WBB-Center were predicted to be lower than the PEC throughout the habitat layer based on this analytical steady state modeling evaluation. Therefore, no further modeling was performed for mercury in these areas.

Given the long time periods required to reach steady state for a more highly sorbing compound such as mercury, a secondary set of conservative model runs using the numerical model was employed. In the model areas remaining following the steady state evaluation described above, mercury was evaluated using the numerical model to evaluate long-term effectiveness under transient conditions using the approach listed below:

- Apply the same parameters used in the steady state analysis (maximum values for porewater concentration, best estimate for all others)
- Evaluate mercury concentrations, using a deterministic simulation, throughout the habitat layer over a 1,000-year evaluation period
- Conservatively ignore reductions in porewater concentrations that will result from siderite and GAC (where present)

If the maximum mercury concentration throughout the habitat layer was predicted to be less than the PEC based on this conservative transient modeling, then no further modeling of mercury was required for a given area. This transient modeling evaluation indicated that an 8 in. sand chemical isolation layer would be sufficient to ensure mercury remains below the mercury PEC throughout the habitat layer in all modeling areas for at least 1,000 years (see Table 1).

7.2 VOCs and Phenol

The eight VOCs (see table above) and phenol were initially evaluated within each model area using the analytical steady state model, assuming no GAC was present. Deterministic simulations were performed using the following input configuration:

- Maximum contaminant concentrations measured in porewater (or calculated based on sediment concentrations and partitioning theory for phenol)
- Biological decay was assumed to be zero with the exception of phenol in areas having a native pH of 8 or less (i.e., Areas A1, E1, E2, E3)
- Best estimate (mean value) of all other parameters

Based on the results from these simulations, if the maximum concentration throughout the habitat layer was less than the performance criteria (i.e., PEC or SSC), then no further modeling of that compound was conducted in a given model area.

Results for VOCs and phenol in each model area based on the initial conservative analytical steady state modeling are provided in Table 1. As shown in that table, in Model Areas A1 and E1 all eight VOCs and phenol were predicted to be less than the performance criteria throughout the habitat layer at steady state. This was true in Model Areas B2 and WBB-East as well, with the exception of phenol and naphthalene, respectively. For the remaining areas, concentrations of two or more of the nine compounds (i.e., eight VOCs plus phenol) were predicted to be higher than the performance criteria under this conservative modeling evaluation. Therefore, the remaining contaminants in each model area were further simulated with the numerical model to evaluate long-term effectiveness of a GAC amended cap under transient conditions based on the approach described below.

- Iterative deterministic simulations were performed over a 1,000 year evaluation period using the 95th percentile porewater concentration and best estimate (mean value) for all other inputs to determine the GAC application rate required to meet the performance criteria (i.e., each remaining compound's PEC/SSC). Biological decay rates were based on the slow end of literature rates as defined in the Feasibility Study and supported by the site specific bench and column testing described in Section 4 of the design report. Based on the results of the site specific bench testing, safety factors (as described in Attachment 1) were applied to the Feasibility Study decay rates for benzene, chlorobenzene, and naphthalene.
- To allow adequate time for a biological community to establish in the cap material, a lag period during which no biological decay would occur was specified in the model. The lag period was set at 5 years for those areas where no pH amendment is required (Model Areas A1, E1, E2, and E3). The lag period was set at 100 years in areas requiring pH amendment. This extended lag period in the pH amendment areas conservatively allows time for a robust biological community to establish after pH conditions within the cap reach steady-state (on the order of 1-2 years), thereby buffering pH throughout the full thickness of the cap.
- Following the iterative deterministic simulations described above, iterative probabilistic simulations were performed (see Section 6.6). The probabilistic simulations (based on full distributions for all key inputs, as available) were used to further evaluate the GAC application rate required to meet the performance criteria (i.e., each remaining compound's PEC/SSC) over a 1,000-year evaluation period. Starting with the GAC application rates established by the deterministic modeling (described above), probabilistic simulations were conducted, and the GAC application rate was increased if needed, until 90 percent of the realizations were predicted to meet the performance criteria over the 1,000-year evaluation period.
- Following the deterministic and probabilistic evaluations described above, GAC application rates were selected for each model area based on the more conservative estimate of GAC application rate--i.e., the higher of the two rates determined from the deterministic or probabilistic evaluation.

The GAC application rates and the contaminant that dictated the carbon amendment requirement in each area are presented in Table 2. In addition, the results from the Monte Carlo modeling at the final GAC application rates are provided in Table 3. The table lists the percent realizations meeting the PEC/SSC for all CPOIs included in the numerical probabilistic modeling at various points in time (100, 200, 500, 750, and 1,000 years).

7.3 PAHs/PCBs

Total PCBs and 15 PAHs were initially evaluated in each model area using the analytical steady state model assuming no GAC was present. Deterministic simulations were performed using the following inputs:

- Maximum porewater concentration was calculated from sediment data as described in Attachment 2
- Biological decay was assumed to be zero

- Best estimate (mean value) of all other parameters

Based on these results, if the maximum concentration throughout the habitat layer was predicted to be less than the PEC at steady state, then no further modeling of that compound was required in a given area. In Model Areas A1, A2, B2, ILWD-East, E1, E3, and WB1-8 all fifteen PAHs were predicted to be less than the performance criteria throughout the habitat layer at steady state. This was true in Model Areas B1/C1, E2 and WBB-East as well, with the exception of one PAH in each area (phenanthrene, fluorene, and anthracene, respectively). Total PCBs were predicted to be less than the performance criteria throughout the habitat layer in all model areas. Table 1 provides the results from this steady state evaluation for PCBs/PAHs.

Given the long time periods required to reach steady state for strongly sorbing compounds such as PAHs, a secondary set of conservative model runs using the numerical model was conducted. The remaining PAHs in each remaining model area (i.e., B1/C1, C2, C3, the remaining three subareas of ILWD, E2, and the three subareas of the WBB/HB Outboard Area) were further evaluated using the numerical model to evaluate long-term effectiveness under transient conditions using the approach listed below:

- Apply the same input parameters used in the steady state analysis (i.e., maximum values for porewater concentration, best estimate for all others)
- Use the GAC application rates established from the modeling analysis conducted for VOCs and phenol described above in Section 7.2, conservatively assuming that sorption to GAC for all PAHs is described by the site-specific measurements for naphthalene
- Evaluate concentrations, using a deterministic simulation, throughout the habitat layer over a 1,000-year evaluation period

If the maximum concentration throughout the habitat layer was predicted to be less than the PEC for 1,000 years, then no further modeling was required for a given PAH/area. The results from these conservative transient simulations for PAHs are provided in Table 1. As Table 1 shows, in Model Areas B1/C1, C3, D-West, D-Center, D-SMU2, E2 and WBB-East, all PAHs simulated were predicted to remain below the performance criteria throughout the habitat layer for 1,000 years.

The remaining PAHs in Model Areas C2 (11 compounds) and WBB-West and WBB-Center (two compounds each) were further evaluated using the numerical model to evaluate long-term effectiveness under transient conditions using the approach described below. These runs were conducted to evaluate whether the GAC application rates determined based on the modeling of VOCs and phenol described above needed to be increased further to address any of the individual PAHs.

- Deterministic simulations were performed over the 1,000-year evaluation period used for VOCs and phenol based on the 95th percentile porewater concentration and best estimate (mean value) for all inputs to evaluate if the PAHs met their performance criteria over this period.

- Probabilistic simulations (based on full distributions for all key inputs, as available) were also used to verify that 90 percent or more of realizations meet each individual PAH's PEC over a 1,000-year evaluation period.

If the results from the modeling described above indicated that the performance criteria were not met from the deterministic (1,000-year evaluation period) or probabilistic (1,000 year evaluation period) model simulations, then the GAC application rate was increased to address the PAHs. The results from this additional PAH modeling indicated that the GAC application rates established for VOCs and phenol (i.e., as shown in Table 2) would not need to be increased to address PAHs in Model Areas WBB-Center and WBB-West. However, the results for Model Area C2 indicated that PAHs required additional GAC (beyond that which was required to meet performance criteria for VOCs and phenol). The GAC application rate and the contaminant that dictated the carbon amendment requirement in that area are presented in Table 2 and the results from the Monte Carlo modeling of PAHs (where required) at the final GAC application rates are provided in Table 3.

7.4 Cap in 6-9 Meter Zone of Remediation Areas A and E

As discussed in Section 4.1.7 of the design report, a modified cap containing a 0.5 ft. chemical isolation layer was considered for the portions of Remediation Areas A and E having water depths from 20 ft. to 30 ft. (6 to 9 meters), since the ROD specified that a thin-layer cap may be appropriate for such areas. To evaluate the effectiveness of a 6 in. chemical isolation layer in these areas, a series of steady-state model simulations with a 4 in. chemical isolation layer (to provide for additional conservatism) was conducted for the 6 to 9 m zones of Model Areas A1, E1 and E3. Given the relatively higher VOC concentrations and the proximity to the ILWD, a modified cap was not considered for the 6 to 9 m zone of Model Area E2, which covers a relatively small area. The model inputs for these simulations were the same as those described above (except that the isolation layer thickness was set to 4 in. for steady state modeling and transient mercury modeling and to 6 in. for GAC performance modeling [where needed]).

Simulations were first performed with the steady state analytical model using the same approach as described in Sections 7.1 through 7.3 (i.e., maximum values for porewater concentration, mean values for all other inputs, no simulation of GAC). The results from these simulations, which are presented in Table 4, indicated that:

- All chemicals except mercury were predicted to be below performance criteria at steady state in Model Areas A1 and E1 with the thinner isolation layer.
- Mercury, a few VOCs, and one PAH were predicted to be above performance criteria in Model Area E3, which is generally consistent with the results from the initial conservative steady state modeling of these areas summarized in Table 1.

To further assess mercury in these three areas, deterministic simulations with the transient numerical model were conducted using the same approach described in Section 7.1 (i.e., maximum values for porewater concentration, mean values for all other inputs, 1,000 year evaluation period), for a 4 in. chemical isolation layer thickness. The results from these simulations indicated that the predicted concentrations throughout the habitat layer were below the mercury PEC for over 1,000 years.

To evaluate the remaining VOCs and PAH in the 6-9 m zone of Model Area E3 (i.e., those that were not screened out by the initial steady state modeling), additional transient numerical modeling of a GAC-amended cap was performed based on the following approach:

- Deterministic simulations of the VOCs (i.e., ethylbenzene, xylenes, dichlorobenzene, and naphthalene) with the transient numerical model were conducted using the same approach described in Section 7.2 (i.e., 95th percentile pore water concentrations, and mean values for all other inputs, 1,000 year evaluation period), for a 6-in. isolation layer composed of sand and GAC. The model was run iteratively to determine the GAC application rate needed to meet the PEC of all four compounds for 1,000 years, as summarized in Table 5. Based on that GAC application rate, probabilistic modeling was then conducted using the same approach described above Section 7.2 (model inputs sampled from full distributions, and GAC application rate increased as needed until 90 percent or more of the realizations met the PECs over the 1,000 year simulations). No increase in GAC application rate in the 6-9 m zone of Model Area E3 was required based on the results of this probabilistic modeling.
- For the one PAH (i.e., acenaphthylene) a secondary set of conservative model runs with the transient model was performed, following the approach described in Section 7.3 (i.e., maximum pore water concentrations, mean values for all other inputs, GAC application rate determined based on VOC modeling, 1,000 year evaluation period) to evaluate whether the additional GAC would be needed to address PAHs. The results of these simulations indicated that additional GAC is not necessary.

Based on the results of the simulations of the 6 to 9 m zones of Remediation Areas A and E, the following can be concluded with respect to the effectiveness of a modified cap (see Tables 4 and 5):

- A 6 in. sand chemical isolation layer will meet performance criteria for 1,000 years or longer for all chemicals in Model Areas A1 and E1 and for mercury in all of the model areas evaluated (i.e., A1, E1, E3).
- In the Model Area E3 6 to 9 m zone, a 6 in. chemical isolation layer amended with GAC (at an application rate that is slightly higher than that of the larger model area) will meet performance criteria for 1,000 years or longer for all chemicals.

7.5 Sub-area Modeling

Additional modeling was performed for several sub-areas, where certain measurements were not consistent with the characteristic ranges of values used to represent these model areas in the model input distributions or where there were slight differences in the cap design specifications or design criteria as compared to the modeling approach described above. These sub-areas included the following:

- One sampling location in Model Area A2
- Two sampling locations in Remediation Area D-Center
- One sampling location in Model Area E1
- The Remediation Area D shoreline

- The Ninemile Creek spits

For each such location, the isolation cap design was based on the sub-area modeling described below.

Sampling Location OL-VC-40197 in Model Area A2

In Model Area A2, porewater concentrations of ethylbenzene and xylene at location OL-VC-40197 were elevated in comparison to all other porewater concentrations in Model Area A2 (see Figures B-15 and B-16) and therefore data from this location were not included in the data set for Model Area A2. A GAC application rate was developed using iterative deterministic transient model simulations based on the maximum porewater concentration measured at this location. All other model inputs were set to the best estimate (mean value) established for Model Area A2. Additionally, Monte Carlo simulations based on mean porewater concentration at the OL-VC-40197 location and all other parameters varying according to their respective distributions were performed to evaluate the robustness of the GAC application rate determined through the deterministic modeling (i.e., by confirming that 90% or more of the realizations met the PECs at 1,000 years, consistent with the probabilistic modeling approach described in Section 7.2). Due to the higher porewater concentrations, a higher GAC application rate was required for this localized area relative to that needed for the larger Model Area A2 (Table 5). The areal extent of this sub-area where this higher GAC rate will be applied is shown in Figure 4.1.

Sample Locations OL-VC-10140 and OL-VC-10138 in Model Area D-Center

In Model Area D-Center, benzene porewater concentrations at two locations were elevated in comparison to other porewater data collected in that area, including samples collected from depths deeper than the data selected to define porewater concentrations in the ILWD cap modeling, which were based on samples from 1-meter above to 2-meters below the dredge elevation at a given sample location (see Attachment 1). A GAC application rate specific to concentrations measured in the vicinity of these two sample locations was therefore developed using deterministic simulations based on an alternate porewater data set (data from Model Area D-Center for 1-meter above to 3-meters below the dredge elevation, which includes the high benzene concentrations at depth from locations OL-VC-10140 and OL-VC-10138) and all other inputs the same (i.e., mean values) as those used in the base modeling for Model Area D-Center. Due to the higher porewater concentrations in the alternate data set used to evaluate these two locations, a higher GAC application rate was required for this localized area relative to that needed for the larger Model Area D-Center (Table 5). The areal extent of this sub-area where this higher GAC rate will be applied is shown in Figure 4.4.

Sample Location OL-GP-60155 in Model Area E1

The upwelling velocity at sample location OL-GP-60155 (16.8 cm/yr) in Model Area E1 was an order of magnitude higher than the average upwelling velocity in the overall model area. Sediment porewater concentrations are low throughout Model Area E1, and concentrations in the vicinity of OL-GP-60155 are generally at the low end of the area's overall distribution. To evaluate the elevated groundwater velocity at this location, the Model Area E1 steady state model was used based on the approach discussed in Sections 7.1-7.3, except that 1) the

porewater concentration was set equal to the maximum value measured at sample locations in the vicinity of OL-GP-60155 (approximately a 7 acre area), and 2) the upwelling velocity was set to 16.8 cm/yr. The results of this model analysis, which are shown in Table 4, indicated that concentrations were predicted to be less than the performance criteria throughout the habitat layer at steady state for all CPOIs (i.e., mercury, VOCs, phenol, PCBs, and PAHs). Consistent with the larger Model Area E1, these results indicate that an 8 in. sand isolation layer would be protective in this localized area as well.

Remediation Area D Shoreline

The in-lake planting area within Remediation Area D, which covers a 25-ft strip along the shoreline adjacent to Model Areas D-East, D-Center, and D-West, were also considered for sub-area modeling. This 25-ft strip is being designed to contain higher total organic carbon (TOC) in the cap's habitat layer as compared to the remainder of Remediation Area D. To evaluate the higher habitat layer TOC specific to these areas, sensitivity analyses were conducted to evaluate the impacts on carbon amendments (see Attachment 6). The results of these sensitivity analyses indicated that the differences in GAC application rate were small, and considering the other model conservatisms associated with how these areas are modeled (e.g., see Section 3.3), sub-area-specific GAC application rates are not needed for this relatively limited portion of Remediation Area D.

Ninemile Creek Spits

The Ninemile Creek spits have been incorporated into the cap design for Remediation Area A and were evaluated using the model inputs developed for Model Area A2. However, the cap effectiveness criteria within the spits are established in the Ninemile Creek ROD and differ from those defined in the lake ROD. As discussed in more detail in Attachment 5, the only CPOI that required additional modeling in the spits was mercury. Therefore, using the model inputs for Model Area A2, the approach described in Section 7.1 was followed for the evaluation of the spits, with the exception that model results for mercury were compared to the criterion established in the Ninemile Creek ROD for mercury of 0.15 mg/kg. As discussed in Attachment 5, the model results indicated that the cap design specified for Model Area A2 would also be protective of the Ninemile Creek ROD criteria for 1,000 years in the spits.

7.6 Sources of Uncertainty in Model Results

The input parameters to which the model is most sensitive are porewater concentration, groundwater upwelling velocity, biodegradation rate, and contaminant sorption parameters (including GAC Freundlich coefficients). For each of these parameters, extensive data sets derived from field investigation and bench-scale testing were developed to provide site-specific information. As described in Section 6 specific model areas were developed to address spatial variability and to develop cap designs (i.e., GAC application rates) specific to the conditions in each area. Additional sources of variation and parameter uncertainty were addressed by a combination of conservative initial modeling (e.g., based on maximum measured pore water concentrations) and probabilistic modeling that accounted for the full range of variation in key input parameters (including worst case conditions).

Sources of uncertainty in the modeling have been addressed through the extensive data gathering effort used to support model input specification, the conservatisms described in Section 3.3 and the design optimization process described in Section 6.0.

8.0 CONCLUSIONS

Design of the Onondaga Lake sediment cap chemical isolation layer considers an extensive collection of site-specific data and evaluation of performance based on the rigorous modeling effort described above. Recommended cap profiles and GAC application rates based on a 1,000 year evaluation period are presented in the table below. The cap thicknesses and carbon amendment doses listed below are the minimums required based on design evaluations and do not include over-placement or over-dosing required to meet these minimums during construction.

CHEMICAL ISOLATION LAYER DESIGN SUMMARY

Model Area	Design Thickness and Profile	GAC Application Rate
A1 (0-6m)	12-in. (8-in. required) sand cap	None
A2 (including Ninemile Creek Spits)	12-in. amended cap (9-in. GAC, 3-in. sand/siderite)	0.66 lb/sf
B1/C1	12-in. amended cap (9-in. GAC, 3-in. sand/siderite)	0.60 lb/sf
B2	12-in. amended cap (9-in. GAC, 3-in. sand/siderite)	1.22 lb/sf
C2	12-in. amended cap (9-in. GAC, 3-in. sand/siderite)	0.01 lb/sf
C3	12-in. amended cap (9-in. GAC, 3-in. sand/siderite)	0.24 lb/sf
D-SMU2	12-in. amended cap (9-in. GAC, 3-in. sand/siderite)	0.044 lb/sf
D-West	12-in. amended cap (9-in. GAC, 3-in. sand/siderite)	1.33 lb/sf
D-Center	12-in. amended cap (9-in. GAC, 3-in. sand/siderite)	0.93 lb/sf
D-East	12-in. amended cap (9-in. GAC, 3-in. sand/siderite)	0.44 lb/sf
E1 (0-6m)	12-in. (8-in. required) sand cap	None
E2	12-in. GAC amended cap	0.27 lb/sf
E3 (0-6m)	12-in. GAC amended cap	0.008 lb/sf
WBB-East	12-in. GAC amended cap	0.02 lb/sf
WBB-Center	12-in. amended cap (9-in. GAC, 3-in. sand/siderite)	0.50 lb/sf
WBB-West	12-in. amended cap (9-in. GAC, 3-in. sand/siderite)	0.61 lb/sf
WB1-8	12-in. amended cap (9-in. GAC, 3-in. sand/siderite)	1.20 lb/sf
6-9 Meter Zone		
A1	6-in. (4-in. required) sand cap	None
E1	6-in. (4-in. required) sand cap	None
E3	6-in. GAC amended cap	0.084 lb/sf

Sub-Areas		
A2 (40197)	12-in. amended cap (9-in. GAC, 3-in. sand/siderite)	6.6 lb/sf
D-Center (10138 and 10140)	12-in. amended cap (9-in. GAC, 3-in. sand/siderite)	5.0 lb/sf

9.0 REFERENCES

- Go, J., D.J. Lampert, J.A. Stegman, D.D. Reible. 2009. Predicting Contaminant Fate and Transport in Sediment Caps: Mathematical Modeling Approaches, *Journal of Applied Geochemistry*, 24, 7, 1347-1353.
- Lampert, D. J. and Reible, D. 2009. An Analytical Modeling Approach for Evaluation of Capping of Contaminated Sediments, *Soil and Sediment Contamination: An International Journal*, 18:4, 470 – 488.
- Neville, C. 2005. ADFL Analytical Solution – Version 4, User’s Guide. S.S. Papadopoulos & Associates, Inc. Bethesda, MD.
- New York State Department of Environmental Conservation and United States Environmental Protection Agency Region 2. 2009. Record of Decision. *Operable Unit 2 of the Geddes Brook/Ninemile Creek Site*. Operable Unit of the Onondaga Lake Bottom Subsite of the Onondaga Lake Superfund Site. October 2009.
- Palermo, M.R., S. Maynard, J. Miller, and D. Reible. 1998. Guidance for *In Situ* Subaqueous Capping of Contaminated Sediments. Environmental Protection Agency, EPA 905-B96-004, Great Lakes.
- Parsons. 2009a. Lake Pre-Design Investigation: Phase VI Work Plan. Prepared for Honeywell, Morristown, New Jersey and Syracuse, New York.
- Parsons, 2009b. Draft Onondaga Lake Capping and Dredge Area and Depth Initial Design Report, Appendix B Attachment 3.2. Prepared for Honeywell.
- USEPA. 1997. Guiding Principles for Monte Carlo Analysis. Risk Assessment Forum, U.S. Environmental Protection Agency. EPA/630/R-97/001.
- Zheng, C., and P. Wang. 1998. MT3DMS: A Modular Three-Dimensional Multispecies Transport Model for Simulation of Advection, Dispersion and Chemical Reactions of Contaminants in Groundwater Systems. Documentation and User’s Guide. U.S. Army Corps of Engineers Technical Report, June 1998.

TABLES

TABLE 1

SUMMARY OF COMPOUNDS MEETING PERFORMANCE CRITERIA ASSUMING INITIAL CONSERVATIVE ANALYTICAL STEADY STATE AND TRANSIENT MODEL EVALUATIONS¹

Group	Chemical	Model Area																
		A1	A2	B1/ C1	B2	C2	C3	S ²	W ²	C ²	E ²	E1	E2	E3	WB1-8	WBB -West	WBB- Center	WB- East
Mercury	Mercury	✓✓	✓✓	✓✓	✓	✓✓	✓	✓✓	✓✓	✓✓	✓✓	✓✓	✓✓	✓✓	✓	✓	✓	✓✓
VOCs	Benzene	✓	✓		✓	✓	✓					✓	✓	✓		✓	✓	✓
	Toluene	✓	✓		✓	✓	✓	✓				✓	✓	✓				✓
	Ethylbenzene	✓		✓	✓	✓						✓						✓
	Xylenes	✓			✓	✓						✓						✓
	Chlorobenzene	✓		✓	✓	✓	✓	✓				✓		✓	✓			✓
	Dichlorobenzenes	✓		✓	✓	✓		✓				✓		✓				✓
	Trichlorobenzenes	✓	✓	✓	✓	✓	✓	✓				✓		✓	✓			✓
	Naphthalene	✓	✓		✓							✓						
	Phenol	✓					✓					✓	✓	✓				✓
PAHs/ PCB	Total PCBs	✓	✓	✓	✓	✓	✓	✓	✓	✓	✓	✓	✓	✓	✓	✓	✓	✓
	Fluorene	✓	✓	✓	✓		✓✓	✓✓	✓✓	✓✓	✓	✓	✓✓	✓	✓			✓
	Phenanthrene	✓	✓	✓✓	✓		✓✓	✓✓	✓✓	✓✓	✓	✓	✓	✓	✓			✓
	Acenaphthene	✓	✓	✓	✓		✓	✓	✓✓	✓	✓	✓	✓	✓	✓	✓✓	✓✓	✓
	Acenaphthylene	✓	✓	✓	✓	✓	✓	✓	✓✓	✓	✓	✓	✓	✓	✓	✓✓	✓✓	✓
	Anthracene	✓	✓	✓	✓		✓✓	✓✓	✓✓	✓✓	✓	✓	✓	✓	✓	✓✓	✓✓	✓✓
	Pyrene	✓	✓	✓	✓	✓	✓	✓	✓✓	✓	✓	✓	✓	✓	✓	✓✓	✓✓	✓
	Benzo(a)anthracene	✓	✓	✓	✓		✓	✓	✓✓	✓	✓	✓	✓	✓	✓	✓✓	✓✓	✓
	Benzo(b)fluoranthene	✓	✓	✓	✓		✓	✓	✓	✓	✓	✓	✓	✓	✓	✓	✓	✓
	Benzo(k)fluoranthene	✓	✓	✓	✓	✓	✓	✓	✓	✓	✓	✓	✓	✓	✓	✓	✓	✓
	Chrysene	✓	✓	✓	✓		✓	✓	✓✓	✓	✓	✓	✓	✓	✓	✓✓	✓✓	✓
Fluoranthene	✓	✓	✓	✓		✓	✓	✓	✓	✓	✓	✓	✓	✓	✓✓	✓✓	✓	

TABLE 1 (CONTINUED)

SUMMARY OF COMPOUNDS MEETING PERFORMANCE CRITERIA ASSUMING INITIAL CONSERVATIVE ANALYTICAL STEADY STATE AND TRANSIENT MODEL EVALUATIONS¹

Group	Chemical	Model Area																	
		A1	A2	B1/ C1	B2	C2	C3	S ²	W ²	C ²	E ²	E1	E2	E3	WB1-8	WBB -West	WBB- Center	WB- East	
	Benzo(a)pyrene	✓	✓	✓	✓		✓	✓	✓	✓	✓	✓	✓	✓	✓	✓	✓✓	✓✓	✓
	Dibenz(a,h)anthracene	✓	✓	✓	✓	✓	✓	✓	✓	✓	✓	✓	✓	✓	✓	✓	✓	✓	✓
	Indeno(1,2,3-cd)pyrene	✓	✓	✓	✓		✓	✓	✓	✓	✓	✓	✓	✓	✓	✓	✓	✓	✓
	Benzo(g,h,i)perylene	✓	✓	✓	✓	✓✓	✓	✓	✓	✓	✓	✓	✓	✓	✓	✓	✓	✓	✓

Notes:

- 1) Table summarizes the results from the conservative analytical steady state (✓) and 1,000 year transient evaluations (✓✓) performed using maximum concentrations discussed in Sections 7.1 through 7.3. These compounds were not subject to additional modeling. Check marks (✓) indicate cases where performance criteria were met.
- 2) ILWD Subareas: SMU2 (S), West (W), Center (C), East (E)

TABLE 2
CARBON APPLICATION RATE EVALUATION

Model Area	Acre s	Application rate based on Deterministic Modeling ¹		Application rate based on Probabilistic Modeling ²		Final Carbon Application Rate (lb/sf)
		Controlling Chemical(s)	Carbon Application Rate (lb/sf)	Controlling Chemical(s)	Carbon Application rate (lb/sf)	
A1 (0-6m) ³	39.8	Sand Cap Only				
A2 ⁵	16.1	Xylenes	0.66	NA	No additional carbon	0.66
B1/C1	15.5	Phenol	0.60	NA	No additional carbon	0.60
B2	7.0	Phenol	1.22	NA	No additional carbon	1.22
C2	8.8	Fluorene	0.01	NA	No additional carbon	0.01
C3	12.1	Xylenes	0.24	NA	No additional carbon	0.24
D-SMU2	7.1	Naphthalene	0.044	NA	No additional carbon	0.044
D-West ⁴	11.0	Phenol	1.33	NA	No additional carbon	1.33
D-Center ^{4,5}	33.0	Xylenes	0.93	NA	No additional carbon	0.93
D-East ⁴	53.1	Chlorobenzene	0.44	NA	No additional carbon	0.44
E1 (0-6m) ³	65.6	Sand Cap Only				
E2	21.2	Chlorobenzene	0.27	NA	No additional carbon	0.27
E3 (0-6m) ³	60.5	Ethylbenzene and Naphthalene	0.008	NA	No additional carbon	0.008
WB1-8	2.4	Xylenes	1.11	NA	1.20	1.20
WBB-West	5.7	Chlorobenzene, Dichlorobenzenes, and Naphthalene	0.61	NA	No additional carbon	0.61
WBB-Center	4.7	Dichlorobenzenes	0.50	NA	No additional carbon	0.50
WBB-East	6.0	Naphthalene	0.02	NA	No additional carbon	0.02

Notes:

- 1) Application rate needed to achieve criteria over 1,000-year evaluation period in deterministic simulation based on 95th percentile porewater concentrations and best estimates for other model inputs.
- 2) Application rate needed to achieve criteria over 1,000-year evaluation period in 90% or more of realizations from probabilistic modeling (Monte Carlo Analysis).
- 3) The 6-9 meter zone in this model area was evaluated separately, results are provided in Table 5. Acreages do not include the 6-9 meter zone.
- 4) ILWD sub-area acreage values include portions of the addendum cap area adjacent to each sub-area. Carbon application rates for each sub-area will be applied to the portion of the addendum cap area adjacent to each sub-area.
- 5) A2 and D-Center total acreages include 40197 and 10138/10140 areas, respectively. The acreage for each of these sub-areas is provided in Table 5.

TABLE 3

MONTE CARLO MODELING RESULTS AT FINAL GAC APPLICATION RATES

Model Area	Chemical	Carbon Dose (lb/sf)	Percent Realizations Meeting PEC				
			1,000 years	750 years	500 years	200 years	100 years
A2	Ethylbenzene	0.66	97.2	97.8	98.7	99.8	100.0
	Xylenes		93.5	95.4	97.2	99.6	100.0
	Chlorobenzenes		100.0	100.0	100.0	100.0	100.0
	Dichlorobenzenes		100.0	100.0	100.0	100.0	100.0
	Phenol		98.2	98.2	98.2	98.2	98.3
B1/C1	Benzene	0.6	95.2	95.2	95.2	95.2	95.2
	Toluene		100.0	100.0	100.0	100.0	100.0
	Xylenes		99.9	100.0	100.0	100.0	100.0
	Naphthalene		100.0	100.0	100.0	100.0	100.0
	Phenol		95.4	95.4	95.4	95.4	95.4
B2	Phenol	1.22	92.6	92.6	92.6	92.6	92.6
C2	Naphthalene	0.01	96.7	96.7	96.7	96.7	96.7
	Phenol		95.4	95.4	95.4	95.4	95.4
	Fluorene		94.5	95.5	97.0	98.6	99.3
	Phenanthrene		95.3	96.3	97.8	99.2	99.4
	Acenaphthene		98.7	99.0	99.2	99.8	100.0
	Anthracene		97.5	98.2	98.8	99.5	99.9
	Pyrene		99.3	99.3	99.3	99.7	99.9
	Benzo(a)anthracene		99.3	99.4	99.7	100.0	100.0
	Benzo(b)fluoranthene		99.4	99.6	99.9	100.0	100.0
	Chrysene		99.5	99.7	99.9	100.0	100.0
	Fluoranthene		99.1	99.3	99.3	99.7	100.0
	Benzo(a)pyrene		99.6	99.8	99.9	100.0	100.0

Model Area	Chemical	Carbon Dose (lb/sf)	Percent Realizations Meeting PEC				
			1,000 years	750 years	500 years	200 years	100 years
	Indeno(1,2,3-cd)pyrene		99.8	100.0	100.0	100.0	100.0
C3	Ethylbenzene	0.24	100.0	100.0	100.0	100.0	100.0
	Xylenes		91.0	94.1	97.7	100.0	100.0
	Dichlorobenzenes		99.9	99.9	100.0	100.0	100.0
	Naphthalene		98.2	99.1	99.9	100.0	100.0
ILWD-SMU2	Benzene	0.044	99.6	99.6	99.6	99.6	99.6
	Ethylbenzene		96.2	96.2	96.2	96.2	96.4
	Xylenes		93.6	93.6	93.6	93.9	94.7
	Naphthalene		93.3	93.3	93.4	94.6	97.9
	Phenol		96.0	96.0	96.0	96.0	96.0
ILWD-West	Benzene	1.33	98.4	98.5	98.5	99.0	99.8
	Toluene		99.8	99.8	99.9	99.9	100.0
	Ethylbenzene		100.0	100.0	100.0	100.0	100.0
	Xylenes		99.6	99.9	100.0	100.0	100.0
	Chlorobenzenes		100.0	100.0	100.0	100.0	100.0
	Dichlorobenzenes		100.0	100.0	100.0	100.0	100.0
	Trichlorobenzenes		100.0	100.0	100.0	100.0	100.0
	Naphthalene		99.90	99.98	100.0	100.0	100.0
	Phenol		93.06	93.06	93.06	93.06	93.1
ILWD-Center	Benzene	0.93	93.8	93.8	93.8	93.9	94.2
	Toluene		99.8	99.8	99.8	99.9	100.0
	Ethylbenzene		99.8	99.9	99.9	100.0	100.0
	Xylenes		92.2	95.7	97.7	100.0	100.0
	Chlorobenzenes		96.1	97.4	99.5	100.0	100.0
	Dichlorobenzenes		100.0	100.0	100.0	100.0	100.0
	Trichlorobenzenes		99.9	99.9	99.9	99.9	99.9

Model Area	Chemical	Carbon Dose (lb/sf)	Percent Realizations Meeting PEC				
			1,000 years	750 years	500 years	200 years	100 years
	Naphthalene		97.4	97.6	98.1	100.0	100.0
	Phenol		99.6	99.6	99.6	99.6	99.6
ILWD-East	Benzene	0.44	100.0	100.0	100.0	100.0	100.0
	Toluene		100.0	100.0	100.0	100.0	100.0
	Ethylbenzene		100.0	100.0	100.0	100.0	100.0
	Xylenes		96.3	97.0	97.9	99.9	100.0
	Chlorobenzenes		94.1	94.9	95.7	97.1	99.8
	Dichlorobenzenes		97.9	98.8	99.9	100.0	100.0
	Trichlorobenzenes		100.0	100.0	100.0	100.0	100.0
	Naphthalene		98.0	98.3	99.1	100.0	100.0
Phenol	97.3	97.3	97.3	97.3	97.3		
E2	Ethylbenzene	0.27	99.9	99.9	99.9	100.0	100.0
	Xylenes		98.7	99.2	99.4	99.9	100.0
	Chlorobenzenes		94.6	96.3	98.4	99.9	100.0
	Dichlorobenzenes		96.8	98.3	99.2	99.9	100.0
	Trichlorobenzenes		100.0	100.0	100.0	100.0	100.0
	Naphthalene		97.9	98.6	99.2	100.0	100.0
E3	Ethylbenzene	0.0008	94.6	94.6	94.6	94.6	94.6
	Xylenes		99.4	99.4	99.4	99.4	99.4
	Naphthalene		94.2	94.2	94.2	94.2	94.2
WBB-East	Naphthalene	0.02	93.0	93.9	95.7	100.0	100.0
WBB-West	Toluene	0.61	100.0	100.0	100.0	100.0	100.0
	Ethylbenzene		100.0	100.0	100.0	100.0	100.0
	Xylenes		98.3	99.4	99.8	100.0	100.0
	Chlorobenzenes		91.8	93.7	96.8	99.8	100.0
	Dichlorobenzenes		93.3	96.7	98.9	100.0	100.0

Model Area	Chemical	Carbon Dose (lb/sf)	Percent Realizations Meeting PEC				
			1,000 years	750 years	500 years	200 years	100 years
	Trichlorobenzenes		99.6	99.7	99.7	99.8	99.8
	Naphthalene		93.7	96.1	98.7	99.9	100.0
	Phenol		98.7	98.7	98.7	98.7	98.7
	Fluorene		99.3	99.3	99.4	99.9	100.0
	Phenanthrene		99.6	99.9	100.0	100.0	100.0
WBB-Center	Toluene	0.5	99.9	99.9	99.9	99.9	99.9
	Ethylbenzene		100.0	100.0	100.0	100.0	100.0
	Xylenes		98.0	99.0	99.8	100.0	100.0
	Chlorobenzenes		92.9	94.2	96.8	99.8	99.9
	Dichlorobenzenes		93.5	97.2	99.0	100.0	100.0
	Trichlorobenzenes		99.5	99.6	99.7	99.8	99.8
	Naphthalene		94.0	96.6	98.6	99.9	100.0
	Phenol		98.4	98.4	98.4	98.4	98.4
	Fluorene		99.3	99.3	99.4	100.0	100.0
	Phenanthrene		99.7	99.9	99.9	100.0	100.0
WB 1-8	Benzene	1.2	99.3	99.3	99.3	99.7	99.9
	Toluene		100.0	100.0	100.0	100.0	100.0
	Ethylbenzene		99.9	100.0	100.0	100.0	100.0
	Xylenes		90.3	96.5	99.5	100.0	100.0
	Dichlorobenzenes		100.0	100.0	100.0	100.0	100.0
	Naphthalene		95.9	98.9	99.8	100.0	100.0
	Phenol		93.7	93.7	93.7	93.7	93.7
E3 (6-9m Zone)	Ethylbenzene	0.084	99.3	99.3	99.3	99.3	99.3
	Xylenes		99.4	99.5	99.7	100.0	100.0
	Dichlorobenzene		99.9	99.9	99.9	100.0	100.0
	Naphthalene		94.6	95.1	96.3	98.9	99.8

Model Area	Chemical	Carbon Dose (lb/sf)	Percent Realizations Meeting PEC				
			1,000 years	750 years	500 years	200 years	100 years
OL-VC-40197	Benzene	6.56	100.0	100.0	100.0	100.0	100.0
	Toluene		100.0	100.0	100.0	100.0	100.0
	Ethylbenzene		99.2	100.0	100.0	100.0	100.0
	Xylenes		97.0	100.0	100.0	100.0	100.0
	Chlorobenzenes		100.0	100.0	100.0	100.0	100.0
	Dichlorobenzenes		100.0	100.0	100.0	100.0	100.0
	Trichlorobenzenes		99.9	100.0	100.0	100.0	100.0
	Naphthalene		100.0	100.0	100.0	100.0	100.0

Note:

- 1) Monte Carlo modeling was performed on areas and chemicals that did not meet the PEC during the conservative screening using maximum porewater concentrations.

TABLE 4

SUMMARY OF COMPOUNDS MEETING PERFORMANCE CRITERIA USING INITIAL CONSERVATIVE ANALYTICAL STEADY STATE AND TRANSIENT MODEL EVALUATIONS OF 6-9 M ZONES AND SUB-AREA MODELING ¹

Group	Chemical	Model Area			
		A1 (6-9 M ZONE)	E1 (6-9 M ZONE)	E3 (6-9 M ZONE)	E1 Location OL-GP-60155
Mercury	Mercury	✓✓	✓✓	✓✓	✓
VOCs	Benzene	✓	✓	✓	✓
	Toluene	✓	✓	✓	✓
	Ethylbenzene	✓	✓		✓
	Xylenes	✓	✓		✓
	Chlorobenzene	✓	✓	✓	✓
	Dichlorobenzenes	✓	✓		✓
	Trichlorobenzenes	✓	✓	✓	✓
	Naphthalene	✓	✓		✓
	Phenol	✓	✓	✓	✓
PAHs/ PCB	Total PCBs	✓	✓	✓	✓
	Fluorene	✓	✓	✓	✓
	Phenanthrene	✓	✓	✓	✓
	Acenaphthene	✓	✓	✓	✓
	Acenaphthylene	✓	✓	✓✓	✓
	Anthracene	✓	✓	✓	✓
	Pyrene	✓	✓	✓	✓
	Benzo(a)anthracene	✓	✓	✓	✓
	Benzo(b)fluoranthene	✓	✓	✓	✓
	Benzo(k)fluoranthene	✓	✓	✓	✓
	Chrysene	✓	✓	✓	✓
	Fluoranthene	✓	✓	✓	✓

TABLE 4 (CONTINUED)

SUMMARY OF COMPOUNDS MEETING PERFORMANCE CRITERIA USING INITIAL CONSERVATIVE ANALYTICAL STEADY STATE AND TRANSIENT MODEL EVALUATIONS OF 6-9 M ZONES AND SUB-AREA MODELING ¹

Group	Chemical	Model Area			
		A1 (6-9 M ZONE)	E1 (6-9 M ZONE)	E3 (6-9 M ZONE)	E1 Location OL-GP-60155
	Benzo(a)pyrene	✓	✓	✓	✓
	Dibenz(a,h)anthracene	✓	✓	✓	✓
	Indeno(1,2,3-cd)pyrene	✓	✓	✓	✓
	Benzo(g,h,i)perylene	✓	✓	✓	✓

Notes:

- 1) Table summarizes the results from the conservative analytical steady state (✓) and 1000 year transient evaluations (✓✓) performed using maximum concentrations discussed in Sections 7.1 through 7.3. These compounds were not subject to additional modeling. Check marks (✓) indicate cases where performance criteria were met.

TABLE 5

CARBON APPLICATION RATE FOR 6-9 M ZONES AND SUB AREA MODELING

Model Area / Location	Acres	Application rate based on Deterministic Modeling ¹		Application rate based on Probabilistic Modeling ²		Final Carbon Application Rate (lb/sf)
		Controlling Chemical(s)	Carbon Application Rate (lb/sf)	Controlling Chemical(s)	Carbon Application rate (lb/sf)	
A1 (6-9 M)	29.9	Sand Cap Only				
E1 (6-9 M)	12.6	Sand Cap Only				
E3 (6-9 M)	15.6	Naphthalene	0.084	NA	No additional carbon	0.084
A2 OL-VC-40197	0.2	Xylenes	6.6	NA	No additional carbon	6.6
D-Center OL-VC-10138 & OL-VC-10140	1.6	Benzene	5.0	Not modeled		5.0
E1 OL-GP-60155	NA	Sand Cap Only				
Ninemile Creek Spits ³	1.9	NA	0.66	Not modeled		0.66

Notes:

- 1) Application rate needed to achieve criteria over 1,000-year evaluation period in deterministic simulation based on 95th percentile porewater concentrations and best estimates for other model inputs.
- 2) Application rate needed to achieve criteria over 1,000-year evaluation period in 90% or more of realizations from probabilistic modeling (Monte Carlo Analysis).
- 3) Cap design for Ninemile Creek spits same as Model Areas A2 (see Attachment 5)

FIGURES

ATTACHMENT 1

MODEL INPUTS

1.0 MODEL INPUT PARAMETERS

Model inputs were derived from extensive site sampling efforts and bench-scale testing, as well as literature in some cases. Based on the initial modeling conducted during the FS, as well as analyses conducted since that time, model predictions have been found to be most sensitive to underlying porewater concentration, groundwater upwelling velocity, biological decay rate and sorption parameters (including partitioning to sand cap materials and to GAC amendments). Therefore, an extensive data collection effort and a series of bench-scale evaluations were conducted between 2005 and 2011 to increase understanding and provide site-specific information for these key parameters. The following subsections describe the data collection efforts and basis for developing the input values used for these key model input parameters.

Both deterministic and probabilistic model evaluations were used in developing the chemical isolation layer design. Input parameters for the deterministic simulations were fixed values specified based on the references and rationale provided in detail in Table A1.1. Probabilistic model simulations were completed to assess cap performance against the full range of potential input parameter values (including the “worst-case” values as they pertained to predications of cap performance). Statistical distributions were developed for key input parameters and used in these probabilistic modeling evaluations. The distributions used for such model input parameters, and the basis for their selection (including applicable references and data sources) are also provided in Table A1.1.

1.1 Porewater Concentrations

Multiple sampling methods were used to measure porewater concentrations within the remediation areas of the lake. These methods are described further in the Onondaga Lake Phase I Pre-Design Investigation Porewater Methods Evaluation Report (Parsons, 2006). Sampling methods included *in situ* diffusion samplers (peepers), groundwater upwelling pumps and porewater generated via centrifugation of sediment. Peepers and centrifuged samples, in general, produced consistent results and provided readily implementable approaches for collecting a large number of porewater samples. Therefore, data from all three methods (i.e., centrifugation, peepers, and upwelling pumps) were generally used to develop model inputs for porewater concentration.

In consultation with the NYSDEC, correction factors were developed and applied to the porewater data to account for any potential losses during sample collection, handling or analysis. Correction factors varied by compound and sampling methodology. Correction factors for peeper data were based on the results of the Phase II Pre-Design Investigation: Data Summary Report, Appendix J - Diffusion Sampler Equilibrium Study (Parsons, 2009a). For porewater samples generated via centrifugation, correction factors were based on average Matrix Spike/Matrix Spike Duplicate (MS/MSD) recoveries. Groundwater data collected from upwelling pumps in 2002/2003 were discarded, with the exception of mercury and phenol results, due to the potential for losses along the pump tubing. Groundwater data collected from the upwelling pumps, following modification of the tubing during the Phase I Pre-Design Investigation (PDI), were incorporated into the model data set without correction factors. Table A1.2 provides a summary of the correction factors employed.

For certain contaminants, the ability to collect porewater samples was limited by the volume required for analysis. Therefore, in the case of PAHs, phenol and PCBs, sediment data from the lake PDI as well as the Remedial Investigation (RI) were used (in conjunction with measurements of TOC, bulk density, and porosity) to calculate porewater concentrations based on equilibrium partitioning equations for use in the modeling effort. Attachment 2 to Appendix B of this design report describes the calculation of porewater concentrations for these compounds.

Initial concentrations used in the model inputs were based on the data selection and calculation methods described above and are further detailed in Table A1.1. Based on the porewater concentration data set for each compound in each model area, empirical distributions were developed. Addendum 1 describes the approach for generating these cumulative distribution functions (CDFs) for each compound in each model area. For deterministic simulations, either the maximum value (for initial conservative screening level modeling) or the 95th percentile of the distribution was used (as described in Appendix B). Probabilistic modeling was based on sampling from the full distributions. Plots of the full distributions for each compound are provided with the electronic model input files in Appendix B Attachment 4.

1.2 Groundwater Upwelling Velocities

Appendix C to this design report details the field effort and results of the extensive groundwater upwelling investigation conducted on the lake, and describes the development of the groundwater upwelling inputs that were used in cap modeling. This work was completed to characterize the groundwater upwelling velocities that the sediment cap will be subjected to following construction.

Direct measurements of groundwater upwelling velocity were collected in most of the remediation areas, as detailed in Appendix C. Thus, the measurements of groundwater upwelling velocity collected in the capping areas of Remediation Areas A, E, and in Model Area C2 were used to generate the groundwater upwelling data sets (i.e., empirical CDFs) used in the cap modeling for those areas.

The upwelling rates used in the cap modeling for the four subareas in Remediation Area D, Model Areas B1/C1, B2, C3, WBB-West, WBB-Center, WBB-East and the WB1-8 connected wetlands were based on predictions of conditions that would exist once the upland hydraulic containment systems are in place. Estimates of these future upwelling distributions were developed based on calculations of vertical flow through the underlying silt and clay unit based on measurements of thickness, vertical hydraulic conductivity, and hydraulic gradient of that unit in each of these areas. Additional discussion is provided in Appendix C.

For all modeling areas, the specific upwelling velocities used in the model runs were based on the upwelling velocity distributions developed as described above (i.e., based on empirical data or estimated based on calculations of flow through the slit and clay unit). For deterministic simulations, the best estimate (i.e., mean value) of the distribution was used, and probabilistic modeling was based on sampling from the full distributions, as provided in Appendix C.

1.3 Consolidation Induced Porewater Expression

Settlement calculations indicate that there will be some upward expression of porewater associated with sediment consolidation due to cap placement. This porewater expression would be equivalent to an additional advective flux into the cap during the time that such consolidation occurs. That flux will occur over a relatively short timeframe, after which the long-term conditions represented by the steady-state model would prevail. For steady state model behavior, such an initial expression of porewater does not change the ultimate steady state concentration profile calculated by the model. Therefore, consolidation effects were not included in the steady state analytical modeling. Porewater expression may have a more significant impact on shorter-term performance evaluations of amended cap effectiveness, as simulated with the numerical transient modeling. Therefore, porewater expression was represented in the transient modeling of amended cap areas by adding the calculated porewater flux during the consolidation period to the base upwelling velocity (described above). Appendix E of this design report presents the basis for how predictions of settlement induced porewater expression as a function of time were developed for the purposes of the cap modeling, and Table A1.1 provides more detail on how this process was simulated in the model.

1.4 Sorption Parameters for Sediment and Sand Cap Material

As noted above, porewater concentrations within the sediment beneath the cap used for modeling were based on direct measurements of porewater concentrations, as well as calculations of porewater concentrations from sediment data and partitioning theory, as described in Section 1.1. Partitioning theory was also used to predict partitioning between porewater and sediments beneath the cap and between porewater and the cap materials. The basis for specification of the sorption parameters used in the model is summarized in Table A1.1; details are provided in Attachment 2 to Appendix B of this design report.

1.5 GAC Adsorption Parameters

Site-specific isotherms for various solid media with potential for use as an amendment material were generated for VOCs, mercury and naphthalene during the Phase IV PDI (Parsons, 2009b). Additional isotherm testing for the same list of parameters, with the addition of phenol, was conducted during the Phase VI PDI to validate the Phase IV PDI results and evaluate each isotherm point in triplicate to reduce variability (as compared to the initial testing). Screening studies conducted during the Phase VI isotherm experiments indicated a potential influence of pH on GAC sorption for some compounds. As a result, a second round of isotherms was conducted at neutral pH. Results from the Phase VI adjusted pH isotherms were generally consistent with or more conservative than the Phase IV results. Because of this and the higher levels of QA/QC employed in the Phase VI studies, the Phase VI amended pH GAC isotherms were used in the cap modeling evaluation for all cap areas within the lake and the WB1-8 connected wetlands to simulate GAC amendments, where used. Isotherm data were also generated within the Outboard Area following a similar methodology. Adjusted pH isotherms were developed based on porewater from the WBB-West area, and unadjusted isotherms were developed based on porewater from the WBB-East area. These data were used for modeling GAC amendments in these areas.

GAC isotherm data for PAHs and PCBs were not included in the scope of the site-specific evaluations. In order to model these compounds, the site-specific results for naphthalene were conservatively used to represent PAHs and PCBs. PAHs are composed of multiple benzene rings bonded in a planar configuration. With only two bonded benzene rings, naphthalene is the simplest and smallest of the PAH compounds. All other PAHs consist of greater numbers of bonded benzene rings and are therefore of higher molecular weight, larger molecular size, and greater hydrophobicity; the same is true of PCBs, as these compounds consist of two benzene rings to which between one and ten chlorine atom(s) are bonded. These characteristics all lend themselves to higher relative GAC sorbability than naphthalene. For example, in one study the equilibrium sorbed concentration values for naphthalene and phenanthrene at a water concentration of 0.1 mg/L were determined to be 50 mg/g and 80 mg/g, respectively (USEPA, 1980). Since the addition of each benzene ring (or chlorine atoms in the case of PCBs) will increase the sorptivity relative to naphthalene, applying the site-specific derived Freundlich parameters for naphthalene to the other PAHs and PCBs will yield a highly conservative modeling estimate for the GAC cap amendment.

Model inputs from the Phase VI and Outboard Area studies included site-specific Freundlich isotherm parameters (K_f and $1/n$) for each compound, as described in Table A1.1. K_f and $1/n$ values used for the deterministic simulations of each chemical were based on the best estimate for these two parameters as determined through nonlinear regression analysis of the isotherm data. A 95 percent confidence interval was also generated directly from the experimental data using joint uncertainty bounds for the two parameters in the fitted Freundlich equations (K_f , $1/n$). In order to quantify uncertainty around the best estimate of K_f and $1/n$ for the probabilistic simulations, coefficient pairs were generated by randomly sampling from within these 95 percent confidence regions.

1.6 Biological Decay

Biological degradation of organic contaminants within the chemical isolation layer is an important contaminant fate process considered in the design of the chemical isolation layer. Over time, natural biological processes will degrade organic contaminants as they slowly migrate upwards into the cap and reduce contaminant concentrations throughout the isolation layer and the overlying habitat layer. Several stages of bench-scale experiments were conducted to evaluate the rate of biological decay anticipated to occur within the cap for key compounds present in lake sediments and porewater (Parsons 2008, 2009a, 2009c, 2009d).

Rapid decay under aerobic conditions (which will occur within the upper portion of the cap's habitat layer) was consistently observed for all VOCs evaluated in the bench studies. Based on test results, anaerobic biodegradation is expected to occur within the chemical isolation layer for benzene, toluene, ethylbenzene, xylene, chlorobenzene, dichlorobenzenes, naphthalene, and phenol, provided porewater pH is 8 or less. Thus, there is evidence from the laboratory testing and in the literature that over time biological decay will occur in the isolation cap for all of the volatile organic compounds (VOCs), including naphthalene evaluated with the cap model. Given the inherent complexities in replicating long-term environmental processes in the relatively short-term investigation period, it was difficult to generate a robust data set to adequately quantify site-specific biological degradation rates for all organic contaminants of concern evaluated with the

cap model. Therefore, when simulating decay for VOCs, including naphthalene, and phenol, the rates were based on the slow end of the literature range developed during the FS (as discussed in Table A1.1). Based on the degree of variability in the results from the site specific bench testing, safety factors were applied to the FS decay rates for three CPOIs: benzene, chlorobenzene, and naphthalene (see Table A1.1). Although development of site-specific degradation rates was difficult based on the batch studies, the range of literature-based rates from the FS used in the cap model are well within the range of rates supported by the batch study results.

To account for a period of time over which a sufficient microbial community is established and acclimated such that it can achieve these decay rates within the chemical isolation layer in areas where pH is elevated above 8, a lag period before biodegradation is assumed to become effective was incorporated into the modeling. This lag period was set to 5 years in model areas with pH ≤ 8 (Model Areas A1, E1, E2 and E3) and to 100 years in areas where pH is elevated above 8 (Model Area A2, all model areas in Remediation Areas B, C, and D, WB1-8 and the WBB-West and WBB-Center areas). Degradation was conservatively excluded from the model in the WBB-East Model Area since there are a few samples in that area with elevated pH, but a pH amendment is not being included in the cap for that area.

2.0 REFERENCES

- Parsons. 2006. *Onondaga Lake Phase I Pre-Design Investigation: Porewater Methods Evaluation Report*. Prepared for Honeywell, Morristown, New Jersey and Syracuse, New York.
- Parsons. 2008. *Onondaga Lake Pre-Design Investigation: Phase IV Work Plan*. Prepared for Honeywell, Morristown, New Jersey and Syracuse, New York.
- Parsons. 2009a. *Onondaga Lake Pre-Design Investigation: Phase II Data Summary Report, Appendix J – Diffusion Sampler Equilibrium Study*. Prepared for Honeywell, Morristown, New Jersey and Syracuse, New York.
- Parsons. 2009b. *Onondaga Lake Pre-Design Investigation: Phase IV Data Summary Report*. Prepared for Honeywell, Morristown, New Jersey and Syracuse, New York
- Parsons. 2009c. *Onondaga Lake Pre-Design Investigation: Phase III Data Summary Report*. Prepared for Honeywell, Morristown, New Jersey and Syracuse, New York
- Parsons. 2009d. *Onondaga Lake Pre-Design Investigation: Phase V Work Plan*. Prepared for Honeywell, Morristown, New Jersey and Syracuse, New York.
- USEPA. 1980. *Carbon Adsorption Isotherms for Toxic Organics*. U.S. Environmental Protection Agency. EPA/600/8-80-023. April 1980.

**TABLE A1.1
MODEL INPUT PARAMETERS AND BASIS**

Model Input	Site-specific or Literature Based	Reference	Rationale
<p>Initial porewater concentration in underlying sediment:</p> <p>Fixed value (maximum concentration or 95th percentile) used for deterministic simulations.</p> <p>Distribution (CDF) used for probabilistic simulations.</p>	<p>Site-specific</p>	<p>Based on concentrations measured in porewater for the following contaminants: benzene, toluene, ethylbenzene, xylene, chlorobenzene, dichlorobenzenes, trichlorobenzenes, naphthalene, phenol, and mercury (where available).</p> <p>Porewater concentrations for the following contaminants were calculated based on sediment concentrations and equilibrium partitioning formulae: phenol, PAHs, and total PCBs (see Attachment 2). Phenol and mercury data from groundwater upwelling pumps were used, where available, to supplement these values.</p> <p>Data were selected from the following depth intervals: 1 meter above to 2 meters below the dredge cut in Remediation Area D, 0-3 m in Remediation Areas A, B, C and E, 0-5 meters in WBB-East and WBB-West/Center and 0-6 meters in WB 1-8. Correction factors were applied as appropriate (see Table A1.2). Depth intervals were selected considering the proposed dredge plan and generally include the data from above to at least two meters below the maximum dredge cut in an area which provides a robust data set and reflects the concentrations that will directly influence the cap. Modeling in sub areas was conducted around sample locations OL-VC-10138 and OL-VC-10140 in the ILWD Center; for this evaluation, data were selected from the IWD Center from 1 meter above to 3 meters below the dredge cut. <i>Honeywell Onondaga Lake Locus Database, 2010.</i></p>	<p>Spatial variability exists across the lake capping areas. The ILWD has been broken into four subareas to account for larger-scale differences in contaminant concentration distributions. Likewise, Remediation Areas A, B, C and E have each been separated into smaller Modeling Areas: A1, A2, B1/C1, B2, C2, C3 and E1, E2, E3 based on differences in porewater concentration.</p> <p>WB1-8 was modeled as a single area due to its small size and limited variation in porewater concentrations. The Outboard Area was broken into 3 areas (WBB-West, WBB-Center, and WBB-East) based on differences in porewater concentration and upwelling. Because no spatial differences in porewater concentration were observable between WBB-West and WBB-Center, the data from those two areas were combined to develop CDFs that were used in both areas.</p> <p>Probabilistic simulations were based on empirical CDFs developed from the concentration datasets for each CPOI within a given modeling area (except in the case of the sub-area probabilistic modeling conducted for location OL-VC-40197, which was based on the mean concentration at that sample location). CDFs are provided in Attachment 5. Further explanation of the</p>

Model Input	Site-specific or Literature Based	Reference	Rationale
			development of the CDFs is provided in Addendum 1.
Molecular diffusion coefficient: Fixed value	Literature	Fixed value by compound. <i>Lyman, W.J, Reehl, W.F. and Rosenblatt D.H. 1990. Handbook of Chemical Property Estimation Methods. American Chemical Society, Washington, D.C.</i>	Little to no spatial variability or uncertainty anticipated.
Hydrodynamic dispersivity: Fixed value	Literature	Conservative value fixed at 10 percent of the total cap thickness. Homogenous cap layer expected to exhibit significantly smaller dispersivity. <i>Domenico and Schwartz (1990), Physical and Chemical Hydrogeology, John Wiley.</i>	Upper bound employed, model is not sensitive to this parameter.
Partition coefficient (Koc / Kd) for isolation sand and underlying sediment: Fixed value used for VOCs in deterministic simulations (best estimate – mean value). Distribution used for VOCs in probabilistic simulations. For mercury, phenol,	Site-specific for VOCs and mercury Literature for PCBs, PAHs, and phenol	Log Koc values for VOCs (mean and standard error ¹) calculated using regression of paired sediment/porewater measurements from Phase I-VI data. Normal distribution of log Koc specified based on these values for probabilistic simulations. Paired data were also used for estimating mercury Kd's in the native sediments (for use in numerical modeling); <i>see Attachment 2.</i> No paired sediment/porewater data existed for the WB1-8 and the WBB Outboard areas, so Koc/Kd values were set equal to those estimated for lake areas based on similarities in properties (e.g., due to elevated pH conditions and presence of	The variability observed is likely due to sampling methodology and analytical limitations. To evaluate the impact of this variability, the distribution for log Koc is modeled by a normal distribution defined by the mean and standard error, with the standard error representing uncertainty about the mean value. For the literature-based values used for PAH, PCB, and phenol modeling, uncertainty was not represented, since there is no information available to estimate site-specific variation in the values derived from NYSDEC Guidance.

¹ The uncertainty in the mean is characterized by the standard error, as opposed to the standard deviation, which characterizes the variability of individual values. Therefore, distributions used in the probabilistic analysis were mostly normal or lognormal distributions developed using the mean and the standard error (= standard deviation / sqrt (number of observations)) of the data (or the log transformed data in the case of a lognormal distribution).

Model Input	Site-specific or Literature Based	Reference	Rationale
<p>PCBs, and PAHs: a fixed value was used for all simulations.</p>		<p>waste material in the WBB-West area, the Koc/Kd values were based on those from ILWD).</p> <p>Literature value used for phenol based on <i>NYSDEC Technical Guidance for Screening Contaminated Sediment (NYSDEC, 1999)</i>.</p> <p>Values used to represent partitioning to cap material for PAHs and PCBs based on NYSDEC screening guidance values; corrected literature values to represent partitioning in underlying sediment, as described in <i>Attachment 2</i>.</p> <p>Mercury partitioning coefficients for sand based on data from: <i>Reible, D, 2009. Phase IV Addendum 2 Report –Isotherm Experiments with Organic Contaminants of Concern with Sand, Organoclay and Peat and for Mercury with Sand, Organoclay, Peat and Activated Carbon.</i></p>	
<p>Porosity (isolation and habitat layers): Fixed value</p>	<p>Literature</p>	<p>Fixed value of 0.4, based on porosity testing of the capping material conducted in January 2012.</p>	<p>Little to no spatial variability or uncertainty anticipated.</p> <p>Given the relatively small percent by weight or volume of GAC that will be present in the isolation layer the value of 0.4 is also appropriate for the bulk mixed media.</p> <p>In places where the habitat layer will consist of gravel material, use of this value is also appropriate because: 1) the porosity of typical gravel material would likely only be slightly lower than this value; 2) the model is not sensitive to such small differences in</p>

Model Input	Site-specific or Literature Based	Reference	Rationale
			<p>porosity. For example, Domenico and Schwarz (1990) list the following ranges of porosity values for sands and gravels:</p> <ul style="list-style-type: none"> • Gravel, coarse: 0.24 to 0.36 • Gravel, fine: 0.25 to 0.38 • Sand, coarse: 0.31 to 0.46 • Sand, fine: 0.26 to 0.53
<p>Porosity (underlying sediment): Fixed value</p>	Site-specific	<p>Average porosity in each area modeled (A1, E1, E2, etc.) was calculated from sediment/soil samples collected in that area. <i>Honeywell Onondaga Lake Locus Database, 2010.</i></p>	<p>The critical model input parameter is the initial porewater concentration (C_0), which was either measured or calculated from sediment data. Since the calculated value is a function of sediment characteristics such as fraction organic carbon, porosity and particle density (along with sediment contaminant level), it is difficult to coherently apply distributions to all these parameters simultaneously. The decision was made to prioritize C_0, and use fixed values for the underlying sediment characteristics. Model is not sensitive to this parameter.</p>
<p>Particle density of sand cap material (un-amended isolation layer and habitat layer) and underlying sediment: Fixed value</p>	Literature	<p>Fixed value of 2.6 g/cm^3 <i>Freeze, R.A., Cherry, J.A. 1979. Groundwater. Prentice-Hall, Inc., Englewood Cliffs, New Jersey.</i></p>	<p>Little to no spatial variability or uncertainty anticipated. Model is not sensitive to this parameter. This value is appropriate for either a sand or gravel habitat layer.</p>
<p>GAC concentration in GAC amended</p>	Design parameter	<p>The transient numerical model was developed to primarily simulate a sorptive amendment as a thin layer that consists</p>	<p>Value for each amended cap area determined as part of design to establish</p>

Model Input	Site-specific or Literature Based	Reference	Rationale
<p>layer: Fixed value</p>		<p>entirely of amendment material (i.e., placement as a mat). In order to simulate a bulk mixture of sand and GAC in a single layer, the input parameters for the “active layer” in the model are specified such that the thickness of the layer equals the thickness of the bulk media, and that the specified thickness, along with the input values for “particle density”, which in this case refers to the GAC concentration (mass of GAC per unit volume of mixed media), and porosity of that layer result in the desired GAC application rate.</p> <p>For example, to achieve a GAC application rate of 0.3 lb/ ft² over a 12” layer of bulk sand and GAC, the following are specified for model inputs in that layer:</p> <ul style="list-style-type: none"> • thickness: 30.48 cm • porosity: 0.4 • GAC concentration: 0.008 g/cm³ <p>and the resulting GAC application rate is: $(0.008 \text{ g/cm}^3) * (1-0.4) * (30.48 \text{ cm}) * (1 \text{ lb} / 453.6 \text{ g}) * (30.48 \text{ cm} / \text{ft})^2 = 0.3 \text{ lb/ft}^2$</p> <p>Essentially, the input value for GAC concentration accounts only for the mass of GAC amendment in the layer. Setting the parameters in this way implicitly (and conservatively) assumes that the sand material in the amended isolation layer has no sorptive capacity.</p>	<p>recommended GAC application rate.</p>
<p>foc (sand material used for isolation layer and lower portion of habitat layer): Fixed value</p>	<p>Site-specific</p>	<p>Model input value based on the average foc of 0.022 percent (222 mg/kg) measured in samples of the sand cap material during the Phase VI PDI. <i>Honeywell Onondaga Lake Locust Database, 2010.</i></p>	<p>Little to no spatial variability or uncertainty anticipated. This value for foc is also applicable in the lower portion of the habitat layer (e.g., below the upper mixing zone). In areas where the habitat layer will consist of gravel materials, the foc is</p>

Model Input	Site-specific or Literature Based	Reference	Rationale
			anticipated to be minimal, so this value is applicable for gravel habitat layer material as well.
foc (underlying sediment): Fixed value	Site-specific	Average values calculated from individual sediment/soil sample results collected in each modeling area. <i>Honeywell Onondaga Lake Locus Database, 2010.</i>	The critical model input parameter is the initial C_0 , which was either measured or calculated from sediment data. Since the calculated value is a function of sediment characteristics such as fraction organic carbon, porosity and particle density (along with sediment contaminant level), this makes it difficult to coherently apply distributions to all these parameters simultaneously. The decision was made to prioritize C_0 , and use fixed values for the underlying sediment characteristics. Model is not sensitive to this parameter.
foc (upper 6 inches of the habitat layer in lake areas or upper 8 inches of the habitat layer in wetland areas): Fixed value (best estimate) for deterministic simulations. Distribution for probabilistic simulations.	Site-specific and literature	For lake model areas except Remediation Area A: Normal distribution based on mean and standard error of site-specific (ln-transformed) TOC data in the top 6 inches of lesser-impacted non-ILWD SMUs (SMU 4 and 5); length weighted averages were developed for cores where multiple sample intervals were collected in the top 0-6". <i>Honeywell Onondaga Lake Locus Database, 2010.</i> For wetland model areas (WB1-8, WBB-West, WBB-Center, WBB-East): average value of 10 percent was used for deterministic simulations and uniform distribution ranging from 5 to 15 percent was used for probabilistic simulations. These same values were used for modeling Remediation Area A (due to the presence of an in-lake planting habitat module over a large portion of that area) and for location-specific modeling conducted to evaluate the 25-ft wide planting areas	Inherent uncertainty exists in trying to estimate the ultimate post-remedy TOC that will be established in the upper layer of the sediment cap within the lake. Site-specific data may provide a suitable estimate of this input parameter in areas of the lake not impacted (or impacted to a lesser degree) by Metro processes and Solvay Waste materials, both of which tend to produce higher TOC values. To address the uncertainty around future TOC levels in the upper layer of the cap data in the 0-6 inches interval from SMUs 4 and 5 were used to develop a range of surficial TOC. The SMU 4/5 data do not exhibit any spatial structure and are expected to be an overestimate of post-remedy TOC given recent decreases in

Model Input	Site-specific or Literature Based	Reference	Rationale
		along the Remediation Area D shoreline. Expected range of foc in wetland soils of 5 to 15 percent is generally consistent with site-specific data (SYW-10 and Geddes Brook floodplain) as well as literature (e.g., Bruland et al. 2006). <i>Bruland, G. L., and C. J. Richardson. 2006. Comparison of soil organic matter in created, restored and paired natural wetlands in North Carolina. Wetlands Ecology and Management 14:245–251.</i>	<p>organic loading and lake productivity associated with Metro upgrades. This data set was described by a log normal distribution represented by the mean and standard error. This value for foc is based on the assumption that clean sediment will be deposited in the habitat layer over time. This assumption is not impacted by the application of a sand or gravel habitat layer material.</p> <p>Higher foc values for wetland areas based on literature and measurements in other constructed wetlands.</p>
<p>Freundlich coefficients for GAC:</p> <p>Fixed value (best estimate based on nonlinear regression of isotherm data) for deterministic simulations.</p> <p>Distribution for probabilistic simulations based on sampling from 95 percent joint confidence region.</p>	Site-specific	<p>Isotherm experiments were conducted by Carnegie-Mellon to establish sorption characteristics of the proposed activated carbon to be used. Parsons conducted a series of isotherm experiments during the Phase VI PDI to verify the Carnegie Mellon results, reduce variability through analysis of triplicate samples, and account for impacts of neutralized pH. Model inputs were based on the Phase VI isotherm data and data collected following the same methodology for the Wastebed B Outboard Area. <i>Draft Report submitted in February 2011, updated draft report provided in October 2011 which included results from WBB isotherm studies.</i></p> <p>Naphthalene isotherm parameters were conservatively used to represent isotherm parameters for PAHs and PCBs.</p>	<p>The best estimates of Kf and 1/n (as determined by nonlinear regression of the isotherm data) were used for deterministic model runs. In order to quantify uncertainty around the mean values used for Kf and 1/n, a 95 percent confidence region was generated around the means, and estimates of the coefficient pairs randomly taken from within that range were used for the probabilistic simulations. The 95 percent confidence interval was generated directly from experimental data (a two parameter (Kf, 1/n) nonlinear sorption isotherm).</p>

Model Input	Site-specific or Literature Based	Reference	Rationale
Boundary layer mass transfer coefficient: Fixed value	Site-specific	Fixed value of 0.363 cm/hr. Eqn 11 of <i>Thibodeaux and Becker, 1982 (4 m/s windspeed, 5m water depth, benzene, 500m fetch). Thibodeaux, L. J., and Becker, B., (1982). "Chemical transport rates near the sediment of a wastewater impoundments", Environmental Progress, Vol 1; no. 4, p 296-300.</i>	Little to no spatial variability or uncertainty anticipated.
Particle biodiffusion coefficient (upper mixing zone [top 6"] of habitat layer): Fixed value (best estimate) for deterministic simulations. Distribution for probabilistic simulations.	Literature	Normal distribution of log transformed values. <i>Thoms, S.R., Matisoff, G., McCall, P.L., and Wang, X. 1995. Models for Alteration of Sediments by Benthic Organisms, Project 92-NPS-2, Water Environment Research Foundation, Alexandria Virginia</i>	Uncertainty associated with size, depth and distribution of benthic organisms. Data from freshwater sites employed to generate a lognormal distribution.
Porewater biodiffusion coefficient (upper mixing zone [top 6"] of habitat layer): Fixed value (best estimate) for deterministic simulations. Distribution for probabilistic simulations.	Literature	Normal distribution based on mean and standard error of log transformed values derived from literature. <i>Wood, L.W. (1975) Role of oligochaetes in the circulation of water and solutes across the mud-water interface. Verhandlungen der Internationalen Vereinigung fur Theoretische und Angewandte Limnologie. 19: 1530-1533. Svensson, J.M., and L. Leonardson. (1996) Effects of bioturbation by tube-dwelling chironomid larvae on oxygen uptake and denitrification in eutrophic lake sediments. Freshwater Biology. 35: 289-300. Cunningham (2003) Unpublished PhD dissertation, Louisiana State University, D. Reible, Advisor.</i>	Uncertainty associated with size, depth and distribution of benthic organisms. Data from freshwater sites employed to generate a lognormal distribution.

Model Input	Site-specific or Literature Based	Reference	Rationale
<p>Darcy velocity: Fixed value (best estimate – mean value) for deterministic simulations. Distribution for probabilistic simulations.</p>	Site-specific	<p>Site-specific groundwater upwelling data used to generate an empirical cumulative distribution function for the data sets in Model Areas A1, A2, C2 and Remediation Area E (Model Areas E1, E2, and E3 combined).</p> <p>Upwelling velocities used in Remediation Areas B, C (excluding Model Area C2) D, WBB-East, WBB-Center, WBB-West, and WB 1-8 were based on the best estimate of conditions that would exist once the upland hydraulic containment systems are in place. To represent these anticipated conditions in the cap modeling, a probabilistic simulation approach was used to calculate a distribution of upwelling velocities within each modeling area. These simulated distributions were generated based on the variations in hydraulic conductivity, hydraulic gradient, and thickness of the underlying clay layer, and were found to closely follow lognormal distributions, which formed the basis of the model inputs. Further detail is provided in Appendix C.</p> <p>In all cases, the best estimate (i.e., mean value) of the distribution was used for deterministic simulations, and probabilistic modeling was based on sampling from the full distributions (empirical CDF or lognormal), as provided in Appendix C.</p>	<p>Simulation of separate sub-areas and model areas (with the exception of Remediation Area E as described below) captures major spatial variation in upwelling rate (resulting from differences in underlying clay thickness and underlying sediment/soil structure). The impacts of smaller-scale variations in upwelling within these subareas/model areas are quantified by the probabilistic results (i.e., the distribution in outputs captures measurement uncertainty as well as spatial variability).</p> <p>No significant spatial variability was observed within Remediation Area E; thus, data from the three model areas were pooled and used to specify the same CDF for each individual area. Additional discussion on groundwater data sets used in the modeling is provided in Appendix C.</p>
<p>Biological decay rate (isolation and habitat layers): Fixed value</p>	Site-specific	<p>Anaerobic biological degradation rates for VOCs including benzene, toluene, xylene, ethylbenzene, chlorobenzene, dichlorobenzene, trichlorobenzene, phenol and naphthalene based on slow end of literature range used in the FS. Based on the results of the site specific bench testing, safety factors were applied to the FS decay half lives for benzene, chlorobenzene and naphthalene (1.5, 3.0, and 2.0, respectively). Resulting decay half lives used in the modeling were as follows: benzene</p>	<p>The modeling evaluation employed literature-based degradation rates that are consistent with or more conservative than anaerobic decay rates measured in the site specific testing. Safety factors were applied to benzene, chlorobenzene and naphthalene half lives to account for variable results in the site-specific testing. Degradation was</p>

Model Input	Site-specific or Literature Based	Reference	Rationale
		<p>1,080 days, chlorobenzene 1,800 days, dichlorobenzene 720 days, ethylbenzene 228 days, toluene 365 days, trichlorobenzene 720 days, xylene 767 days, naphthalene 450 days, phenol 28 days.</p> <p><i>Howard, P.H., R.S. Boethling., W.F. Jarvis., W.M. Meylan, and E.M. Michalenko. 1991. Handbook of Environmental Degradation Rates. Lewis Publishers, Inc., Chelsea, Michigan.</i></p> <p><i>Interim Report on Phase V PDI Biotreatability Study Interim Report submitted in July 2010, results of additional testing and supplemental analysis provided to DEC via e-mail in May and June 2011.</i></p>	<p>also conservatively omitted in the WBB-East Model Area since a few porewater samples in that area indicate elevated pH, and no pH amendment is included in the cap for that area.</p>
<p>Lag time for biological decay: Fixed value</p>	Literature	<p>Lag time is used in the model to represent a period over which microbial populations capable of degrading the compounds of interest (i.e., VOCs) build up and acclimate. Lag time of 5 years was specified for areas with native pH ≤ 8; lag time of 100 years was specified for pH-amended areas.</p>	<p>Longer lag times used in pH amendment areas given expected time for pH equilibration in cap following initial consolidation period (see Appendix I).</p>
<p>Consolidation induced porewater expression: Fixed value that varies over time</p>	Site-specific	<p>For each remediation area, a power function was used to represent the cumulative consolidation-induced porewater flux over time. These functions were developed based on conservative estimates of the consolidation flux (primary and secondary) for each remediation area:</p> <ul style="list-style-type: none"> • Within non-ILWD areas, the maximum settlement magnitude and corresponding time rate of settlement within each remediation area, which takes into account the full range of sediment characteristics and consolidation parameters, was used to develop power function parameters. • For the ILWD, the consolidation flux parameters of 	<p>Values selected to represent conservative estimates of the total porewater flux associated with consolidation and timeframe over which such consolidation would occur in each remediation area based on settlement estimates, as described in Appendix E.</p>

Model Input	Site-specific or Literature Based	Reference	Rationale
		<p>the subarea within ILWD having the highest settlement estimate (using average/representative consolidation parameters within that subarea) was used for modeling of all four ILWD model areas. Model sensitivity analyses were conducted to evaluate alternate upper bound values as well (see Attachment 6 to Appendix B of this design report).</p> <p>The total consolidation used in the model ranges from 0.67 ft (Remediation Area D) to 3.1 ft (Remediation Area E). The time to reach 90 percent of those values varies from approximately 3 years (Remediation Areas A, B, and E) to around 20 years (Remediation Area D).</p> <p>The time-derivative of the resulting consolidation vs. time curve is used by the model to calculate a time-varying upwelling velocity that is added to the base-upwelling rate input to the model. This process was modeled over a 30-year timeframe (because at longer times, the incremental upwelling velocity becomes negligible).</p> <p>Details are provided in Appendix E.1 for non-ILWD areas and in Appendix E.2 for the ILWD and the Outboard Area. Consolidation in WB 1-8 was assumed to be the same as that estimated for the adjacent Remediation Area B.</p>	

**TABLE A1.2
CORRECTION FACTORS FOR POREWATER
CONCENTRATIONS**

Porewater Sample Collection Method	Correction Factor
Peepers (Phases I, II & III)	
Xylenes (total)	1.1
Chlorobenzene	1.1
Toluene	1.1
Ethylbenzene	1.1
Benzene	1.1
1,3-Dichlorobenzene (phases I & II)	1.2
1,3-Dichlorobenzene (phase III)	1.1
1,4-Dichlorobenzene (phases I & II)	1.2
1,4-Dichlorobenzene (phase III)	1.1
1,2-Dichlorobenzene (phases I & II)	1.2
1,2-Dichlorobenzene (phase III)	1.1
Naphthalene (phases I & II)	1.2
Naphthalene (phase III)	1.1
Mercury (Tuffryn)	1.1
1,2,4-Trichlorobenzene (phases I & II)	1.2
1,2,4-Trichlorobenzene (phase III)	1.1
1,2,3-Trichlorobenzene (phases I & II)	1.2
1,2,3-Trichlorobenzene (phase III)	1.1
1,3,5-Trichlorobenzene (phases I & II)	1.2
1,3,5-Trichlorobenzene (phase III)	1.1
Centrifuge (Phases I, II, III & IV)	
Xylenes (total)	1.11
Chlorobenzene	1.11
Toluene	1.08
Ethylbenzene	1.07
Benzene	1.09
1,3-Dichlorobenzene	1.10
1,4-Dichlorobenzene	1.14
1,2-Dichlorobenzene	1.15
Naphthalene	1.54
Mercury	1.06
1,2,4-Trichlorobenzene	1.45
1,2,3-Trichlorobenzene	1.53
1,3,5-Trichlorobenzene	1.07

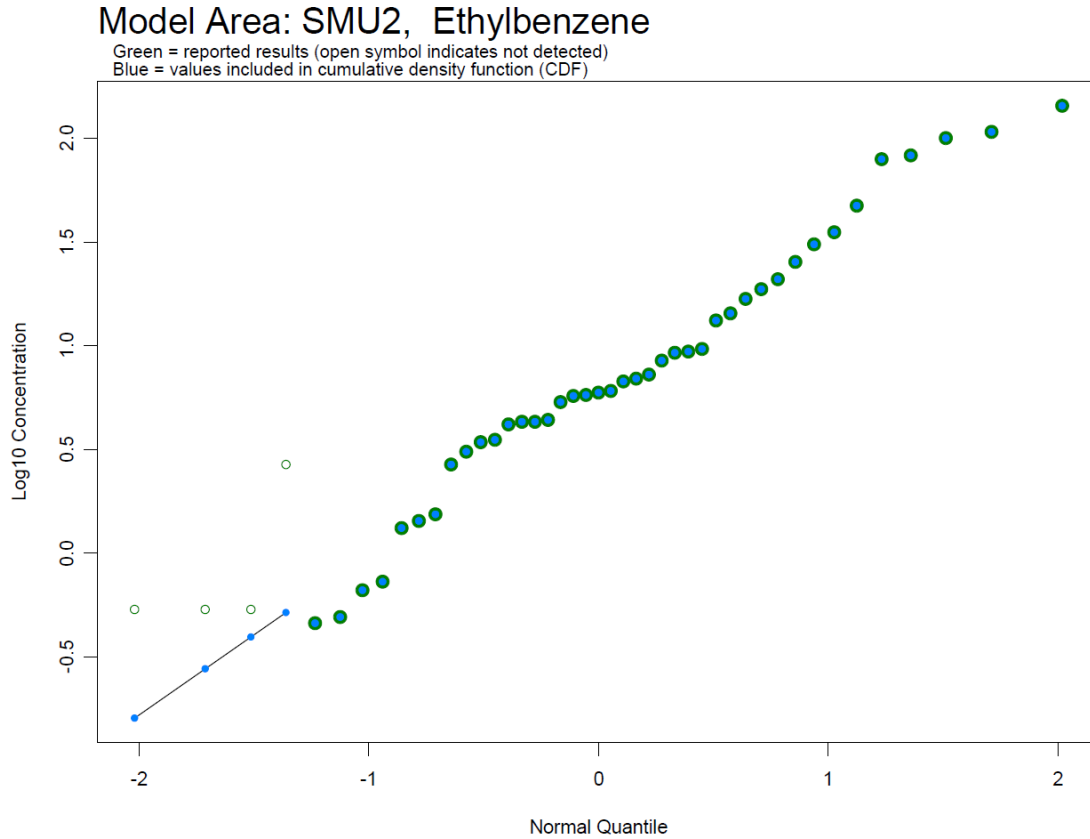
ADDENDUM 1

CUMULATIVE DISTRIBUTION FUNCTIONS FOR POREWATER CONCENTRATION

The contaminant concentrations in the porewater of the sediments underlying the cap were characterized by data collected in Onondaga Lake. There were certain cases where the presence of a relatively high proportion of non-detect results introduced uncertainty at the lower end of the concentration distribution. For example, Figure A.1 shows the distribution of ethylbenzene concentrations in SMU 2, with non-detect sample concentrations plotted at the detection limit (5 ug/L) as green open symbols. Clearly, assuming all non-detect results are equal is inappropriate, whether at the detection limit which would be overly conservative or at zero which is equally inappropriate.

The approach used to estimate the full distribution of contaminant concentrations was based on the observation that the detected concentrations generally follow a log-normal distribution (that is, the detected data are roughly linear in Figure A.1); thus a reasonable and logical assumption is that the non-detect concentrations follow this same distribution. A cumulative distribution function was derived based on the detected concentrations, and this function was then used to estimate values for the non-detect results. Specifically, a truncated log-normal distribution was fit to only the detected concentrations by fitting a linear regression to predict log-concentration from the normal z-score values (i.e., a regression through the green filled symbols was used to generate the resulting black line in Figure A.1). Z-score values were assigned assuming all of the detected concentrations were higher than the non-detect sample results. The fitted regression line was then used to predict log-concentrations for the normal z-score values attributed to the non-detect samples (see open symbols in Figure A.1). Finally, the empirical cumulative distribution function was used to characterize the distribution of porewater concentrations for the probabilistic simulations, restricted to the range of detected and estimated concentrations. This approach is recommended by Ginevan and Splitstone 2004.

Figure A.1
Ethylbenzene concentrations in the porewater of sediment from SMU2



Reference:

Ginevan, Michael E., and Douglas E. Splitstone, 2004. Statistical tools for environmental quality measurement. CRC Press LLC. p. 229.

ATTACHMENT 2

PARTITIONING COEFFICIENTS AND SEDIMENT TO

POREWATER CALCULATIONS

ATTACHMENT 2**PARTITIONING COEFFICIENT EVALUATION AND SEDIMENT
TO POREWATER CALCULATION BASIS**

Partitioning coefficients were employed in various aspects of the cap modeling evaluation to describe the equilibrium relationship between contaminant concentrations in the dissolved and sorbed-to-sediment phases within the cap materials as well as in the underlying sediments. This attachment discusses the basis for the selected partitioning coefficients as well as the calculations used to derive porewater concentrations from sediment data or vice versa.

The following sections describe the methods used to estimate partition coefficients for use in the model based on site-specific data or literature studies. Due to differences in data availability, varying methods were used to develop partition coefficients for the different classes of modeled CPOIs (i.e., VOCs, mercury, phenol, PAHs and PCBs). As such, the classes of CPOIs are discussed separately in the sections below.

1.0 PARTITIONING COEFFICIENT EQUATIONS

Partitioning coefficients, by definition, relate equilibrium porewater concentrations to sorbed-to-sediment concentrations. Since the laboratory-reported sediment concentrations for this project account for contaminants in all phases (i.e., sorbed, dissolved, vapor, and NAPL) per dry weight of sediment, the calculation of a partitioning coefficient must relate to this total sediment concentration. The partitioning equation derived from the EPA's Soil Screening Guidance (EPA, 1996) equation 22 of Part 2 (reorganized) for non-NAPL-impacted material is:

$$K_d = \frac{C_{sed}}{C_{pw}} - \frac{\theta}{\rho_b}$$

where

C_{sed} equals the total sediment concentration (dry weight) of the CPOI ($\mu\text{g}/\text{kg}$),

C_{pw} equals the core dissolved porewater concentration ($\mu\text{g}/\text{l}$),

θ is porosity, and

ρ_b is dry bulk density (kg/L).

For hydrophobic organics, the equation is:

$$K_{oc} = \frac{\left[\frac{C_{sed}}{C_{pw}} - \frac{\theta}{\rho_b} \right]}{f_{oc}}$$

where

f_{oc} is the mass fraction of organic carbon of the raw sediment.

The equation, as laid out, assumes there is no NAPL in the sample. The principal reason for doing this is that it is not possible to test for the presence of NAPL using a sample's CPOI

concentrations without first knowing the K_{oc} values. Therefore, the use of this equation would provide an overestimate of mean K_{oc} values since a NAPL-impacted sample would exhibit a higher total sediment concentration than what would be indicated by equilibrium with its porewater phase. This issue affects the assessment of sediments in SMU 1, where NAPL has been observed. However, it is not expected that the presence of NAPL in some of the samples would materially affect the overall estimates, given the large number of usable data pairs in SMU 1 and the lognormal distribution of the data.

As noted above, partition coefficients relate equilibrium porewater concentrations to sorbed-to-sediment concentrations, not to the total sediment concentration as measured in the PDI sampling program. While this distinction, which suggests it is important to account for contaminant mass in the dissolved-phase of a sample, is meaningful for low sorptivity compounds, it is not actually important for highly sorptive compounds. This is due to the fact that for highly sorptive compounds, such as PAHs and PCBs, very little contaminant mass is held in the dissolved-phase of a sediment sample. Therefore in calculating PAH and PCB porewater concentrations from measured sediment concentrations, it is only necessary to also know the f_{oc} of the sediment sample. This procedure actually adds a very small element of conservatism to the estimation of porewater concentration, since complete accounting for the dissolved-phase mass in the sample would lower the estimate of porewater concentration.

For PAHs and PCBs, the equation for calculating the local porewater concentration is:

$$C_{pw} = \frac{C_{sed}}{K_{oc} \cdot f_{oc}}$$

2.0 DEVELOPMENT OF SITE SPECIFIC PARTITIONING COEFFICIENTS FOR VOCs

The analysis of paired sediment and porewater samples, generated via centrifugation procedures in Phases I through VI of the PDI, provided an opportunity to estimate site-specific partitioning coefficients for Onondaga Lake sediments, in the form of an organic carbon-water partitioning coefficient (K_{oc}) for Benzene, Toluene, Ethylbenzene, Xylene, Tri-chlorobenzene, Di-chlorobenzene, chlorobenzene and naphthalene. This section describes the sample processing procedures, and the calculations and analysis methods used to estimate the partitioning coefficients from the sample data (including filtering of the dataset to eliminate unusable results). Results are presented in graphical and tabular formats. The site specific partitioning coefficients generated as described in the following subsections were used in cap modeling to predict partitioning within the sand cap materials used in the chemical isolation and habitat layers, as well as within the underlying sediments for the numerical modeling.

2.1 SAMPLE COLLECTION AND PROCESSING

In Phase I of the PDI, samples of sediment and porewater were collected at 33 locations in SMU 1 and SMU 6. No paired sampling was conducted in Phase II for the purpose of estimating partitioning coefficients. The total number of sample pairs was greatly increased by work

conducted in Phases III through IV. In total over 1,000 samples pairs were collected across the remediation areas over the course of the PDI.

In Phase I, three cores were collected at each location and depth interval to provide material for sediment and porewater analyses. Upon receipt in the lab, the cores were opened and freestanding water decanted and discarded. No homogenization of sediments occurred. One core was used for raw sediment analysis, and the other two were used to fill between four and six centrifuge bottles, which were then centrifuged to generate porewater. All generated porewater was then composited prior to sub-sampling for the various analyses. One of the centrifuged bottles provided material for the dewatered sediment analysis. A sample pair from Phase I, for the purposes of calculating partition coefficients, was comprised of a dewatered sediment sample and an associated porewater sample.

In Phases III through VI, long cores were cut into 2-ft. sections. Upon receipt in the lab the 2-ft. cores were opened, and freestanding water carefully decanted for compositing with porewater subsequently generated by centrifugation of the sediment sample. A portion of the sediment sample from the top of the core was sub-sampled for raw sediment analyses. The balance of the sediment from the 2-ft. core was weighed and placed in centrifugation bottles. The sample bottle was centrifuged and supernatant water was separated and collected. The aqueous sample for volatile organic compounds (VOCs) was then centrifuged again, decanted and placed in volatile organic analyte (VOA) vials for analysis. A sample pair from Phases III through VI, for the purposes of calculating partition coefficients, was comprised of a raw sediment sample and an associated porewater sample.

2.2 AREA-WIDE PARTITION COEFFICIENT ANALYSIS

The partition coefficients estimated from the site data used in the cap modeling effort were developed based on the hypothesis that a single mean partition coefficient could be used to describe the site data within a given area, and that sample-to-sample differences within these areas stem primarily from measurement variability. This is consistent with the fact that partition coefficients are often taken to be chemical-specific properties (after properly normalizing for organic carbon content as appropriate). To estimate the effective partition coefficient for an area containing numerous sediment-porewater sample pairs, the sorbed-to-sediment phase concentration was first calculated for each sample pair. This concentration was calculated by taking the reported total dry weight concentration (C_{sed} in the equations above) and subtracting off the porewater mass (using the measured corrected porewater concentration (see Table A1.2), bulk density, and porosity):

$$C_s = C_{sed} - \left(C_{pw} \frac{\theta}{\rho_b} \right)$$

where C_s is the sorbed-to-sediment phase concentration of a CPOI ($\mu\text{g}/\text{kg}$).

After calculating Cs for all samples within an area, the concentrations were normalized by foc and plotted against their paired porewater concentrations. Plotting these values against porewater concentration in linear space produces a relationship with a slope that is equivalent to Koc. Thus, a least squares regression analysis can be used to calculate the Koc for a given area (and the confidence interval of the regression line can describe its variability). Preliminary analyses indicated that such regressions could be strongly influenced by the highest concentration data pairs. Given that porewater concentrations within the cap would be expected to be within a lower range, the underlying regression equation ($Cs/foc = Koc * Cpw$) was log-transformed to remove the effect of a few high concentration samples driving the regression and therefore all measurements were treated as having the same standard error. By doing this, it was equivalent to the model: $\log(Cs/foc) = \log(Koc) + \log(Cpw)$. Least squares regression formulae were derived for this case, which produced a best estimate of log Koc and an associated standard error. The log-transform was judged appropriate since Koc values are typically found to be lognormally distributed (and are hence typically reported as log Koc).

For the cap modeling effort, the analysis method described above was used to estimate a Koc value for each modeled VOC. The data from Remediation Areas A and E were pooled together, and data from Remediation Area D were analyzed separately since previous analyses had suggested partitioning within ILWD materials differs from that in sediments from other areas of the lake. Data from Remediation Areas B and C were compared with these two groupings and found to exhibit a relationship between particulate and dissolved phase that more closely resembled that of the ILWD. As such, the data from Remediation Areas B, C, and D were combined for the purposes of calculating Koc values for the VOCs. Koc values were also required for modeling of the Wastebed 1-8 connected wetlands (referred to hereafter as WB1-8) and in the three model areas of the Wastebed B Outboard area (referred to hereafter as WBB-West, WBB-Center, and WBB-East). No paired sediment/soil and porewater samples were collected during the investigations conducted in these areas. Therefore, Koc values for these areas were assigned based on those developed from areas of the lake having similar sediment characteristics.

2.3 FILTERING OF DATA PAIRS

After compiling the data from PDI Phases I through VI, any data pair (sediment and porewater) which involved a non-detect result was excluded from the analysis, given the uncertainty of the resulting calculation. Additionally, any result which produced a negative value for the sorbed-to-sediment concentration from the above equation was deleted. This would occur when the CPOI mass measured in the porewater phase exceeded the total CPOI mass measured in the bulk sediment (i.e., solids plus porewater). Since such a scenario—where the total contaminant mass (bulk sediment concentration) is insufficient to produce the measured mass in the dissolved-phase (porewater concentration)—is not possible, even though the analytical results support it, the assumption is that there is some error in one or more of the analyses, and therefore the data pair does not allow for calculation of a partitioning coefficient. Such occurrences were rare ($\approx 8\%$ of sample pairs), with nearly half involving benzene, the least sorptive of the compounds considered in this analysis.

In an effort to assess the potential effects of surface water on porewater concentrations in the surficial samples, the data set was also sorted and samples collected in the 0-1 ft interval were eliminated.

2.4 RESULTS

Following the filtering step described in Section 2.3, the log-transformed regression analyses described in Section 2.2 were conducted. Figures 1 through 12 present these regressions, the resulting Koc values, and standard errors (derived from the confidence limit on the regression line). The data and regression lines on Figures 1-12 indicate that while there is scatter in the data (the degree to which varies by CPOI), when taken together, data from Areas A/E and from Areas B/C/D exhibit a relatively consistent relationship between sorbed-to-sediment and porewater concentrations, with standard errors of regression equal to or less than 0.1 log units (for CPOIs with at least 50 sample pairs or more). The presence of such a relationship is consistent with the concept of the area-based approach used in this analysis. The resulting Koc values tend to differ between Areas B/C/D and Areas A/E, with the former group's values being somewhat higher (on average approximately one-third of a log value across CPOIs) – this difference is consistent with results from previous analyses and likely attributable to the effects of elevated pH within the ILWD materials and/or differences related to the solid matrix of waste material versus natural sediment.

For each CPOI, Table 1 presents the number of data pairs, the resulting Koc values and associated standard errors, and includes a comparison to a range of literature values. The differences in resulting Koc values among these CPOIs follow expected trends (e.g., Koc of chlorobenzenes increases with chlorination level from monochlorobenzene to dichlorobenzenes to trichlorobenzenes), and the calculated values are within the range of the literature values.

As such, the values listed in Table 1 for Areas A/E were used to describe the partitioning of VOCs to sand capping materials in all model areas. These same values were used to simulate partitioning of VOCs within the underlying sediment in the application of the numerical model to Remediation Areas A and E, as well as the WBB-East area, which is similar to these two lake

areas in that there is limited to no impact from ILWD-like materials. Likewise, the Koc values estimated from the Remediation Area B/C/D data set were used to describe partitioning within the underlying sediment/waste materials within those areas, for use in the transient numerical modeling. These values were also used in transient modeling of the underlying sediment in WB1-8, WBB-Center, and WBB-West, because the soil/sediments in these areas are similar in nature to those in the ILWD. The differences in Koc between ILWD and non-ILWD materials are believed to be due to elevated pH and/or solid matrix differences between ILWD materials and natural sediment as discussed above; however, the Koc values derived from non-ILWD data were used to simulate sorption to sand capping materials within the ILWD, Remediation Areas B and C, and Model Areas WB1-8, WBB-West, and WBB-Center because the pH amendment to the cap is designed to lower pH in the isolation layer. Thus, the amended cap approach within these high pH areas is designed to eliminate these effects and result in partitioning behavior within the isolation layer that is consistent with that in other capped areas of the lake.

2.5 MERCURY PARTITIONING COEFFICIENTS

Unlike VOCs, the partition coefficients used for simulating mercury were expressed as a Kd value, since organic carbon is not the only significant sorbing phase for mercury. The values used in the cap modeling conducted for mercury were developed as follows:

- Kd values for the underlying sediment (used in the transient numerical modeling) were calculated from the values for paired sediment / porewater data (i.e., using the data sets/filtering methods described above for VOCs), and the average log Kd for each area was used in the model. This simpler method for calculating the sediment Kd (as compared to the regression-based approach used for VOCs) was used since this parameter only describes the partitioning within the underlying sediment in the numerical model, which has much less influence on predicted concentrations in the cap than the Kd values used to describe partitioning onto capping materials (which are described below). Separate values for the underlying sediment log Kd were calculated for Remediation Areas A, B/C, D, and E, and are presented in Table 2. For the model areas lacking paired sediment-porewater data, underlying sediment mercury Kd values were assigned based on those calculated from data in areas having similar characteristics. Specifically, the Kd for WB1-8 was set equal to that calculated from Remediation Area B and C sediment data, the Kd for WBB-West and WBB-Center was set equal to that calculated from Remediation Area D sediment data, and the Kd for WBB-East was set equal to the average of those calculated from Remediation Area A and E sediment data (due to the generally lower pH and limited to no impact from ILWD-like materials in these areas). The variation in estimated Kd values among these Remediation Areas is believed to reflect differences in the nature of the materials, including elevated pH.
- Kd values for sorption of mercury onto sand capping material in Remediation Areas A and E and in the WBB-East Model Area were estimated based on the data from isotherm studies conducted using porewater from SMU 6/7 sediments (Parsons, 2008). These data were found to best be described by a Freundlich isotherm equation

(Parsons, 2008). As such, the best fit SMU 6/7 isotherm equation was used to calculate a K_d based on the maximum measured porewater concentration in each applicable modeling area. This approach is conservative because at the lower concentrations that would be present in the cap (as compared to the maximum underlying porewater concentration), the SMU 6/7 isotherm relationship produces K_d values that are higher than those calculated for that maximum porewater concentration (thus resulting in even slower transport). The resulting log K_d values for each applicable modeling area (i.e., Model Areas A1, A2, E1, E2, E3, and WBB-East) are presented in Table 2.

- K_d values for sorption onto sand capping material in areas impacted by ILWD-like materials and elevated pH conditions (i.e., Remediation Areas B, C, and D and the WB1-8, WBB-West, and WBB-Center Model Areas) were derived from data generated from isotherm studies performed with SMU 1 porewater (Parsons, 2008). These data were found to follow a linear relationship, so a regression-based approach was used, in which the slope of a linear regression line fit through a plot of sorbed-to-sediment phase mercury concentrations versus porewater concentrations was used to estimate the K_d . The resulting log K_d value is presented in Table 2.

In areas where the isolation cap material will consist of sand mixed with activated carbon as a sorptive amendment, the K_d values described above do not account for any increased sorption of mercury that may occur as a result of the amendment.

3.0 PHENOL PARTITIONING COEFFICIENT

Site-specific porewater data for phenol were limited given the large volumes required or analysis. Additionally, sediment-porewater pairs were not available for the direct estimate of a phenol partitioning coefficient. In lieu of a site specific K_{oc} value the NYSDEC Technical Guidance (NYSDEC, 1999) value for phenol was used to describe partitioning of phenol to both the underlying sediment, to supplement existing porewater data, and to simulate partitioning to the cap material. Similar to VOC compounds, phenol partitioning in the cap model is simulated through use of a K_{oc} value. The Technical Guidance document directly provides an octanol/water partition coefficient or K_{ow} . The Technical Guidance suggests that when applying the equilibrium partitioning methodology K_{oc} and K_{ow} values are very similar, for unchlorinated phenol the Log K_{ow} value is 2.0 (NYSDEC, 1999). This value was used for phenol in all model simulations.

4.0 PCB AND PAH PARTITIONING COEFFICIENTS

Site specific porewater data were not available for PAH and PCB model simulations. Porewater collected during the 2002/2003 groundwater upwelling investigation were mostly non-detect for PAHs and PCBs (Parsons, 2003 and Parsons, 2007). In the absence of site-specific data for PAHs and PCBs a literature review of partitioning of these compounds was conducted. This information was used to calculate initial porewater concentrations in model simulations as well as to describe partitioning to cap materials.

Modeling conducted during the Feasibility Study had used Kow values reported in New York State Department of Environmental Conservation Guidance (NYSDEC, 1999) as estimates of Koc and measured foc values to estimate the concentrations of PAHs and PCBs in sediment porewater beneath the cap. This same approach was taken in the here when modeling fate and transport of PAHs and PCBs within the sand capping material; however, a growing body of literature indicates that the conventional approach of calculating PAH and PCB porewater concentrations in underlying sediments will overestimate actual PAH or PCB porewater concentrations (for discussions see Arp et al., 2009; Hawthorne et al., 2006; and McGroddy et al., 1996). The primary cause of this discrepancy is that natural sediments are composed of different types of organic carbon, with some phases of organic carbon (“hard” carbon, generally derived from anthropogenic sources) sorbing hydrophobic contaminants stronger but more slowly than other phases (“soft” carbon, generally natural organic matter). For purposes of calculating initial porewater concentrations in the underlying sediment, measured foc values and field-derived effective Koc values measured in natural sediment at other sites that account for strongly-sorbing carbon fractions of sediment, were used. Addendum 1 provides a detailed description of the literature review and partitioning coefficient recommendations.

Recommendations from the evaluation presented in Addendum 1 support the use of corrected PAH and PCB Koc values to most accurately model and predict porewater PAH and PCB concentrations within the underlying Lake sediment in the absence of direct measurements. Based on the data presented in Addendum 1 an increase in effective Koc values of 10X from PAH Kow values is recommended for derivation of PAH porewater concentrations in the non-ILWD impacted sediments (which was taken to consist of Remediation Areas A and E, as well as the WBB-East Model Area). Likewise, based on the data presented in Addendum 1, an increase in effective Koc values of 5X from PCB Kow values is recommended for derivation of PCB porewater concentrations in the non-ILWD impacted sediments. Effective Koc values are based on the values presented in the NYSDEC Technical Guidance. Partitioning in the underlying sediments of the ILWD and within Remediation Areas B and C and the WB1-8, WBB-West, and WBB-Center Model Areas is based directly on the Technical Guidance values, as the presence of ILWD-like material and the unusual pH and DOC conditions in those areas create conditions at variance with natural sediments and so are not addressed by the literature cited above. Partitioning to the cap material is simulated in the model using uncorrected values from the Technical Guidance. Fixed values were used for PAHs and PCBs in all model simulations.

5.0 REFERENCES

- NYSDEC, 1999. Technical Guidance for Screening Contaminated Sediments. January 1999.
- Parsons, 2003. Groundwater Upwelling Investigation for Onondaga Lake, Syracuse New York. Prepared for Honeywell, Morristown, New Jersey. Syracuse, New York.
- Parsons, 2007. Onondaga Lake Pre-Design Investigation, Phase I Data Summary Report. Prepared for Honeywell, Morristown, New Jersey. Syracuse, New York.

Parsons, 2008. Onondaga Lake Pre-Design Investigation: Phase IV Work Plan - Addendum 2 Cap Amendment Isotherm Development. Prepared for Honeywell, Morristown, New Jersey. Syracuse, New York.

USEPA, 1996. Soil Screening Guidance: Technical Background Document, Part 2, page 36, EPA/540/R-95/128, May 1996.

TABLES

Table 1. Summary of log K_{OC} values determined by regression analysis, compared to literature-based values.

	Model Areas B,C, and D			Model Areas A & E			Range of log K _{OC} from regression-based formulas in literature ¹		Range of log K _{OC} from published studies (Mackay, et al.) ²	
	No. of data pairs	log K _{OC}	std error of regression	No. of data pairs	log K _{OC}	std error of regression	Min	Max	Min	Max
Benzene	192	1.78	0.040	131	1.69	0.051	1.63	1.97	1.26	2.01
Toluene	278	2.34	0.030	140	2.18	0.059	2.31	2.64	2.25	2.39
Ethylbenzene	187	2.77	0.041	127	2.59	0.045	2.77	3.10	2.21	
Xylene	306	2.76	0.029	188	2.53	0.046	2.77	3.10	2.22	2.52
Chlorobenzene	197	2.51	0.037	143	2.29	0.056	2.46	2.79	1.92	2.73
1,2-Dichlorobenzene	191	3.00	0.036	77	2.64	0.073	3.00	3.32	2.26	3.51
1,3-Dichlorobenzene	14	2.77	0.20	126	2.72	0.066	3.00	3.32	2.14	4.60
1,4-Dichlorobenzene	200	3.08	0.038	99	2.60	0.068	3.00	3.32	2.78	3.26
1,2,3-Trichlorobenzene	7	3.67	0.15	1	3.21	--	3.87	4.19	2.30	4.70
1,2,4-Trichlorobenzene	39	3.54	0.057	32	2.82	0.141	3.87	4.19	3.09	4.70
1,3,5-Trichlorobenzene	--	--	--	52	3.05	0.100	3.87	4.19	2.85	5.10
Naphthalene	331	2.86	0.032	114	2.47	0.077	2.99	3.31	2.66	5.00

Notes:

1. Range from several representative regression formulas that correlate K_{OW} to K_{OC} (log K_{OW} values presented in Table 1 of NYDEC's *Technical Guidance for Screening Contaminated Sediments* (http://www.dec.ny.gov/docs/wildlife_pdf/seddoc.pdf) were used).

These formulas were pooled from the following studies:

- DiToro, D.M., 1985. A Particle Interaction Model of Reversible Organic Chemical Sorption. *Chemosphere* 14 :1503-1538.
- Karickhoff, S.W., 1981. Semi-empirical estimation of sorption of hydrophobic pollutants on natural sediments and soil. *Chemosphere* 10: 833-846.
- Means, J.C., S.G. Wood, J.J. Hassett and W.L. Banwart, 1980. Sorption of polynuclear aromatic hydrocarbons by sediments and soils. *Environmental Science & Technology* 14: 1524-1528.
- Shimizu, Y., S.Yamazaki and Y. Terashima, 1992. Sorption of anionic pentachlorophenol (PCP) in aquatic environments: The effect of pH. *Water Science & Technology* 25: 41-48.

2. Range of values taken from *Illustrated Handbook of Physical-Chemical Properties and Environmental Fate for Organic Chemicals*, Donald Mackay, Wan Ying Shiu, and Kuo Ching Ma, 1992. Only values from studies utilizing field measurements were included.

Table 2. Summary of log K_d values for Mercury.

	Mercury log K_d	
	Underlying Sediment	Sand Cap
Model Area A-1	4.7 ¹	3.3 ³
Model Area A-2		2.8 ³
Remediation Areas B & C	2.5 ¹	3.1 ⁴
Wastebed 1-8 Wetland	2.5 ²	
Remediation Area D	3.1 ¹	
WBB Outboard Area West and Center	3.1 ²	
WBB Outboard Area East	4.4 ²	4.0 ³
Model Area E-1	4.2 ¹	3.3 ³
Model Area E-2		3.8 ³
Model Area E-3		3.2 ³

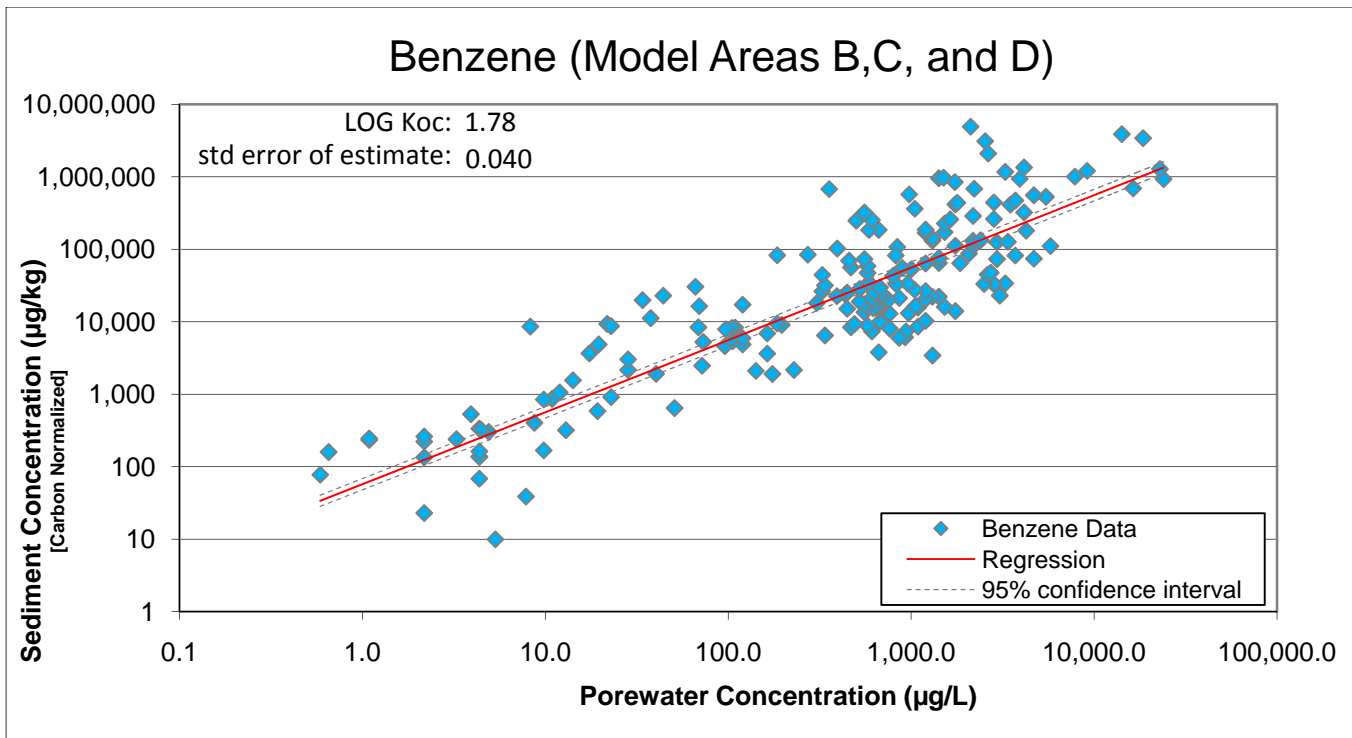
Notes:

1. Values calculated from paired sediment and porewater data.
2. Values assigned based on data from other lake areas having similar characteristics.
3. Values calculated based on isotherm developed from testing of SMU 6/7 porewater and max. measured porewater concentration in given area.
4. Value based on isotherm developed from testing of SMU 1 porewater.

FIGURES

**Relationship between porewater concentration and
carbon-normalized sediment concentration
(with log-transformed regression)**

BENZENE – Model Areas B, C, and D



BENZENE – Model Areas A & E

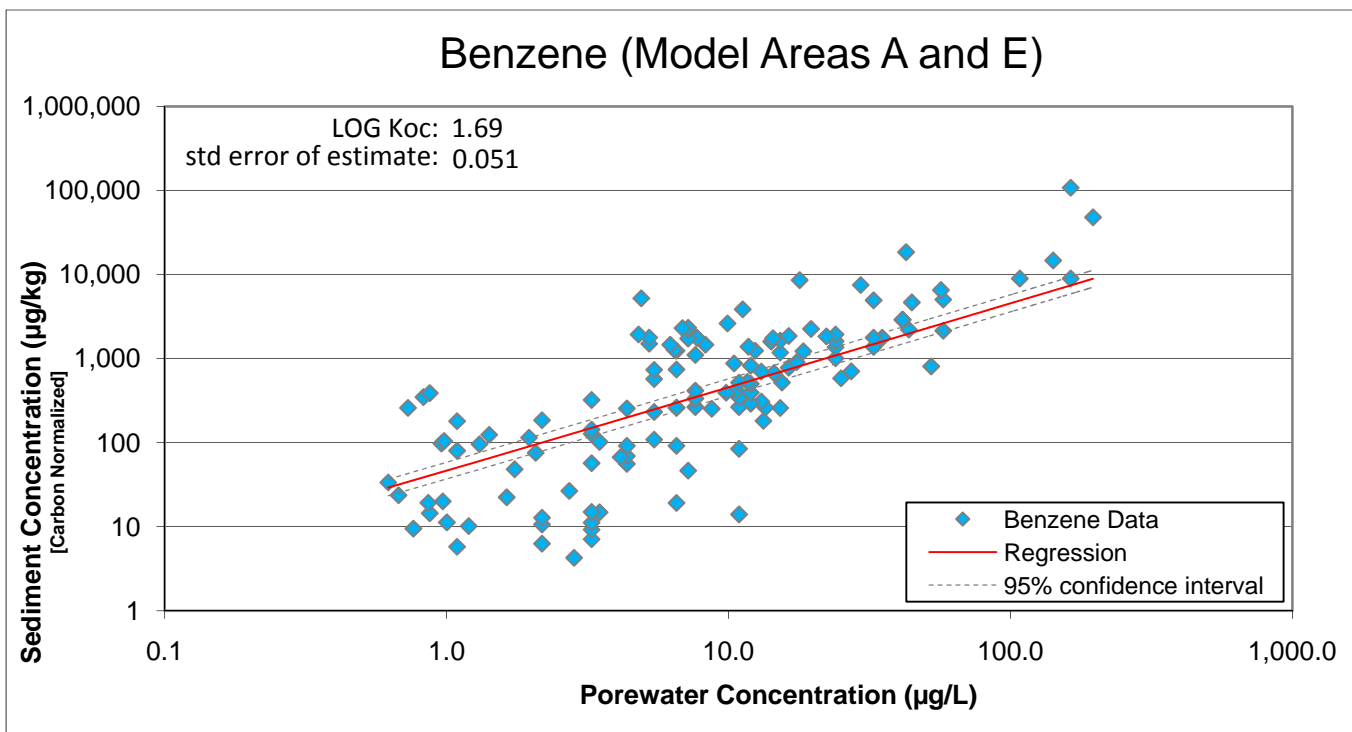
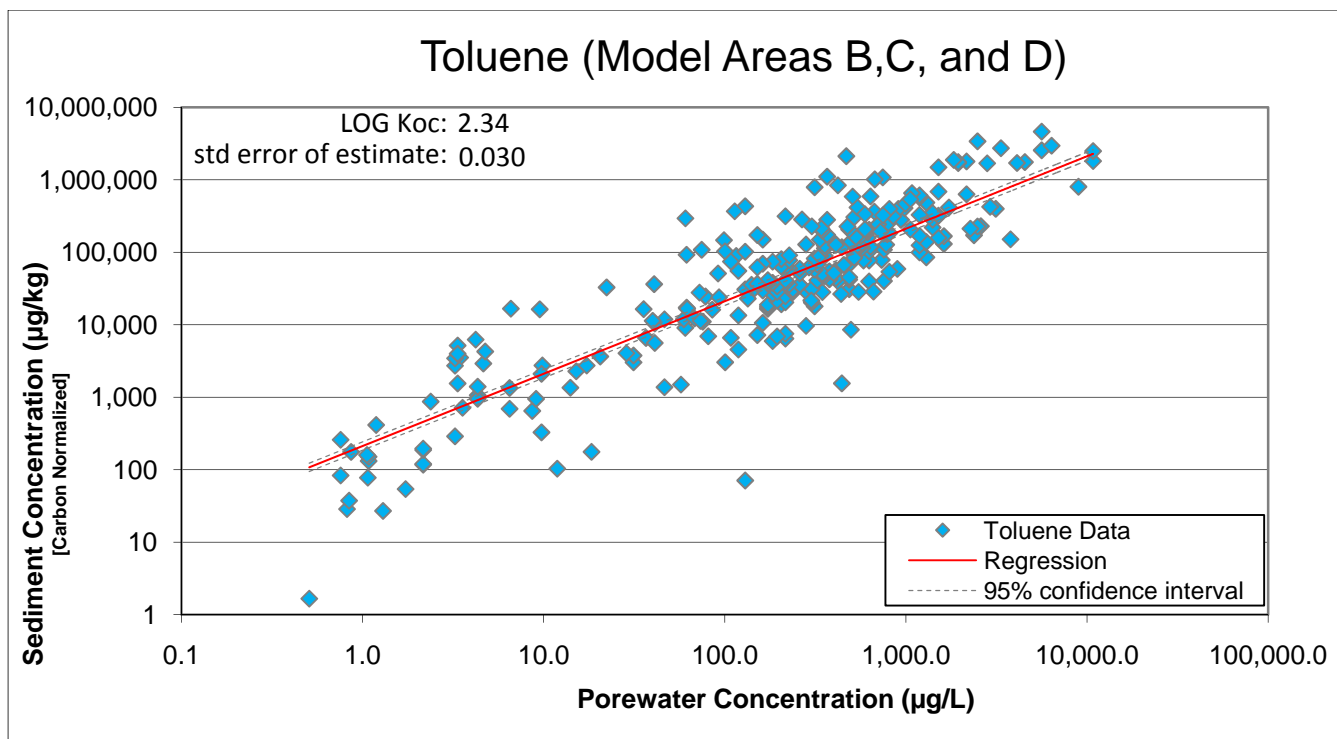


Figure 1. Relationship between *benzene* porewater concentration and carbon-normalized sediment concentration (with log-transformed regression).

TOLUENE – Model Areas B, C, and D



TOLUENE – Model Areas A & E

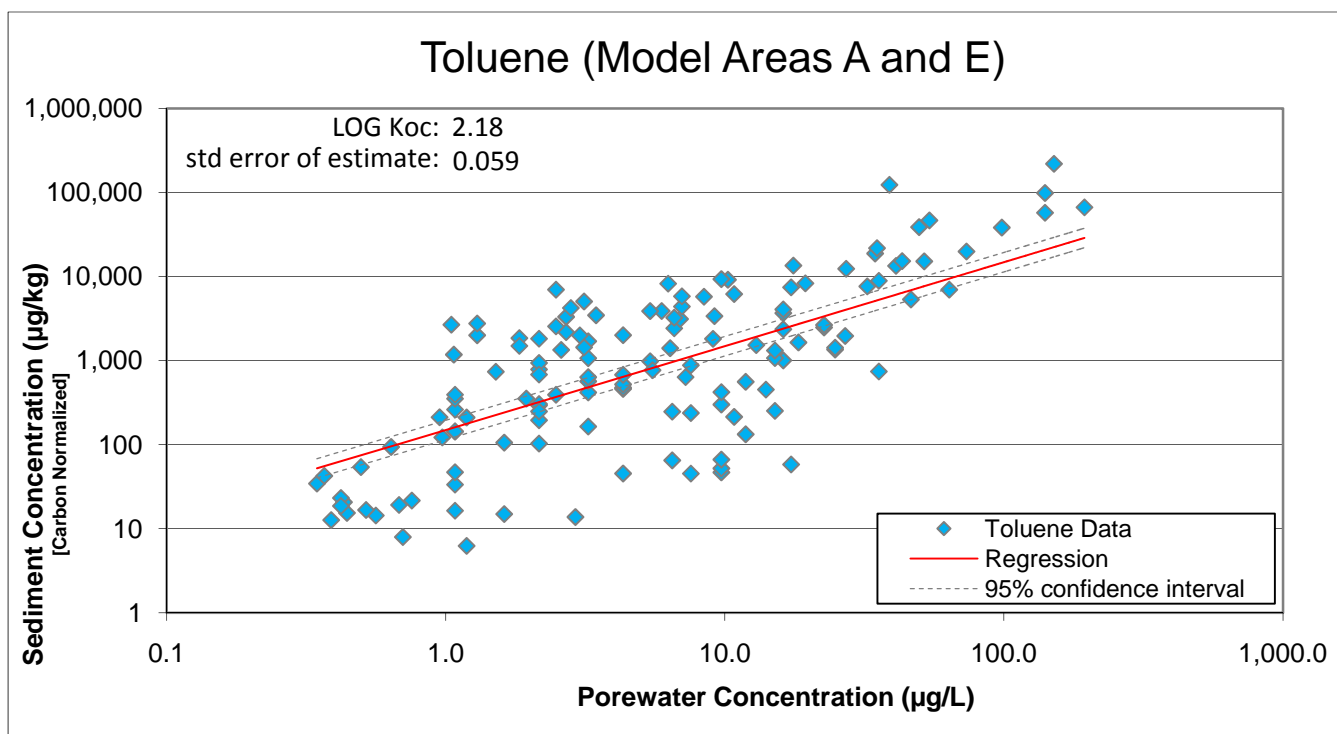
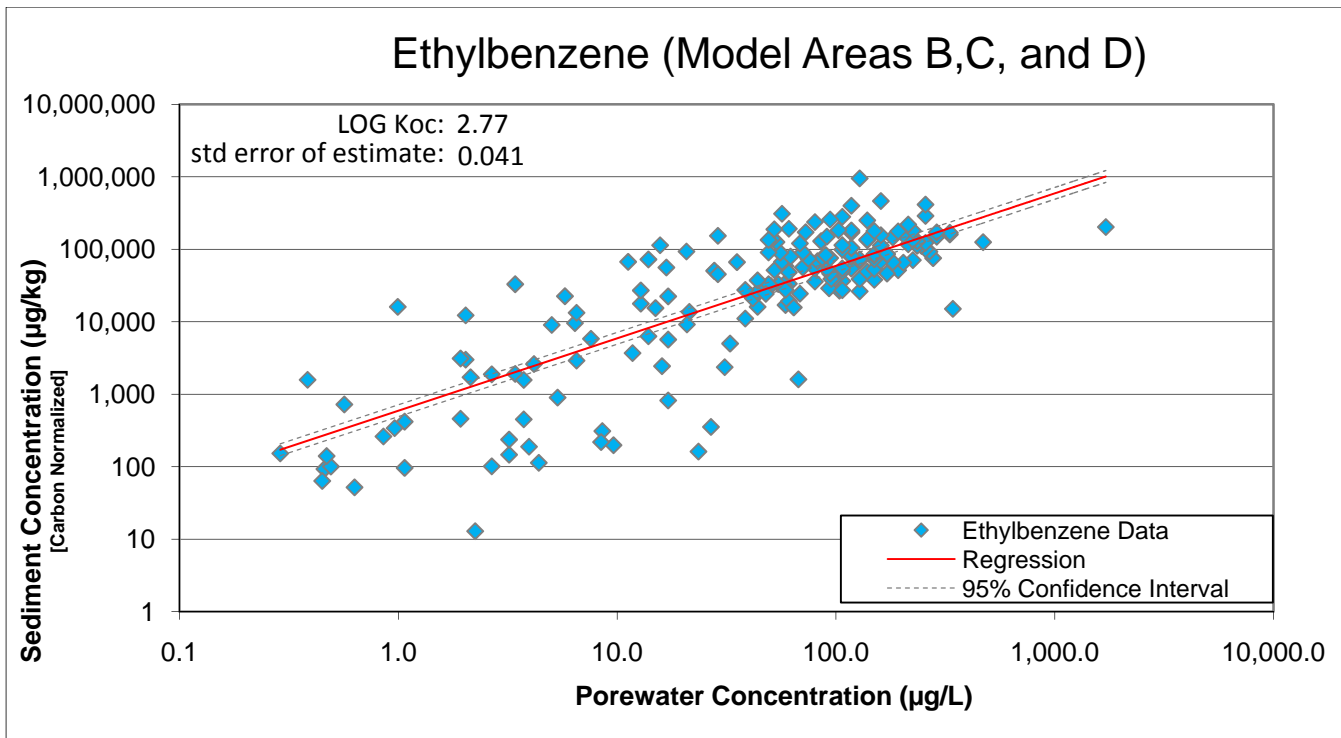


Figure 2. Relationship between *toluene* porewater concentration and carbon-normalized sediment concentration (with log-transformed regression).

ETHYLBENZENE – Model Areas B, C, and D



ETHYLBENZENE – Model Areas A & E

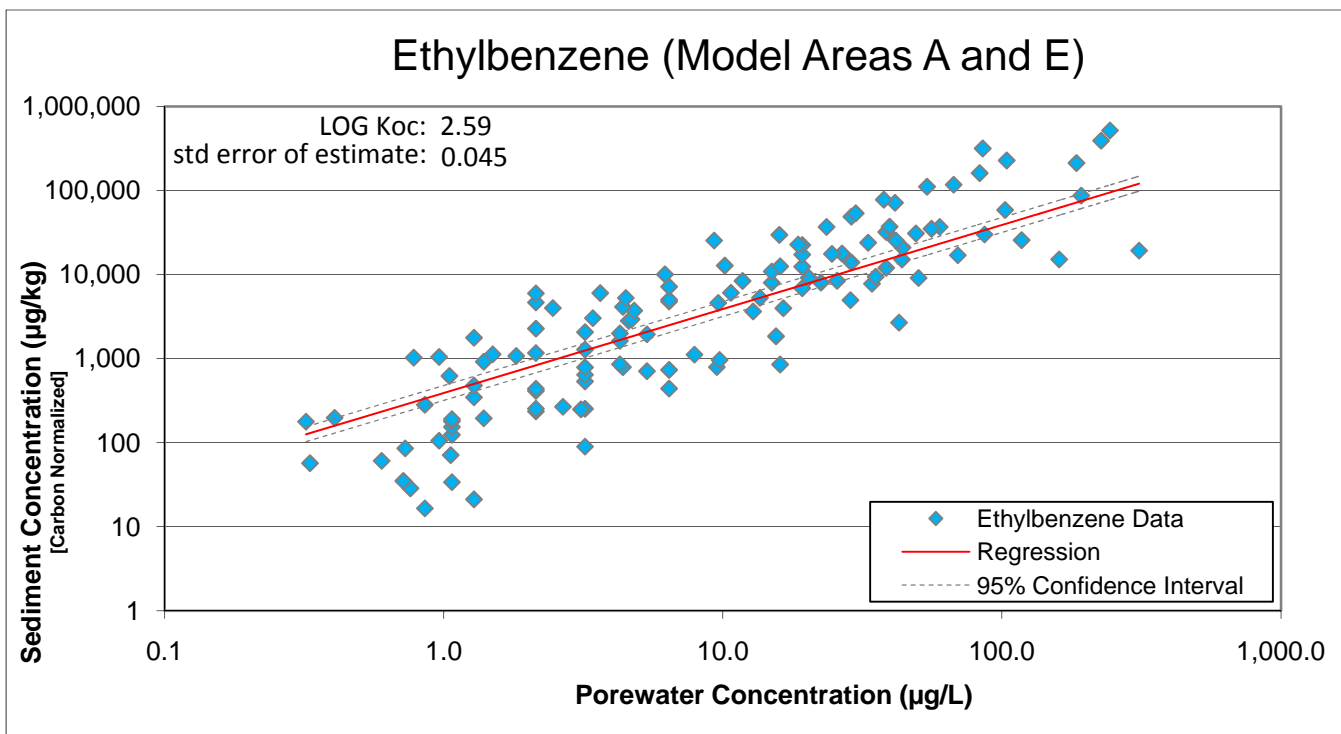
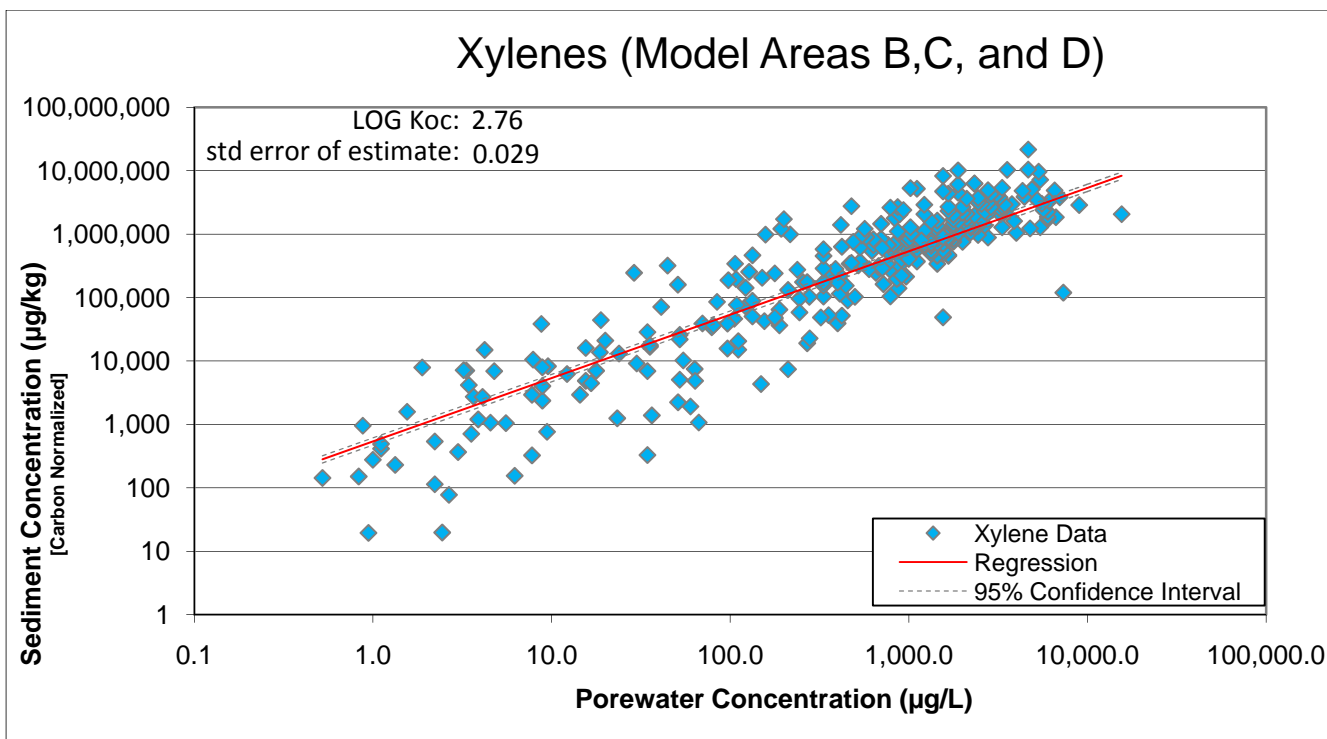


Figure 3. Relationship between *ethylbenzene* porewater concentration and carbon-normalized sediment concentration (with log-transformed regression).

XYLENE – Model Areas B, C, and D



XYLENE – Model Areas A & E

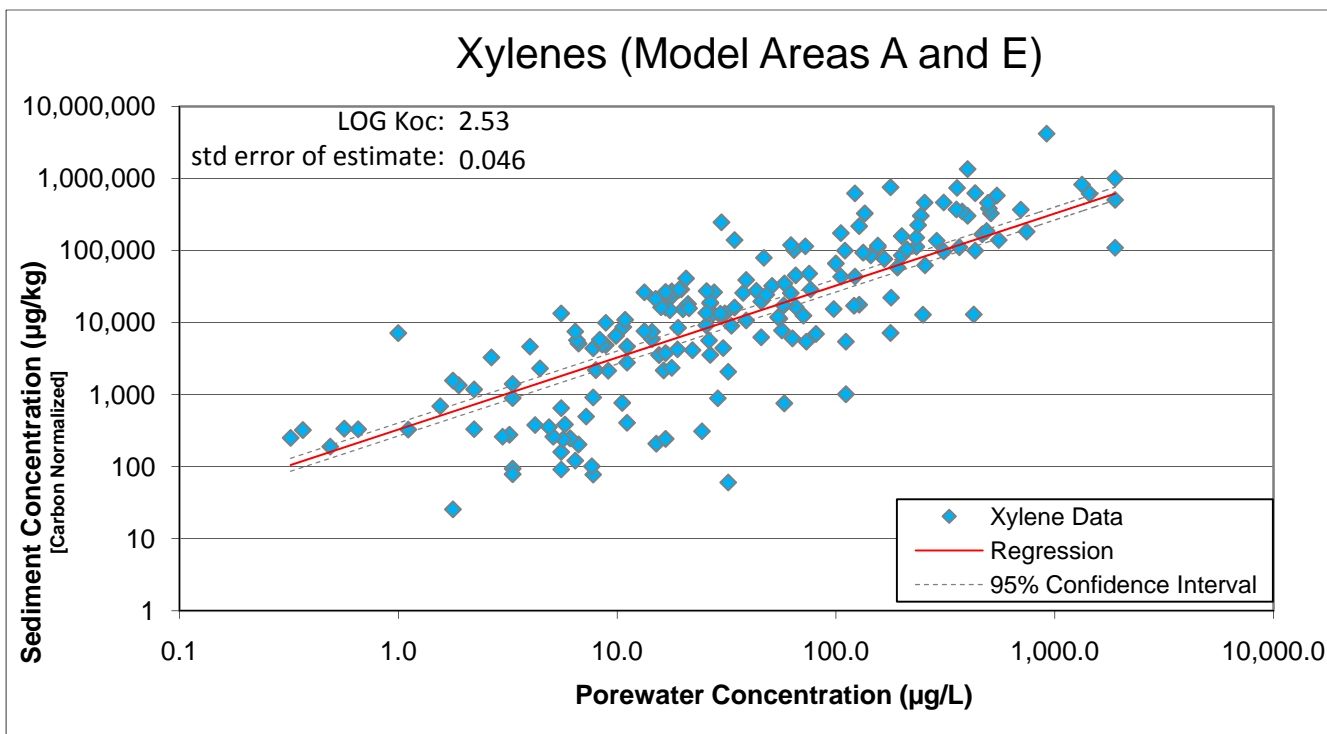
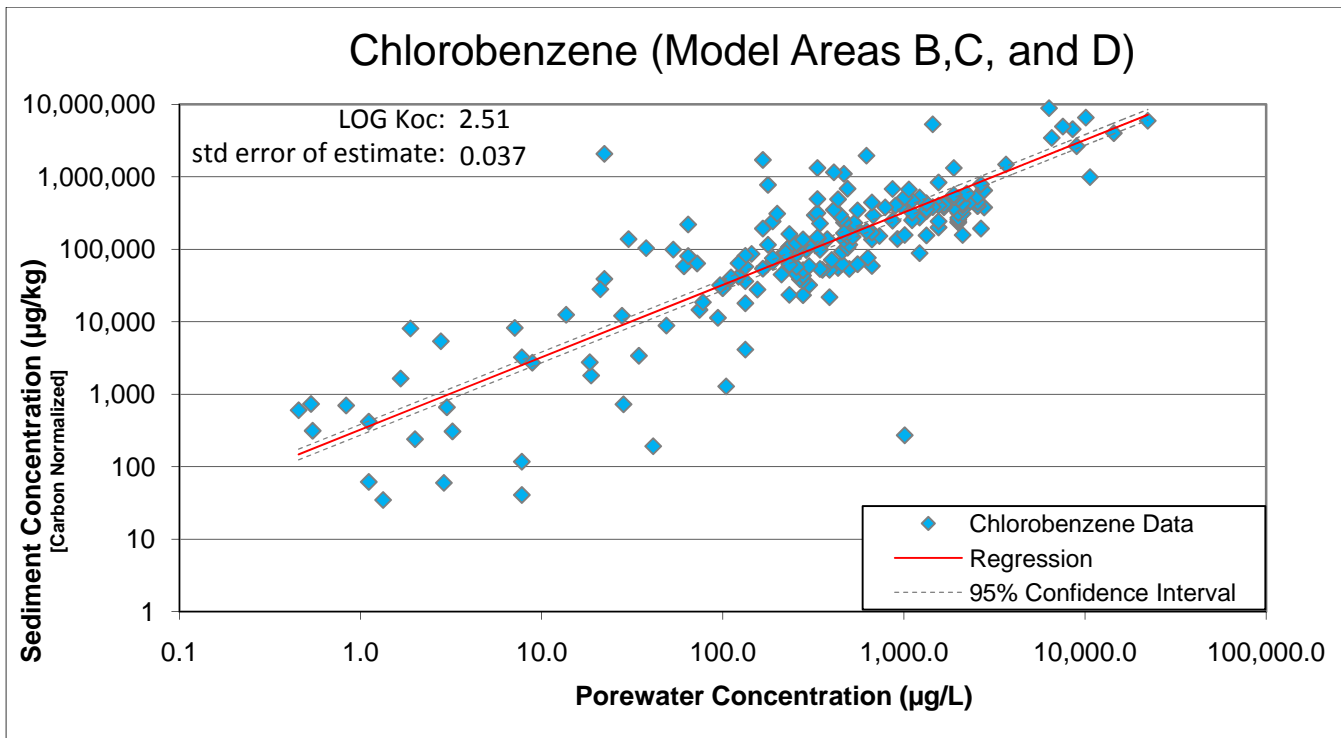


Figure 4. Relationship between *xylene* porewater concentration and carbon-normalized sediment concentration (with log-transformed regression).

CHLOROBENZENE – Model Areas B, C, and D



CHLOROBENZENE – Model Areas A & E

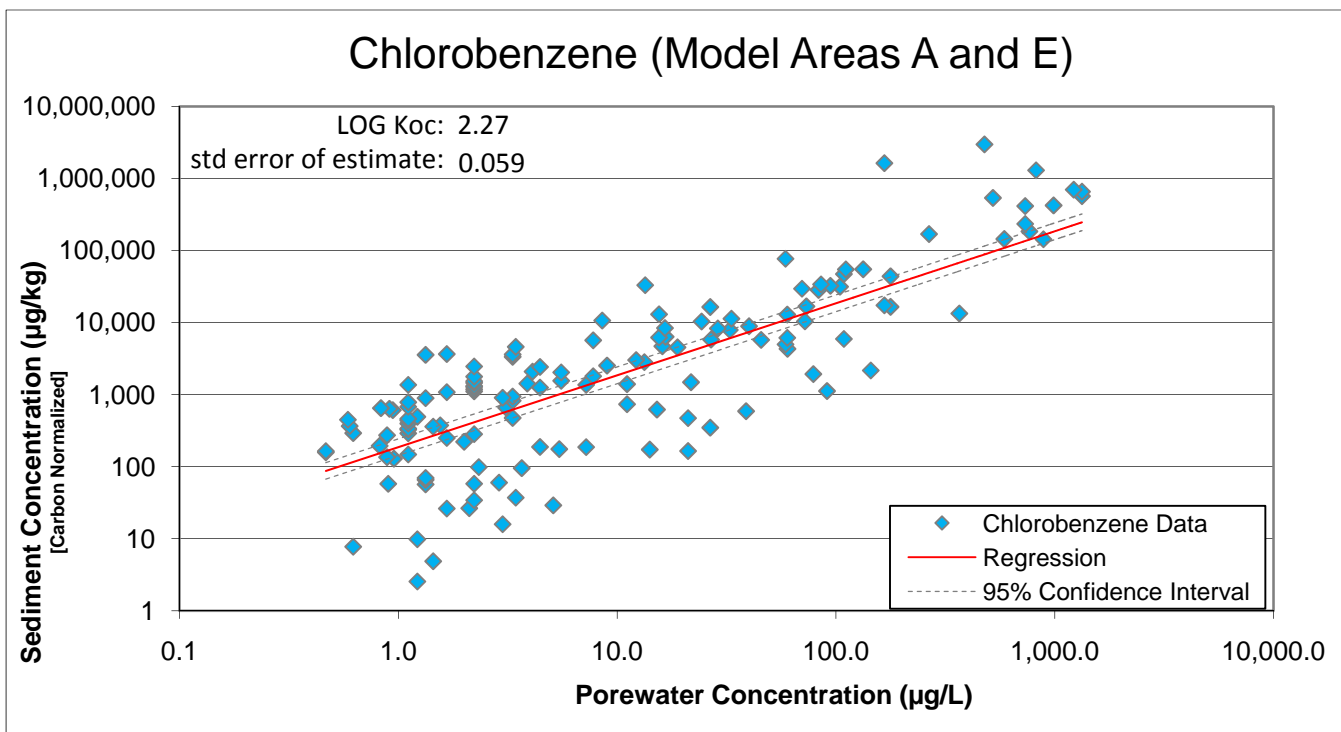
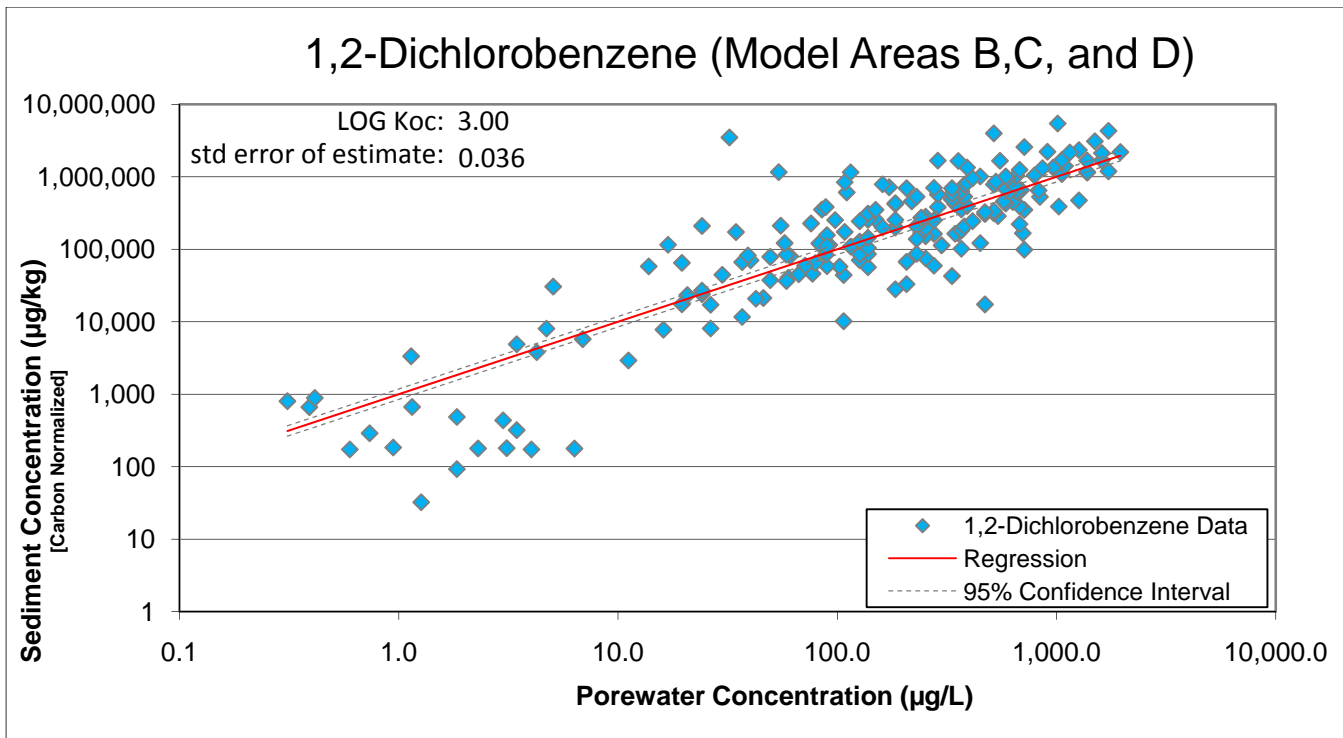


Figure 5. Relationship between *chlorobenzene* porewater concentration and carbon-normalized sediment concentration (with log-transformed regression).

1,2-DICHLOROBENZENE – Model Areas B, C, and D



1,2-DICHLOROBENZENE – Model Areas A & E

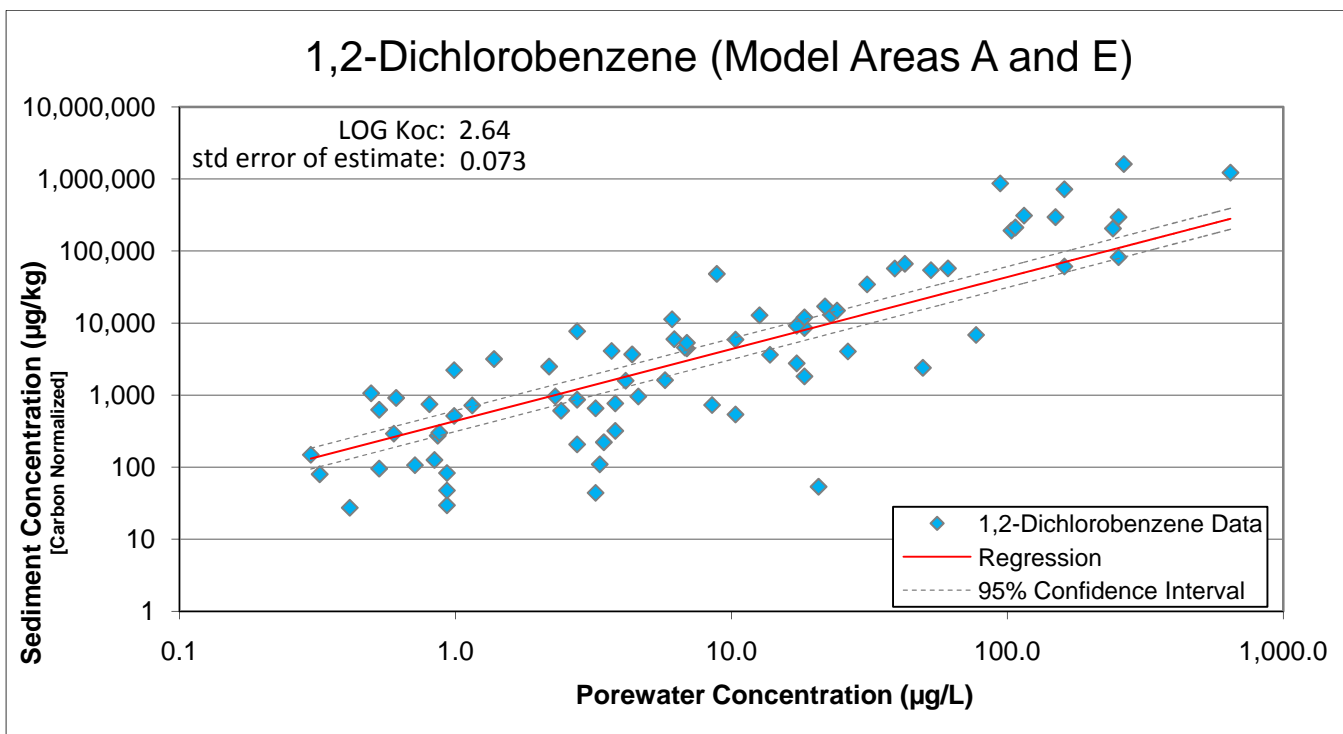
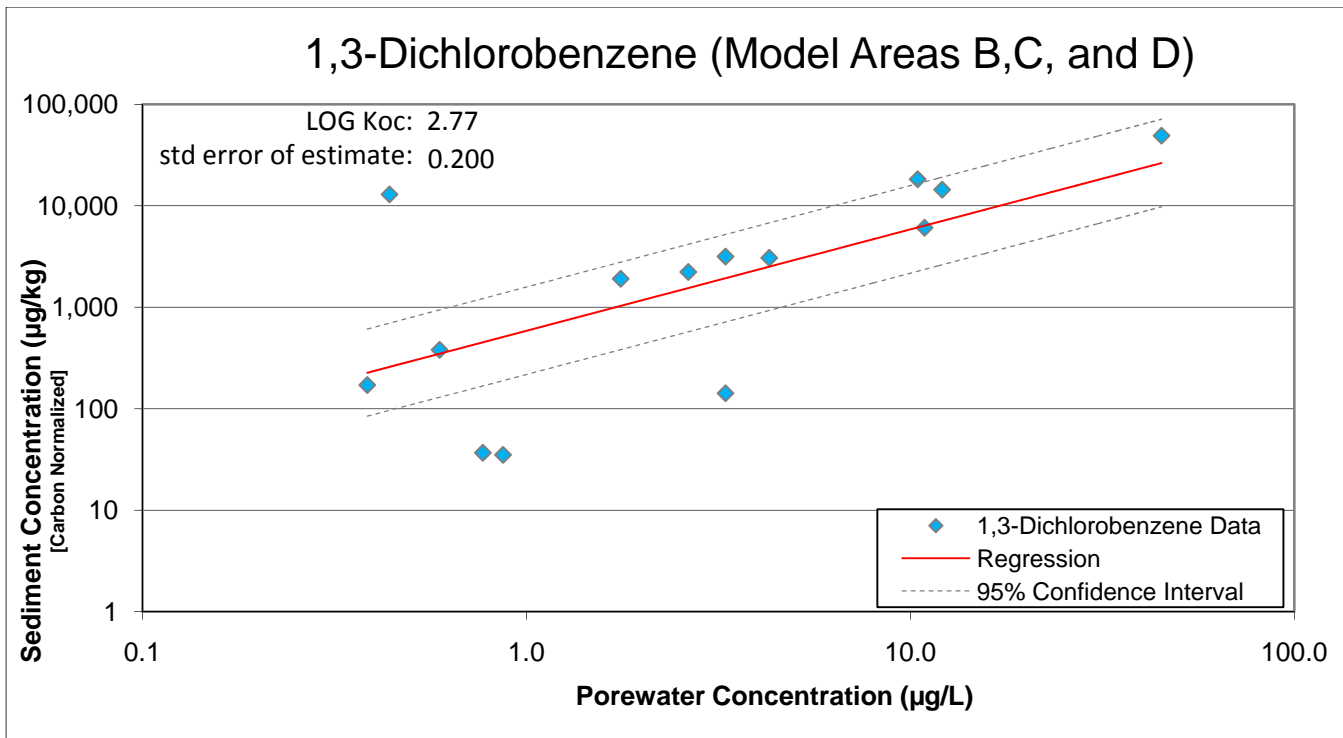


Figure 6. Relationship between 1,2-dichlorobenzene porewater concentration and carbon-normalized sediment concentration (with log-transformed regression).

1,3-DICHLOROBENZENE – Model Areas B, C, and D



1,3-DICHLOROBENZENE – Model Areas A & E

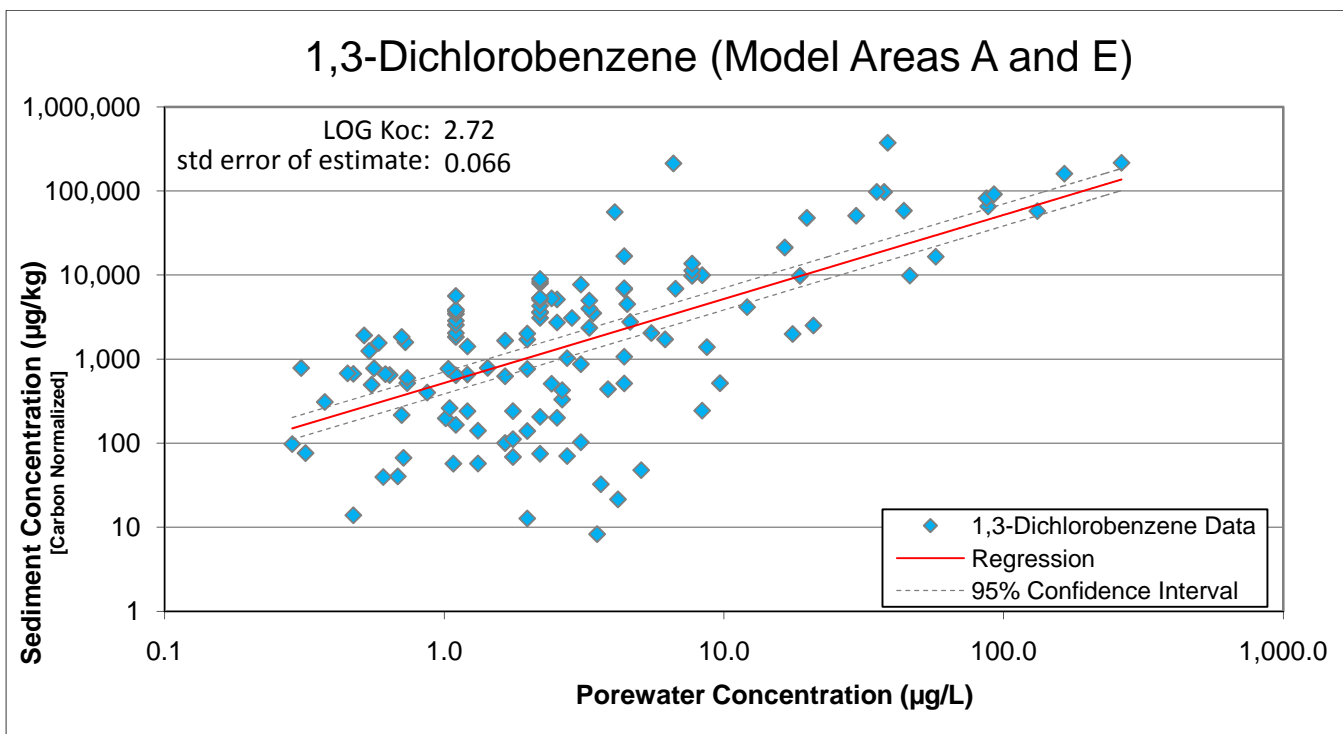
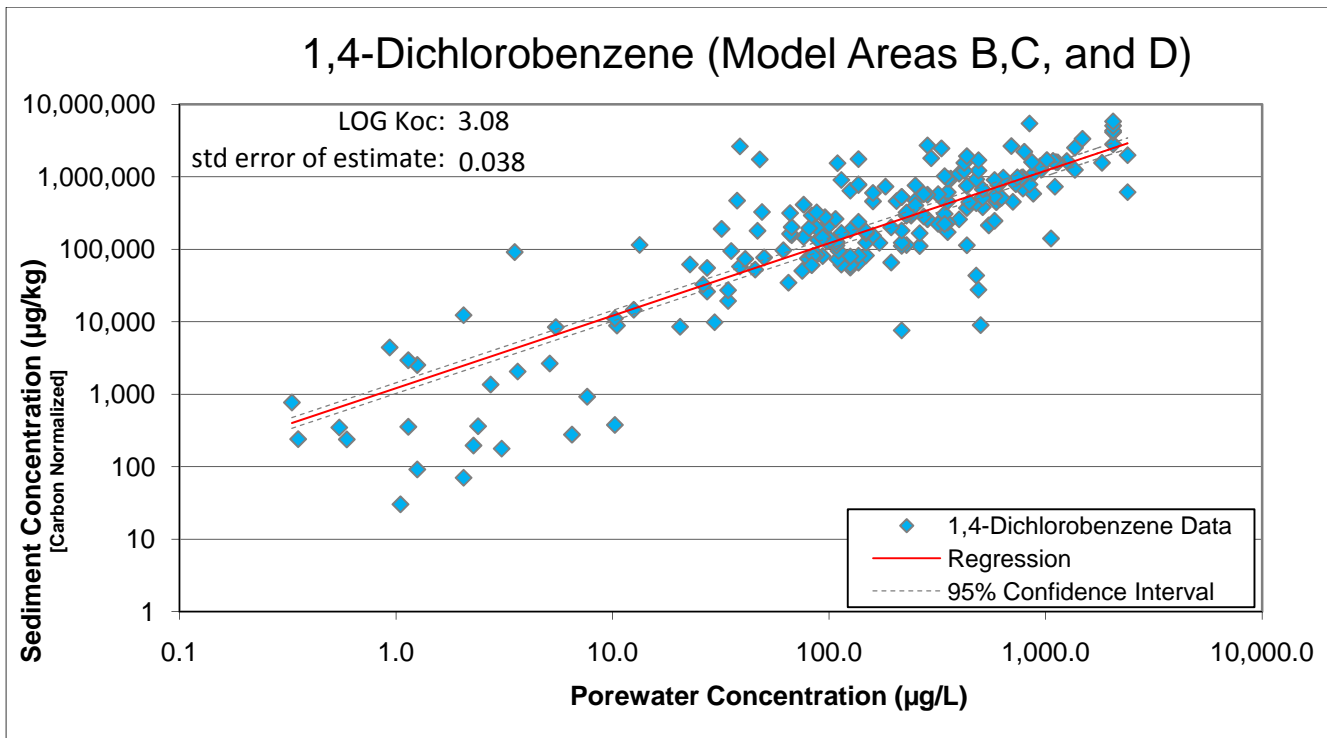


Figure 7. Relationship between 1,3-dichlorobenzene porewater concentration and carbon-normalized sediment concentration (with log-transformed regression).

1,4-DICHLOROBENZENE – Model Areas B, C, and D



1,4-DICHLOROBENZENE – Model Areas A & E

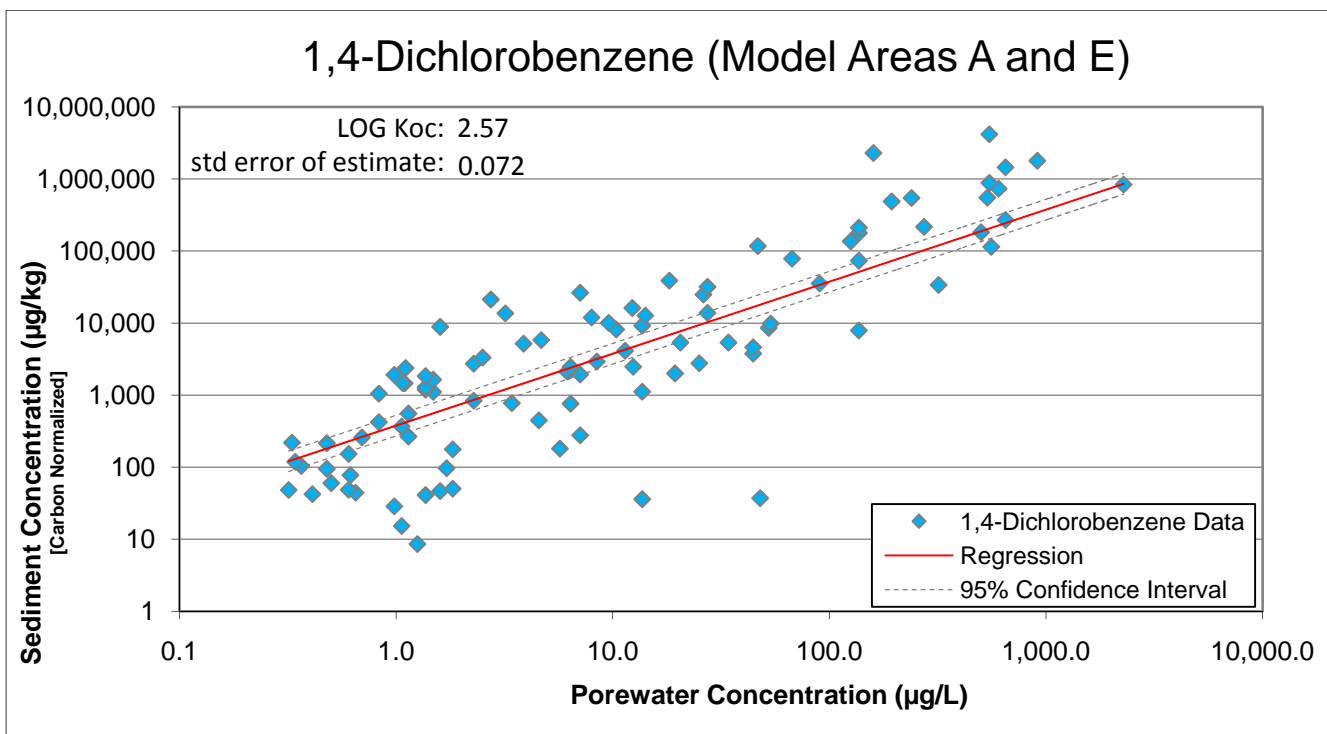
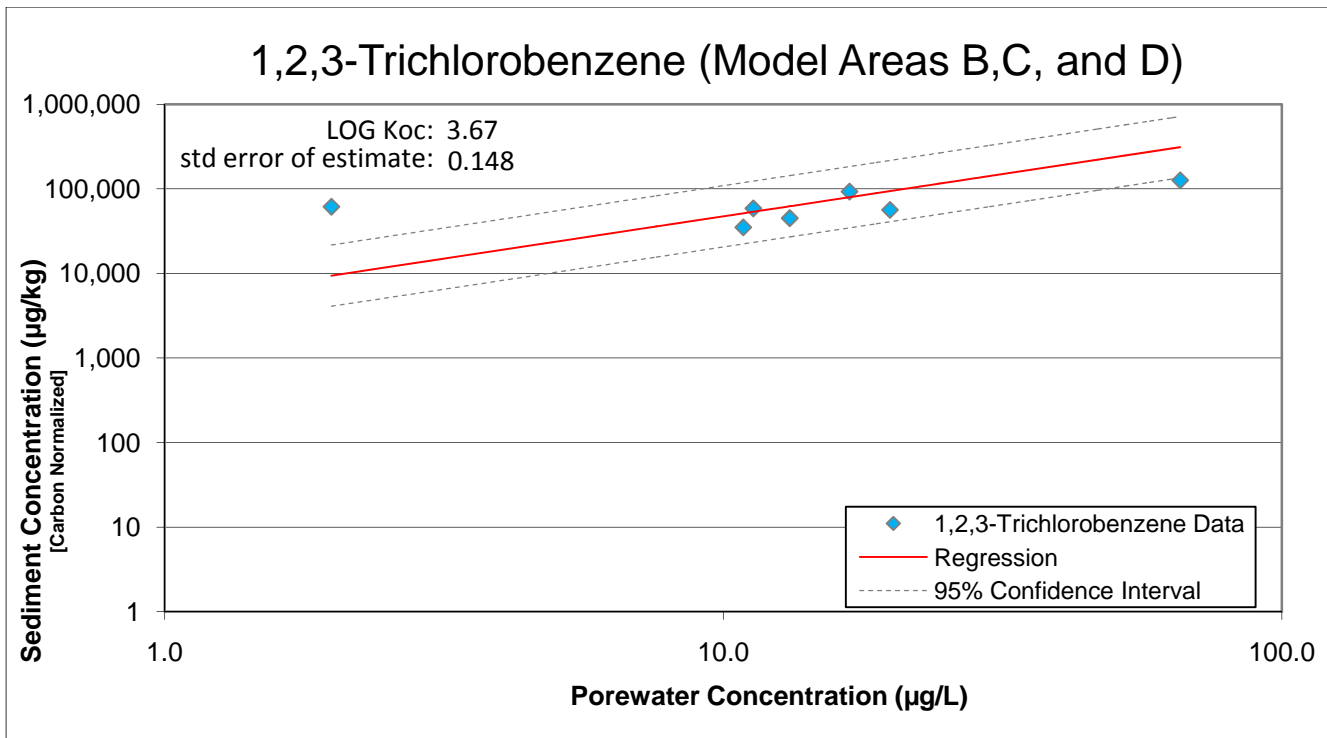


Figure 8. Relationship between 1,4-dichlorobenzene porewater concentration and carbon-normalized sediment concentration (with log-transformed regression).

1,2,3-TRICHLOROBENZENE – Model Areas B, C, and D

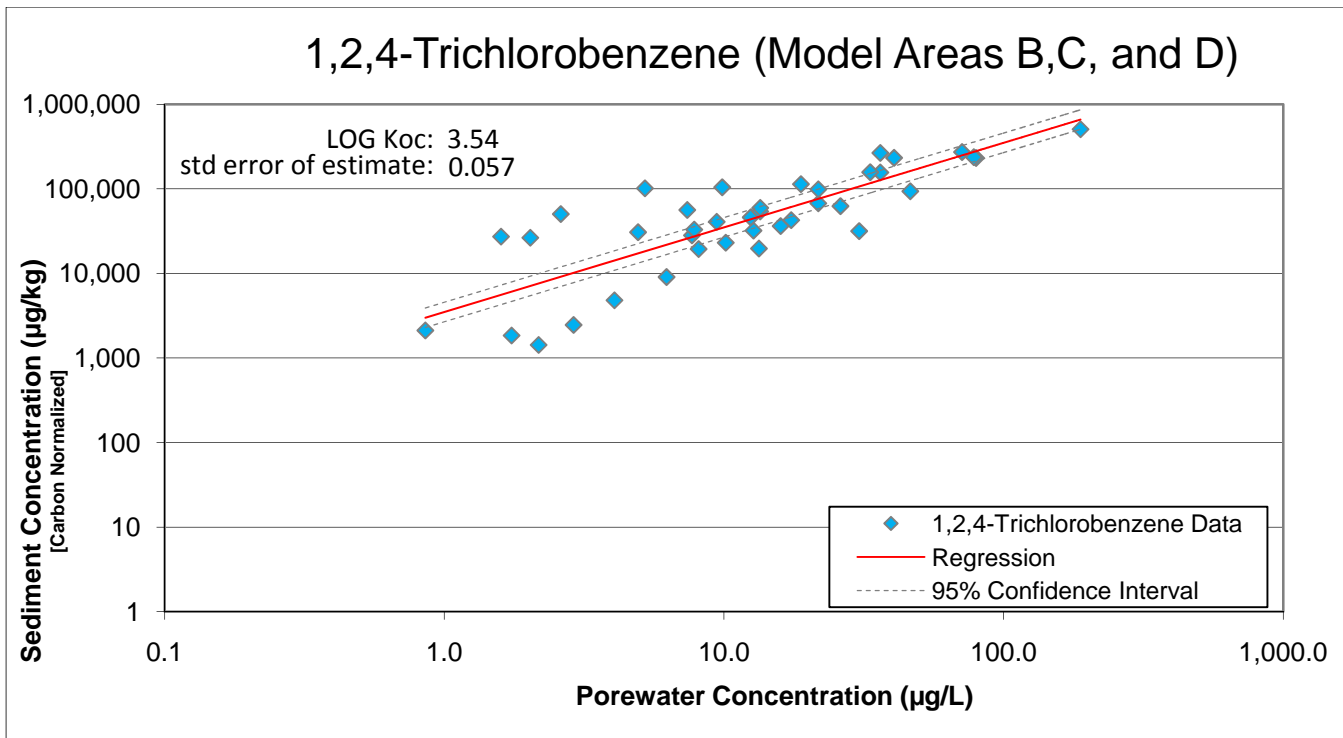


1,2,3-TRICHLOROBENZENE – Model Areas A & E

THERE WAS ONLY A SINGLE USABLE DATA PAIR FOR 1,2,3-TRICHLOROBENZENE IN MODEL AREAS A and E (plot not shown)

Figure 9. Relationship between 1,2,3-trichlorobenzene porewater concentration and carbon-normalized sediment concentration (with log-transformed regression).

1,2,4-TRICHLOROBENZENE – Model Areas B, C, and D



1,2,4-TRICHLOROBENZENE – Model Areas A & E

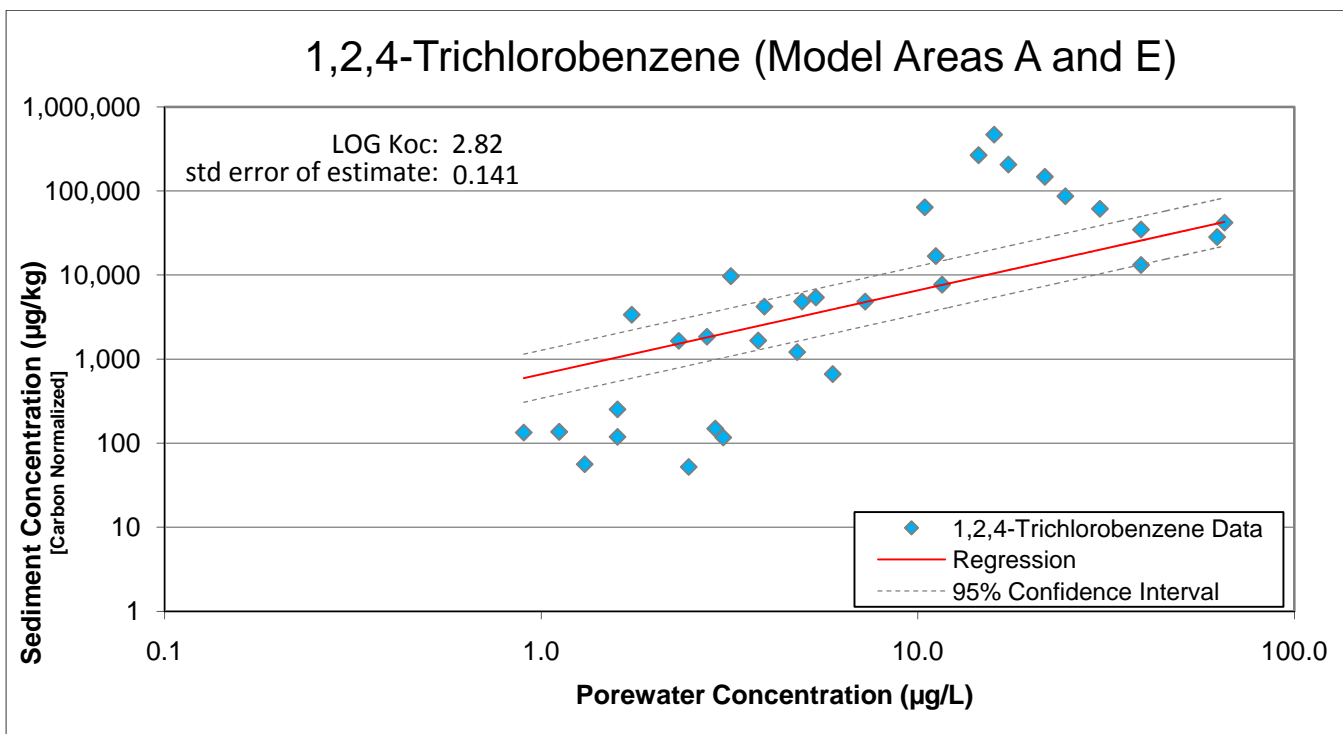


Figure 10. Relationship between 1,2,4-trichlorobenzene porewater concentration and carbon-normalized sediment concentration (with log-transformed regression).

1,3,5-TRICHLOROBENZENE – Model Areas B, C, and D

**THERE WERE NO USABLE DATA PAIRS FOR 1,3,5-TRICHLOROBENZENE
IN MODEL AREAS B, C, and D (plot not shown)**

1,3,5-TRICHLOROBENZENE – Model Areas A & E

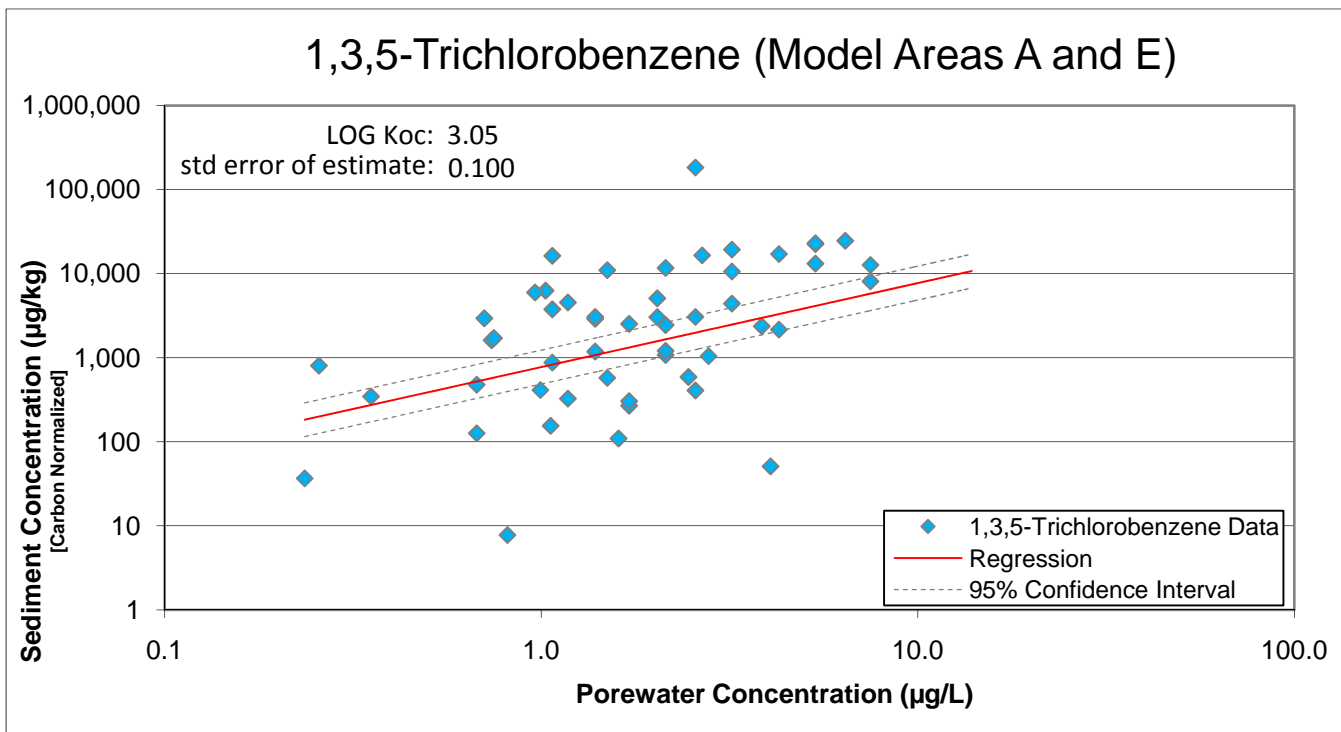
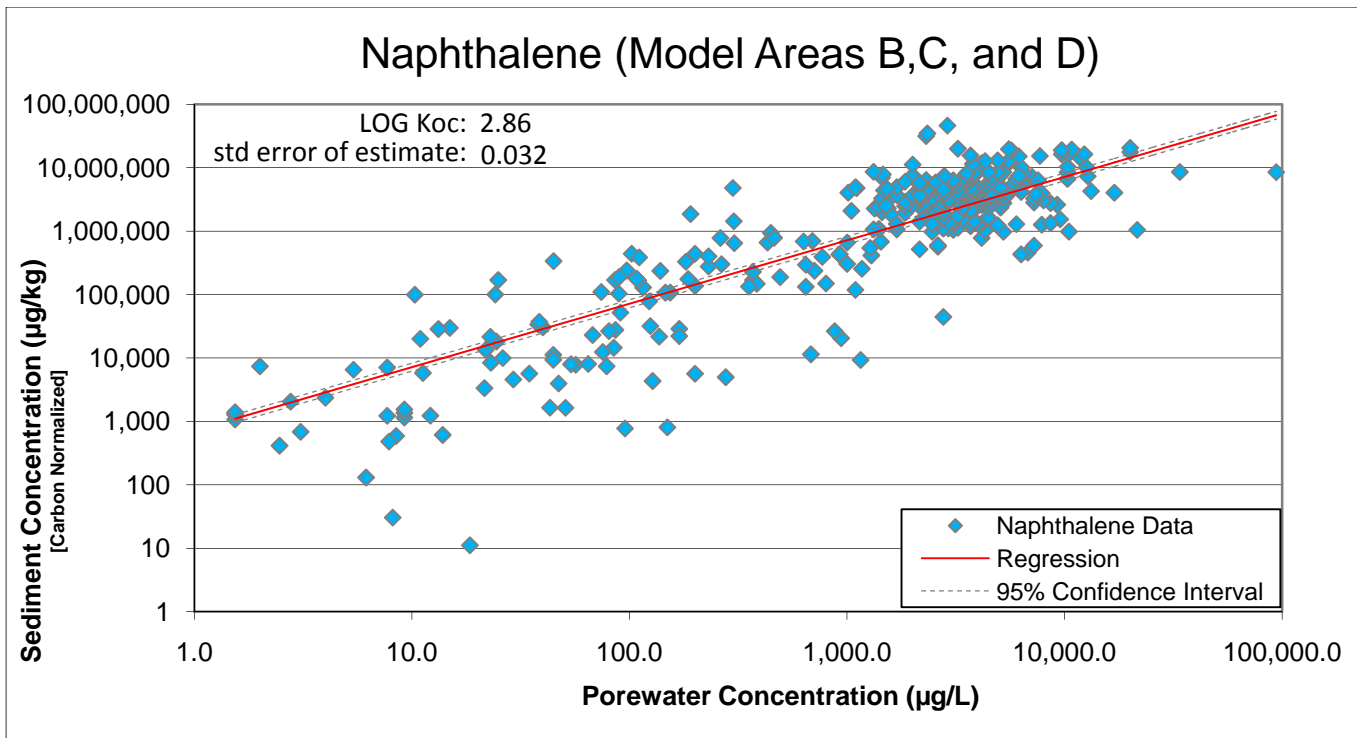


Figure 11. Relationship between 1,3,5-trichlorobenzene porewater concentration and carbon-normalized sediment concentration (with log-transformed regression).

NAPHTHALENE – Model Areas B, C, and D



NAPHTHALENE – Model Areas A & E

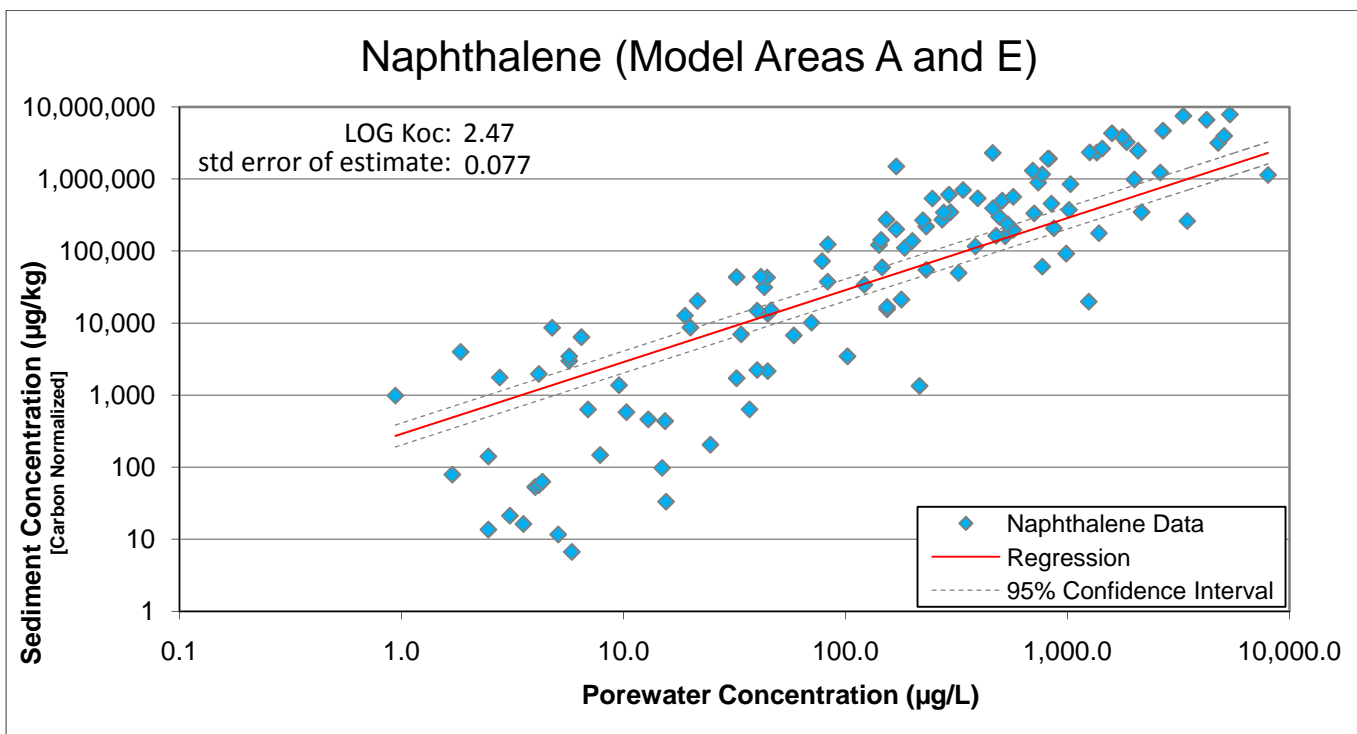


Figure 12. Relationship between *naphthalene* porewater concentration and carbon-normalized sediment concentration (with log-transformed regression).

ADDENDUM 1

TECHNICAL MEMORANDUM

Date: 09 December 2009

To: Edward Glaza – Parsons

Copies to: Caryn E. Kiehl-Simpson and John Nolan – Parsons

From: Tom Krug and David Himmelheber - Geosyntec Consultants
Danny Reible – University of Texas at Austin

Subject: Establishing Representative PAH Sediment-Porewater Partitioning Coefficients Within Sediments for Input into Transport Modeling, Onondaga Lake, Syracuse, New York

1. BACKGROUND AND SCOPE

This memorandum has been prepared by Geosyntec Consultants, Inc. (Geosyntec) to provide recommended values for effective sediment-porewater partitioning coefficients (K_{oc}) in lake sediments to be used to calculate sediment porewater concentrations. The values are intended to be incorporated into transport modeling at areas of Onondaga Lake, Syracuse, New York (the “Site”) not impacted by in-lake waste deposits (ILWD) that are to be managed with an *in situ* sediment cap. A focused literature review of select datasets was performed to examine the phenomenon of porewater polycyclic aromatic hydrocarbon (PAH) and polychlorinated biphenyl (PCB) concentrations measured in actual sediment samples being lower than expected based upon conventional estimates derived from octanol-water distribution coefficients (K_{ow}) and bulk sediment concentration. Direct measurement of porewater concentrations of these compounds are unavailable, hence the need to make the best prediction of porewater concentration for the purposes of modeling.

One approach of estimating porewater concentrations of hydrophobic contaminants, such as PAHs and PCBs, in sediments has been to measure bulk sediment concentration (C_s), then assume linear partitioning into the aqueous phase (C_w) based on solid-liquid distribution coefficients (K_d). The distribution coefficient has been generalized as the product of the fraction organic carbon (f_{oc}) in the sediment and K_{oc} :

$$C_w = \frac{C_s}{K_d} = \frac{C_s}{K_{oc} \times f_{oc}} \quad (1)$$

While this approach does not account for mass held in the dissolved-phase associated with the sediment solids, the correction is extremely small for highly sorptive compounds such as PAH

and PCB. Therefore, pore water concentrations can be related to bulk sediment concentrations (which is based on mass in all phases) with negligible adjustment. Measured f_{oc} values are site-specific while K_{oc} values are chemical-specific and can either be determined experimentally or calculated based on chemical structure and/or properties (e.g., octanol-water partitioning coefficient [K_{ow}]). Note that K_{ow} values are physical constants of a particular compound but that values of K_{oc} are partially dependent upon the particular compound and are also influenced by environmental conditions (including factors such as the nature of the f_{oc}) and whether compounds are sorbing or desorbing. Modeling conducted to date has used K_{ow} values reported in New York State Department of Environmental Conservation Guidance (NYSDEC, 1999) as estimates of K_{oc} and measured f_{oc} values to estimate the concentrations of PAHs and PCBs in sediment porewater beneath the cap. A growing body of literature indicates that this conventional approach of calculating PAH and PCB porewater concentrations in sediments will overestimate actual PAH or PCB porewater concentrations (for discussions see Arp et al., 2009; Hawthorne et al., 2006; and McGroddy et al., 1996). The primary cause of this discrepancy is that natural sediments are composed of different types of organic carbon, with some phases of organic carbon (“hard” carbon) sorbing hydrophobic contaminants stronger but more slowly than other phases (“soft” carbon). An illustration of how different forms of carbon present in sediments results in different effective K_{oc} values for phenanthrene was compiled by Ghosh et al. (2003) and reproduced in this document as Figure 1. As a result, when PAHs or PCBs are introduced into sediments, a portion of the contaminant is sorbed strongly to the “hard” carbon component of organic matter and effectively resistant to desorption. This desorption-resistance is not inherently incorporated into the conventional $K_{oc} \times f_{oc}$ approach of estimating porewater concentrations since compilations of K_{oc} are often based upon short-term sorption experiments in the laboratory or equivalent correlations with K_{ow} . This discrepancy ultimately leads to lower field measurement of porewater PAH concentrations than are predicted by literature K_{oc} values.

A more realistic approach to modeling PAH and PCB transport within sediments is to use measured f_{oc} values and field-derived effective K_{oc} values measured in natural sediment that account for strongly-sorbing fractions of sediment. A compilation of field-derived effective K_{oc} values from several literature sources has been performed.

2. COMPILATION OF DATASETS COMPARING MEASURED PAH POREWATER CONCENTRATIONS WITH ESTIMATED POREWATER CONCENTRATIONS

Figures 2 and 3 present graphs plotting K_{ow} values for PAHs versus field-derived effective K_{oc} values. PAHs included in the analysis are listed in Table 1. Plotted K_{ow} values were obtained from the NYSDEC Guidance Document (1999) for all but three PAH compounds (acenaphthylene, benzo[ghi]perylene, and dibenz[a,h]anthracene) whose K_{ow} values were obtained from Syracuse Research Corporation's (SRC) KowWIN database. The K_{ow} values utilized in this assessment are the same values being employed for modeling efforts to date. The data utilized for the field-derived observed K_{oc} values were actual porewater sampling and

analysis, providing an accurate measurement of aqueous phase PAH concentrations (Arp et al., 2009). Figure 2 contains the compilation of all sediment site data compiled and Figure 3 contains data from sites with freshwater and brackish conditions (i.e., excluding marine sediments).

The K_{ow} values consistently underestimate observed effective K_{oc} values and thus overestimate PAH porewater concentrations associated with sediment containing a known concentration of PAH compared with the field-derived values. On average, the field-derived PAH K_{oc} values are greater than the K_{ow} values currently utilized in modeling efforts by 1.07 ± 0.14 log units (average \pm 95% confidence interval) when examining all the data, and 1.05 ± 0.15 when considering just freshwater and brackish sediment sites. Figures 2 and 3 indicate that adjusting the log K_{ow} values currently employed in modeling efforts by one log unit, or a factor of 10, closely approximates the statistical best-fit lines in both Figures 2 and 3 and falls within the 95% confidence bands of each respective regression line.

3. COMPILATION OF DATASETS COMPARING MEASURED PCB POREWATER CONCENTRATIONS WITH ESTIMATED POREWATER CONCENTRATIONS

Figures 4 and 5 presents graphs of K_{ow} values for PCBs versus field-derived effective K_{oc} values from Arp et al 2009. PCBs included in the analysis are presented in Table 2. Plotted K_{ow} values in Figures 4 and 5 were obtained from the Hawker et al 1988 and Lu et al 2007 respectively.

The K_{ow} values consistently underestimate observed effective K_{oc} values and thus overestimate PCB porewater concentrations associated with sediment containing a known concentration of PCB compared with the field-derived values. On average, the field-derived PCB K_{oc} values are greater than the literature K_{ow} values by a factor of five. Figures 4 and 5 indicate that adjusting the K_{ow} values currently employed in modeling efforts by a factor of five, closely approximates the statistical best-fit lines in both Figures 4 and 5 and falls within the 95% confidence bands of each respective regression line.

4. RECOMMENDATIONS

The literature review described above and relevant experience at other sediment sites supports the use of corrected PAH and PCB K_{oc} values to most accurately model and predict porewater PAH and PCB concentrations within the Onondaga Lake sediment in the absence of direct measurements. Based on the data presented in Figures 2 and 3 an increase in effective K_{oc} values of 10 from PAH K_{ow} values is recommended for derivation of PAH porewater concentrations in the non-ILWD impacted sediments at this time. Based on the data presented in Figures 4 and 5 an increase in effective K_{oc} values of 5 from PCB K_{ow} values is recommended for derivation of PCB porewater concentrations in the non-ILWD impacted sediments.

5. REFERENCES

Arp, H.P.H., Breedveld, G.D., and Cornelissen, G., 2009. Estimating the in situ sediment-porewater distribution of PAHs and chlorinated aromatic hydrocarbons in anthropogenic impacted sediments. *Environ. Sci. Technol.*, 43, 5576–5585.

Cornelissen, G., Gustafsson, O., Bucheli, T. D., Jonker, M. T. O., Koelmans, A. A., and VanNoort, P. C.M., 2005. Extensive sorption of organic compounds to black carbon, coal, and kerogen in sediments and soils: Mechanisms and consequences for distribution, bioaccumulation, and biodegradation. *Environ. Sci. Technol.*, 39 (18), 6881–6895.

Ghosh, U., Zimmerman, J.R., and Luthy, R.G., 2003. PCB and PAH speciation among particle types in contaminated harbor sediments and effects on PAH bioavailability. *Environ. Sci. Technol.*, 37, 2209–2217.

Hawker, D.W., and Connell, D.W., 1988. Octanol-water partition coefficients of polychlorinated biphenyls congeners. *Environ. Sci. Technol.*, 22:382-385.

Hawthorne, S.B., Grabanski, C.B., and Miller, D.J., 2006. Measured partitioning coefficients for parent and alkyl polycyclic aromatic hydrocarbons in 114 historically contaminated sediments: Part 1. K_{oc} values. *Environ. Toxicol. Chem.*, 25 (11), 2901-2911.

Lohmann, R., MacFarlane, J. K., and Gschwend, P. M., 2005. Importance of black carbon to sorption of native PAHs, PCBs, and PCDDs in Boston and New York Harbor sediments. *Environ. Sci. Technol.*, 39 (1), 141–148.

Lu, X., Reible, D.D., and Fleeger, J.W., 2006. Bioavailability of polycyclic aromatic hydrocarbons in field-contaminated Anacostia River (Washington, DC) sediment. *Environ. Toxicol. Chem.*, 25, (11), 2869-2874.

Lu, W., Chen, Y., Liu, M., Chen, X. and Hu, Z., 2007. QSPR prediction of n-octanol/water partitioning coefficient for polychlorinated biphenyls. *Chemosphere*, 69 (2007), 469-478.

McGroddy, S. E., Farrington, J. W., and Gschwend, P. M., 1996. Comparison of the in situ and desorption sediment-water partitioning of polycyclic aromatic hydrocarbons and polychlorinated biphenyls. *Environ. Sci. Technol.*, 30 (1), 172–177.

New York State Department of Environmental Conservation (NYSDEC), 1999. Technical Guidance for Screening Contaminated Sediments. Division of Fish, Wildlife and Marine Resources.

Table 1 - Literature Values for Kow and Koc for Polycyclic Aromatic Hydrocarbons

Data Source in	CAS #	Compound	Average Log Koc	Log Kow	Log Kow
Arp et al, 2009			Arp et al, 2009	NYSDEC, 1999	SRC
7	208-96-8	Acenaphthylene	5.11	ns	3.94
9	208-96-8	Acenaphthylene	4.48	ns	3.94
10	208-96-8	Acenaphthylene	4.47	ns	3.94
4	120-12-7	Anthracene	6.24	4.45	
6	120-12-7	Anthracene	6.08	4.45	
7	120-12-7	Anthracene	5.75	4.45	
9	120-12-7	Anthracene	5.41	4.45	
14	120-12-7	Anthracene	6.61	4.45	
15	120-12-7	Anthracene	5.26	4.45	
1	56-55-3	Benzo[a]anthracene	7.14	5.61	
4	56-55-3	Benzo[a]anthracene	7.38	5.61	
6	56-55-3	Benzo[a]anthracene	6.77	5.61	
7	56-55-3	Benzo[a]anthracene	6.55	5.61	
8	56-55-3	Benzo[a]anthracene	6.95	5.61	
9	56-55-3	Benzo[a]anthracene	6.45	5.61	
14	56-55-3	Benzo[a]anthracene	7.81	5.61	
6	50-32-8	Benzo(a)pyrene	7.03	6.04	
1	50-32-8	Benzo[a]pyrene	7.77	6.04	
4	50-32-8	Benzo[a]pyrene	8.37	6.04	
7	50-32-8	Benzo[a]pyrene	6.68	6.04	
8	50-32-8	Benzo[a]pyrene	7.96	6.04	
9	50-32-8	Benzo[a]pyrene	6.85	6.04	
11	50-32-8	Benzo[a]pyrene	7.25	6.04	
12	50-32-8	Benzo[a]pyrene	6.79	6.04	
13	50-32-8	Benzo[a]pyrene	6.15	6.04	
14	50-32-8	Benzo[a]pyrene	7.81	6.04	
4	205-99-2	Benzo[b]fluoranthene	7.99	6.04	
6	205-99-2	Benzo[b]fluoranthene	7.06	6.04	
8	205-99-2	Benzo[b]fluoranthene	7.42	6.04	
9	205-99-2	Benzo[b]fluoranthene	6.91	6.04	
15	205-99-2	Benzo[b]fluoranthene	6.59	6.04	
1	191-24-2	Benzo[ghi]perylene	8.25	ns	6.70
4	191-24-2	Benzo[ghi]perylene	9.01	ns	6.70
6	191-24-2	Benzo[ghi]perylene	7.58	ns	6.70
7	191-24-2	Benzo[ghi]perylene	7.13	ns	6.70
8	191-24-2	Benzo[ghi]perylene	7.84	ns	6.70
9	191-24-2	Benzo[ghi]perylene	6.94	ns	6.70
14	191-24-2	Benzo[ghi]perylene	8.91	ns	6.70
15	191-24-2	Benzo[ghi]perylene	6.67	ns	6.70
4	207-08-9	Benzo[k]fluoranthene	8.16	6.04	
6	207-08-9	Benzo[k]fluoranthene	7.25	6.04	
8	207-08-9	Benzo[k]fluoranthene	7.41	6.04	
9	207-08-9	Benzo[k]fluoranthene	6.90	6.04	
12	207-08-9	Benzo[k]fluoranthene	6.74	6.04	
15	207-08-9	Benzo[k]fluoranthene	6.41	6.04	

notes:

ns - not specified

Table 1 - Literature Values for Kow and Koc for Polycyclic Aromatic Hydrocarbons

Data Source in	CAS #	Compound	Average Log Koc	Log Kow	Log Kow
Arp et al, 2009			Arp et al, 2009	NYSDEC, 1999	SRC
4	53-70-3	Dibenz[a,h]anthracene	8.06	ns	6.70
6	53-70-3	Dibenz[a,h]anthracene	7.62	ns	6.70
7	53-70-3	Dibenz[a,h]anthracene	6.82	ns	6.70
9	53-70-3	Dibenz[a,h]anthracene	6.88	ns	6.70
6	206-44-0	Fluorantene	6.25	5.19	
1	206-44-0	Fluoranthene	6.26	5.19	
4	206-44-0	Fluoranthene	6.37	5.19	
7	206-44-0	Fluoranthene	5.79	5.19	
8	206-44-0	Fluoranthene	6.04	5.19	
9	206-44-0	Fluoranthene	5.89	5.19	
13	206-44-0	Fluoranthene	6.43	5.19	
14	206-44-0	Fluoranthene	7.41	5.19	
15	206-44-0	Fluoranthene	6.15	5.19	
16	206-44-0	Fluoranthene	6.34	5.19	
7	86-73-7	Fluorene	4.71	4.18	
9	86-73-7	Fluorene	4.65	4.18	
10	86-73-7	Fluorene	4.17	4.18	
15	86-73-7	Fluorene	4.69	4.18	
16	86-73-7	Fluorene	6.49	4.18	
7	91-57-6	2-Methylnaphthalene	4.56	3.86	
16	91-57-6	2-Methylnaphthalene	7.03	3.86	
7	91-20-3	Naphthalene	4.26	3.37	
9	91-20-3	Naphthalene	3.39	3.37	
10	91-20-3	Naphthalene	3.14	3.37	
1	85-01-8	Phenanthrene	5.87	4.45	
4	85-01-8	Phenanthrene	6.15	4.45	
6	85-01-8	Phenanthrene	5.83	4.45	
7	85-01-8	Phenanthrene	5.20	4.45	
8	85-01-8	Phenanthrene	5.70	4.45	
8	85-01-8	Phenanthrene	5.70	4.45	
9	85-01-8	Phenanthrene	5.30	4.45	
10	85-01-8	Phenanthrene	5.03	4.45	
11	85-01-8	Phenanthrene	5.25	4.45	
12	85-01-8	Phenanthrene	4.76	4.45	
13	85-01-8	Phenanthrene	6.50	4.45	
14	85-01-8	Phenanthrene	6.91	4.45	
15	85-01-8	Phenanthrene	4.99	4.45	
16	85-01-8	Phenanthrene	6.59	4.45	
4	129-00-0	Pyrene	6.38	5.32	
6	129-00-0	Pyrene	5.86	5.32	
7	129-00-0	Pyrene	5.82	5.32	
8	129-00-0	Pyrene	6.05	5.32	
9	129-00-0	Pyrene	5.97	5.32	
10	129-00-0	Pyrene	5.08	5.32	
11	129-00-0	Pyrene	5.90	5.32	
12	129-00-0	Pyrene	5.43	5.32	
13	129-00-0	Pyrene	6.06	5.32	
14	129-00-0	Pyrene	6.71	5.32	
15	129-00-0	Pyrene	5.75	5.32	
16	129-00-0	Pyrene	6.80	5.32	

notes:

ns - not specified

Table 2 - Literature Values for Kow and Koc of PCB Congeners

PCB Congener	Log Kow Hawker et al 1988	Log Kow Lu et al 2007	Ave Log Koc Arp et al 2009	PCB Congener	Log Kow Hawker et al 1988	Log Kow Lu et al 2007	Ave Log Koc Arp et al 2009
PCB-18	5.24	5.33	5.94	PCB-118	6.74	6.57	6.83
PCB-18	5.24	5.33	5.54	PCB-118	6.74	6.57	8.02
PCB-28	5.67	5.71	6.25	PCB-118	6.74	6.57	7.58
PCB-28	5.67	5.71	6.44	PCB-118	6.74	6.57	6.85
PCB-28	5.67	5.71	7.18	PCB-118	6.74	6.57	6.86
PCB-28	5.67	5.71	6.28	PCB-126	6.89	na	7.7
PCB-31	5.67	5.68	6.99	PCB-138	6.83	6.73	8.19
PCB-44	5.75	5.73	6.48	PCB-138	6.83	6.73	8.25
PCB-44	5.75	5.73	5.9	PCB-138	6.83	6.73	7.55
PCB-52	5.84	5.79	6.46	PCB-138	6.83	6.73	7.15
PCB-52	5.84	5.79	6.7	PCB-153	6.92	6.8	8.33
PCB-52	5.84	5.79	7.01	PCB-153	6.92	6.8	8.32
PCB-52	5.84	5.79	6.51	PCB-153	6.92	6.8	7.46
PCB-52	5.84	5.79	6.03	PCB-153	6.92	6.8	7.01
PCB-66	6.2	5.98	6.8	PCB-156	7.18	7.44	8.13
PCB-72	6.26	na	6.01	PCB-156	7.18	7.44	7.82
PCB-77	6.36	na	7.32	PCB-156	7.18	7.44	7.38
PCB-77	6.36	na	6.86	PCB-167	7.27	7.29	7.94
PCB-81	6.36	na	7.38	PCB-169	7.42	7.55	7.96
PCB-95	6.13	5.92	6.35	PCB-170	7.27	7.08	8
PCB-101	6.38	na	6.56	PCB-180	7.36	7.21	7.35
PCB-101	6.38	na	7.54	PCB-180	7.36	7.21	8.31
PCB-101	6.38	na	7.71	PCB-180	7.36	7.21	8.3
PCB-101	6.38	na	6.95	PCB-180	7.36	7.21	7.86
PCB-101	6.38	na	6.55	PCB-187	7.17	6.99	7.79
PCB-105	6.65	6.79	8.06	PCB-195	7.56	7.35	7.85
PCB-105	6.65	6.79	7.51	PCB-204	7.3	7.48	8.24

Figure 1 - Phenanthrene K_{oc} values for different types of organic carbon.
Reproduced from Ghosh et al., 2003.

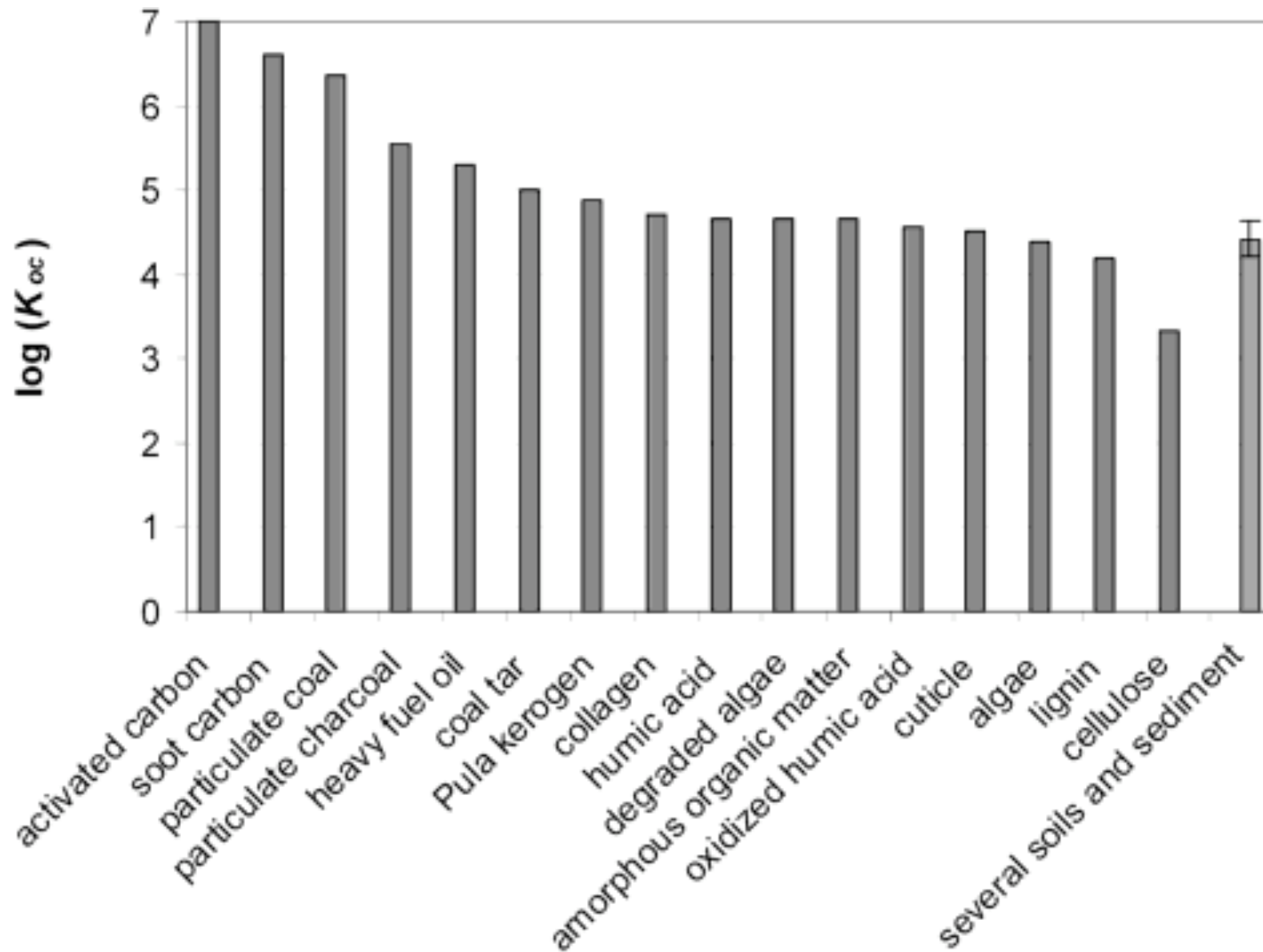


**Figure 2 - Log K_{ow} versus Observed K_{oc}
All Sediment Site Data**

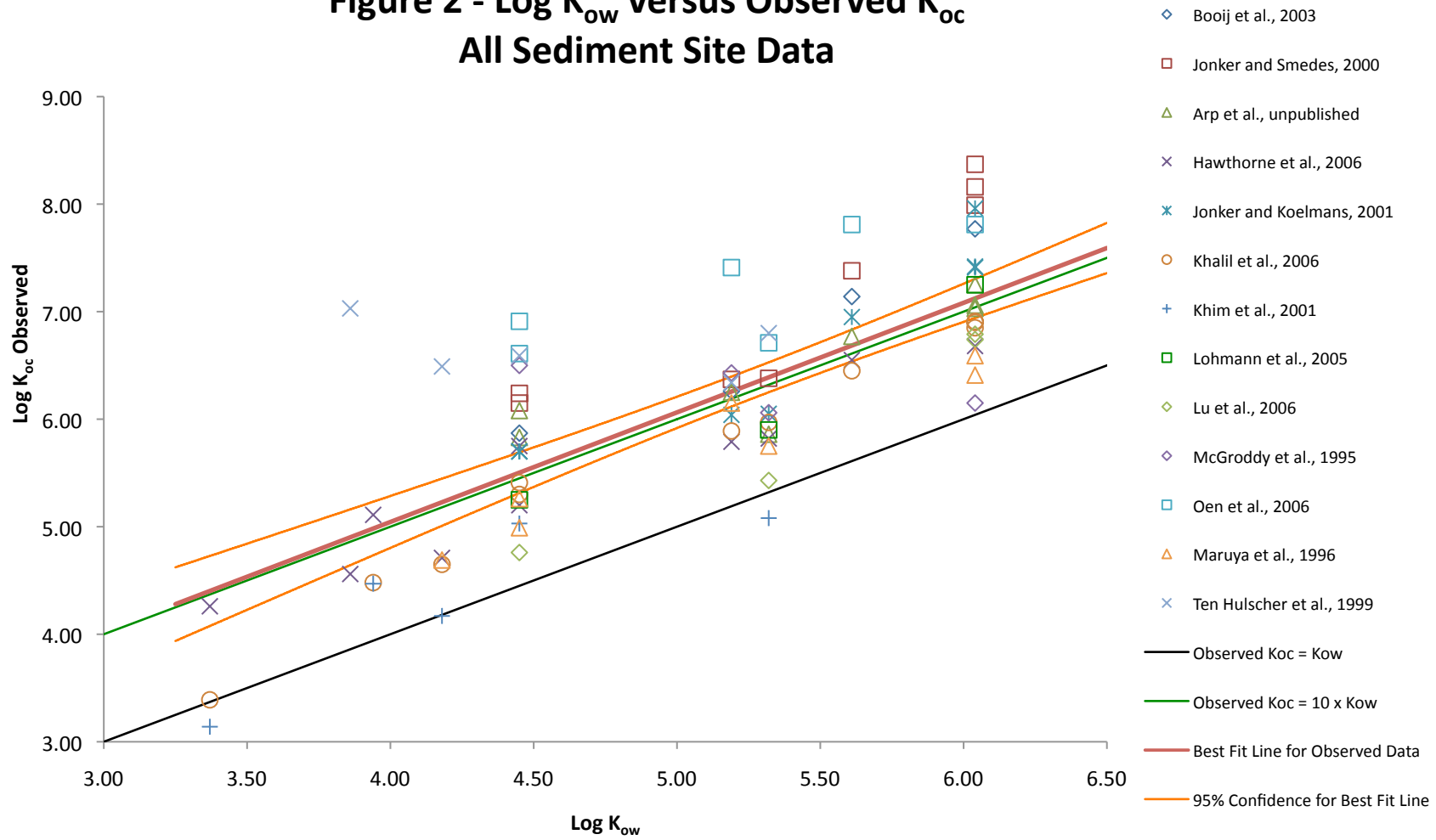


**Figure 3 - Log K_{ow} versus Observed K_{oc}
Freshwater to Brackish Sediment Sites**

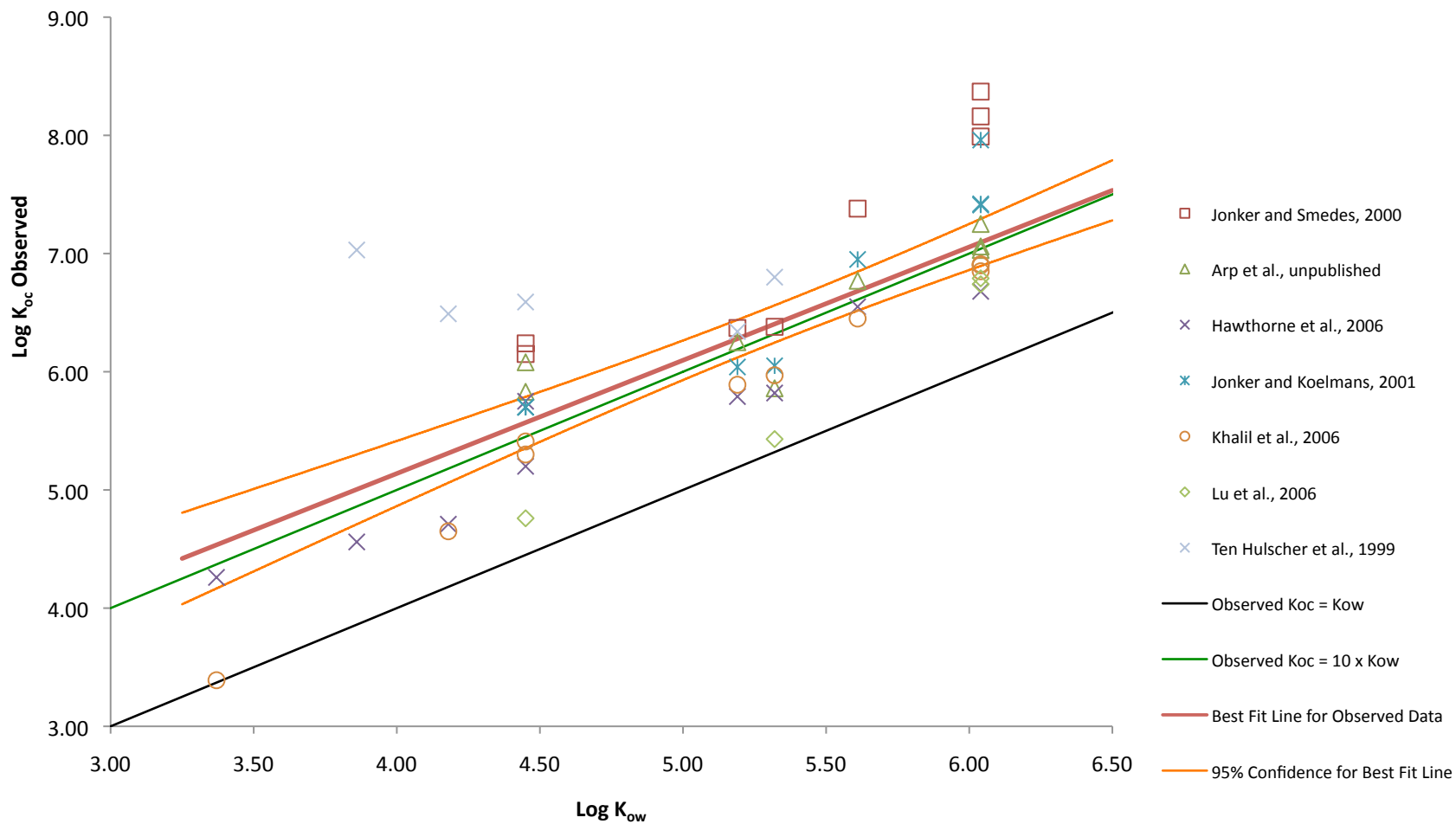
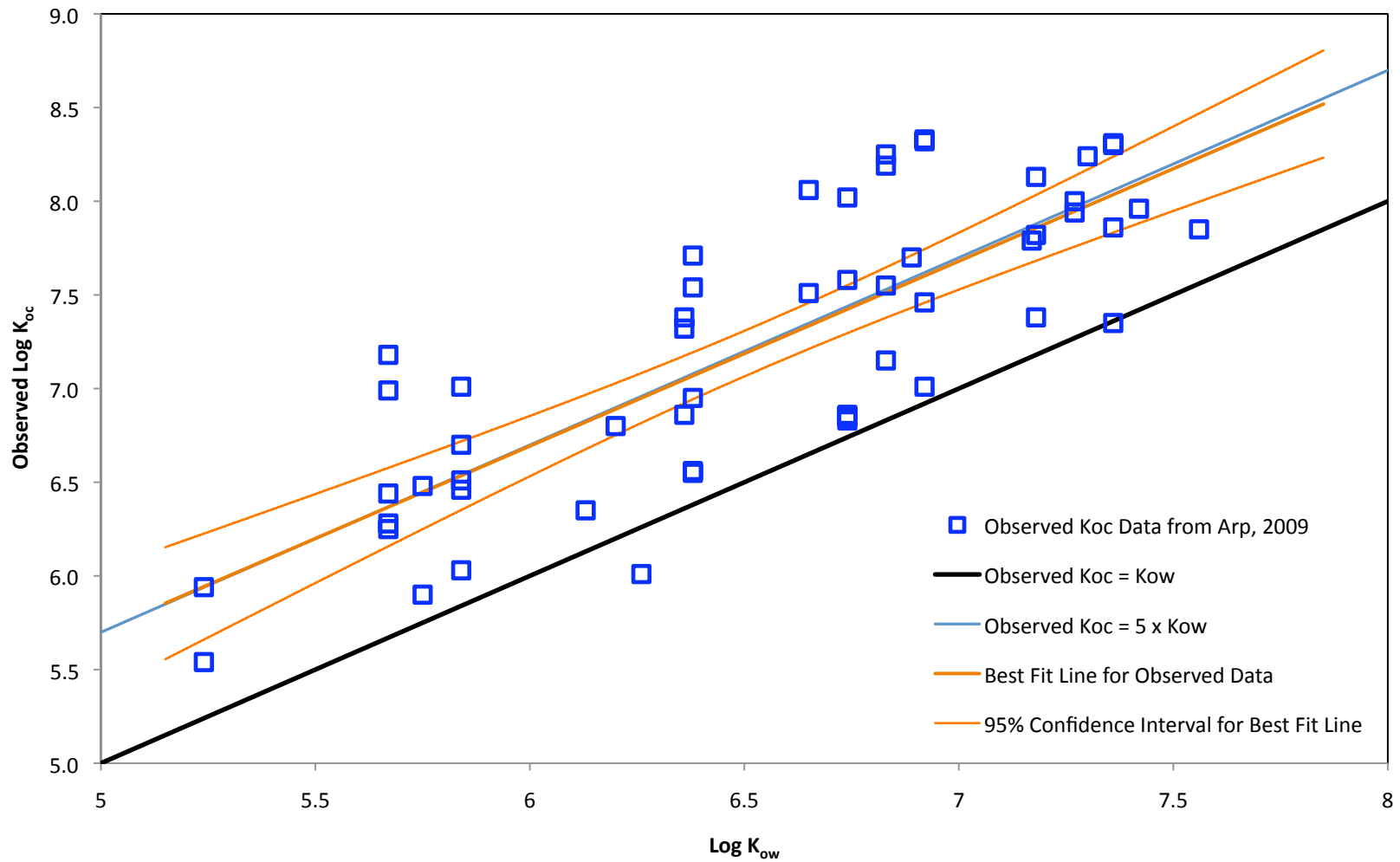
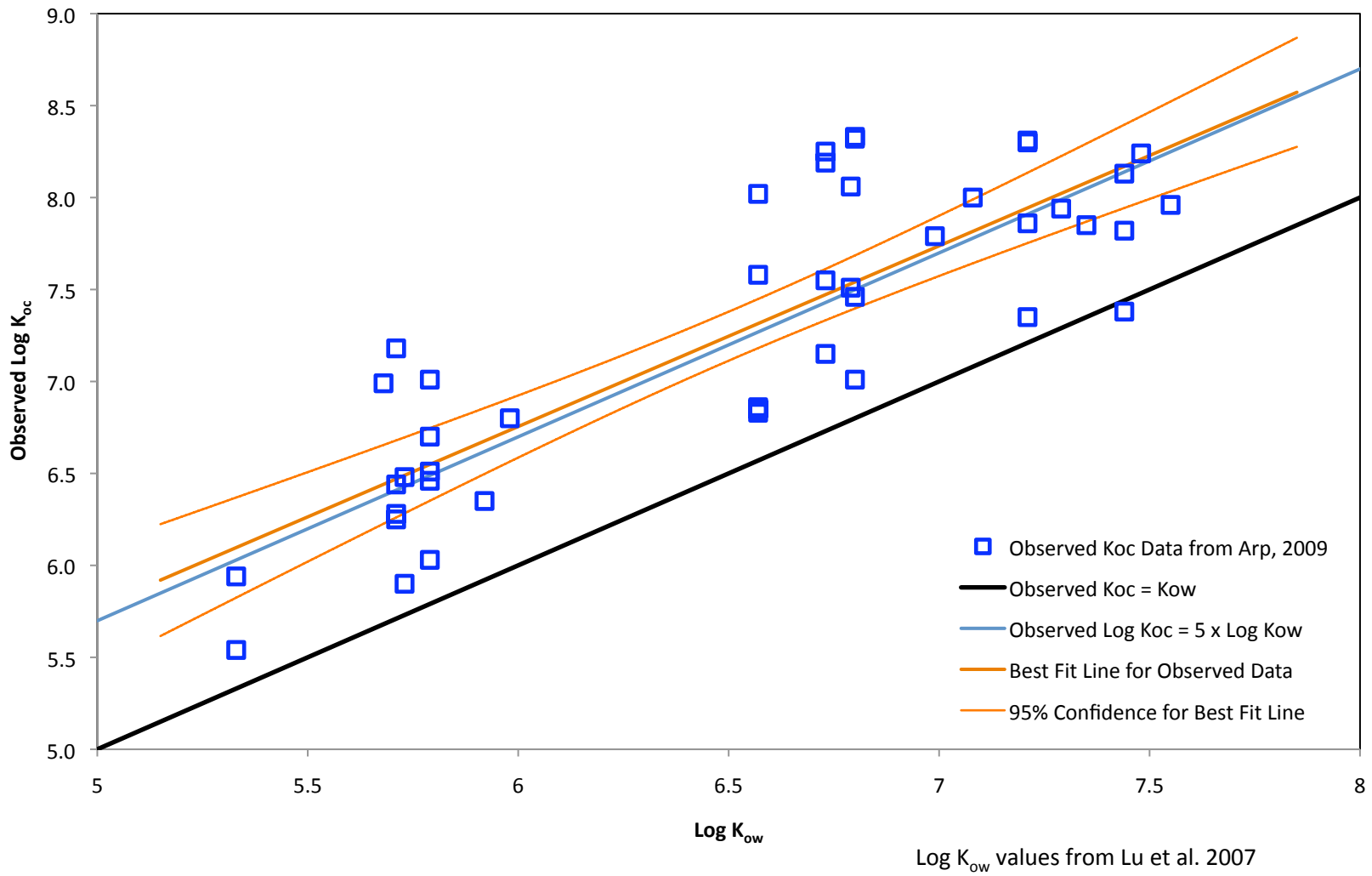


Figure 4 - Log K_{ow} vs Observed Log K_{oc}



Log K_{ow} values from Hawker, 1988

Figure 5 - Log K_{ow} vs Observed Log K_{oc}



ATTACHMENT 3
MODEL VALIDATION

Parsons Engineering Department
Certificate of Software Validation

User Discipline HYDROGEOLOGY

Certification No. HY-009

Software Title. Active Capping Transport Model

Date of Validation 01/06/09

Software Supplier REIBLE⁽¹⁾

Validated Version Version 2.0

Software Description and Use 1-Dimensional, solute transport model through a sediment cap, also see attached documentation.

System Requirements: Operating System Windows XP/Vistas

RAM 512K

Hard Disk yes

Math Coprocessor yes

Windows yes

Other Matlab version 7.7 or later

Restrictions/Limitations see attached documentation

The above-named software is certified as a validated software. The scope of this validation is as follows:

a. The software has demonstrated satisfactory function for its intended tasks, through the following verification methods (check all pertinent items):

(2) By independent verification testing.

By extensive use on active projects.

Industry tested and proven.

NRC/other agency approved (list agency and number if possible). _____

(1) Supplier-performed verification.

Other (describe) _____

b. All users have received/will receive suitable instructions/sufficient documentation to use the software.

Submitted: Software Custodian _____

Date _____

Approved: Section Manager _____

Date _____

(1) Danny Reible, Ph.D., Bettie Margaret Smith Professor of Environmental Health Engineering, Department of Civil, Architectural, Environmental Engineering, The University of Texas at Austin, 1 University Station C1786, Austin, TX 78712-0273.

(2) Model results were compared with well-documented 1-D solute transport equations by Charles Andrews. See attached memorandum.

Printed copies of this document are uncontrolled copies.

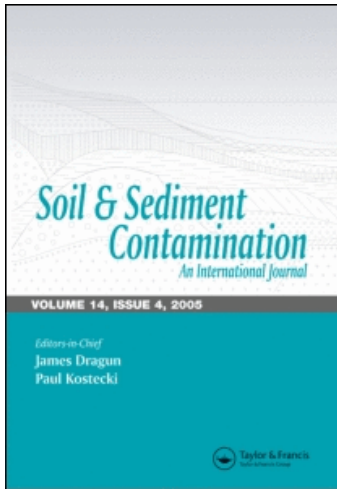
This article was downloaded by: [reible@mail.utexas.edu]

On: 24 June 2009

Access details: Access Details: [subscription number 912623667]

Publisher Taylor & Francis

Informa Ltd Registered in England and Wales Registered Number: 1072954 Registered office: Mortimer House, 37-41 Mortimer Street, London W1T 3JH, UK



Soil and Sediment Contamination: An International Journal

Publication details, including instructions for authors and subscription information:

<http://www.informaworld.com/smpp/title-content=t713401148>

An Analytical Modeling Approach for Evaluation of Capping of Contaminated Sediments

David J. Lampert ^a; Danny Reible ^a

^a Department of Civil, Architectural, Environmental Engineering, The University of Texas at Austin, Austin, TX, USA

Online Publication Date: 01 July 2009

To cite this Article Lampert, David J. and Reible, Danny(2009)'An Analytical Modeling Approach for Evaluation of Capping of Contaminated Sediments',Soil and Sediment Contamination: An International Journal,18:4,470 — 488

To link to this Article: DOI: 10.1080/15320380902962387

URL: <http://dx.doi.org/10.1080/15320380902962387>

PLEASE SCROLL DOWN FOR ARTICLE

Full terms and conditions of use: <http://www.informaworld.com/terms-and-conditions-of-access.pdf>

This article may be used for research, teaching and private study purposes. Any substantial or systematic reproduction, re-distribution, re-selling, loan or sub-licensing, systematic supply or distribution in any form to anyone is expressly forbidden.

The publisher does not give any warranty express or implied or make any representation that the contents will be complete or accurate or up to date. The accuracy of any instructions, formulae and drug doses should be independently verified with primary sources. The publisher shall not be liable for any loss, actions, claims, proceedings, demand or costs or damages whatsoever or howsoever caused arising directly or indirectly in connection with or arising out of the use of this material.

An Analytical Modeling Approach for Evaluation of Capping of Contaminated Sediments

DAVID J. LAMPERT AND DANNY REIBLE

Department of Civil, Architectural, Environmental Engineering,
The University of Texas at Austin, Austin, TX, USA

An analytical design tool is developed to predict performance of a cap for containment of contaminated sediments. Transient conditions within a cap can be modeled by advection, diffusion, and reaction within the typically homogeneous chemical isolation layer for which analytical models exist. After contaminant penetration of the chemical isolation layer, a steady state model is proposed that incorporates pore water advection and diffusion, sediment erosion and deposition, sediment re-working and pore water pumping via bioturbation, and reaction. The steady state model allows the complexities of the biologically active layer to be considered while maintaining an analytical form for convenient and rapid evaluation. In this paper, the model framework, behavior, and limitations are presented.

Keywords Capping, contaminated sediments, modeling

Introduction

Remediation of contaminated sediments is one of the most challenging problems in environmental engineering today. One of the primary risks associated with contaminated sediments is bioaccumulation in benthic organisms, which is a route of entry into the food chain. Thus an important goal of sediment remediation is reducing concentrations to these organisms.

Few alternatives exist for management of contaminated sediments. One promising technology for reducing exposure and risk to contaminated sediments *in situ* is through the use of capping with clean media. Capping with clean media has been shown to reduce surficial sediment concentrations in the lab and to agree well with traditional mass transport models (Thoma et al., 1991). In a field study, Azcue et al. (1998) found that the flux of metals was reduced significantly one year after capping. Zeman and Patterson (1997) discuss the successful implementation of a sand cap in Hamilton Harbor, Ontario, Canada. A capping project in the St. Paul Waterway near Tacoma, Washington, successfully demonstrated habitat restoration (Parametrix, 1998). Ten years of monitoring showed minimal cap disturbance and the ability of capping to contain contaminants. As an added benefit, sand capping restored shallow-water habitat that had been reduced by 90% over the past

Address correspondence to Danny Reible, Bettie Margaret Smith Professor of Environmental Health Engineering, Department of Civil, Architectural, Environmental Engineering, The University of Texas at Austin, 1 University Station C1786, Austin, TX 78712-0273, USA. E-mail: reible@mail.utexas.edu

100 years. Simpson et al. (2002) found that capping was successful at reducing metal fluxes, particularly due to organism-induced mixing (bioturbation) in the clean cap material rather than in the sediments.

The primary purposes of a cap over contaminated sediments are:

1. Armoring contaminated sediments to ensure they are not re-suspended in high flow conditions.
2. Physically isolating contaminated sediments from benthic organisms that typically populate only the upper few cm of sediment.
3. Providing resistance to transport processes that result in chemical release from the sediments.

Because many sediment contaminants are highly sorptive, their migration through a cap can be retarded due to accumulation on the clean cap material. A portion of the cap is typically compromised by the following processes: intermixing between sediment and the lower layer of the cap, expression of contaminated pore water by consolidation of underlying sediment, and bioturbation (organism-related mixing) of the near surface layer. The remaining layer is termed the chemical isolation layer. It has been estimated that the time for typical sediment contaminants to migrate through strongly sorbing chemical isolation layers may be hundreds or thousands of years (Murphy et al., 2006). For other less sorbing caps where the breakthrough time is shorter, capping can serve as a mass transport resistance to reduce the steady state flux and surficial concentrations near the sediment-water interface.

Evaluation and design of sediment caps require a model to predict the relationship of design parameters to chemical fate and transport processes that take place within the contaminated sediment cap containment system. Chemical migration in porous containment layers can be estimated using a transient advection-diffusion model as described by Bear (1972). For example, numerous approaches to the transport of contaminants through soil containment layers have been presented (e.g. Rowe and Booker, 1985; Rubin and Rabideau, 2000; Malusis and Shackelford, 2002). The majority of this work has been applied to soil slurry liners, which differ from sediment caps in several important ways.

The top of the sediment cap (hereafter referred to as the bioturbation layer) is subject to significantly different transport processes and rates than in the underlying cap layer and may exhibit significantly different physical and chemical characteristics, such as increased organic carbon content and sharp gradients in redox conditions. The organisms that reside in this zone also re-work sediment particles; this process significantly affects chemical transport. It is also within this zone that chemical reactivity is highest due to the exchange of nutrients, labile organic matter, and electron acceptors with the overlying water. The thickness of the cap may increase due to deposition or decrease due to erosion. Finally, mass transport at the sediment-water interface requires different boundary conditions than those used in soil slurries due to the presence of turbulent motion in the overlying surface water.

The EPA has provided guidance for *in situ* cap design (Palermo et al., 1998). The important considerations for cap design are minimizing erosion, reducing contaminant flux to biological receptors, and providing appropriate thickness to account for consolidation of the surficial sediments. The EPA guidance document presents a simplistic approach for evaluating contaminant fluxes and concentrations in a sediment cap. In this approach, the transient migration and flux through the cap system is assumed to be controlled by the chemical isolation layer and estimated by advection or diffusion. This approach does not include

important processes such as degradation and cannot predict contaminant concentrations or fluxes in the biologically active zone that is often of primary importance.

In this paper, an approach is presented to address these limitations. The result is a set of analytical models that can be used for initial screening and evaluation of sediment capping. Because the models are analytical, they can be used for rapid evaluation across a range of parameter values and can be used as a check for more complex numerical models, which may be applied to situations where no exact solution to the governing equations exists.

The models developed here enable an assessment of the concentration within the chemical isolation layer of a cap at any time, the time over which a cap is effective, and the potential exposure in the biologically active zone after contaminant penetration of the chemical isolation layer. The recommended approach is to employ a one-layer analytical transient model under the assumption of a semi-infinite domain until penetration of the chemical isolation layer occurs (i.e. while the assumption is valid). Upon penetration of the chemical isolation layer, the relatively rapid transport processes in the surface layer will subsequently quickly lead to steady state conditions. Under steady state conditions it is possible to consider the complexities of the upper boundary and still employ relatively simple analytical solutions to the chemical transport equations. Through use of a steady state model, it is possible to estimate the maximum contaminant concentration and flux that may ever be achieved within the biologically active zone. Thus the model can be used to determine a conservative cap design through estimation of the maximum concentrations and fluxes in the biologically active zone. The transient model presented here is equivalent to the one presented in the EPA guidance document (Palermo et al., 1998) but is included for completeness and discussion of how to adapt the model to evaluate other processes such as burial by sediment deposition. The combination of the transient model for the chemical isolation layer and the steady state model for the chemical isolation and bioturbation layers presented here provide:

1. the concentration profiles during contaminant migration through the chemical isolation layer;
2. the time of complete separation of the benthos from the contaminants;
3. the maximum concentration and flux that will be achieved after penetration of the cap assuming constant concentration in the underlying sediment.

Conceptual Model

The conceptual model divides the system into five different parts: the underlying sediment, the chemical isolation layer, the biologically active or bioturbation layer, the sediment-water interface (benthic boundary) layer, and the overlying water column. The placed cap layer, with thickness h_{cap} , consists of both the chemical isolation layer, with thickness h_{eff} , and the bioturbation layer, with thickness h_{bio} . The underlying sediment layer also includes the zone in which cap and sediment have intermixed during placement as the pore water concentrations in this region are essentially indistinguishable from those in the underlying sediment. In transient calculations any portion of the cap compromised by chemical migration due to consolidation should also be considered part of the underlying sediment (Palermo et al., 1998). Under steady state conditions, however, pore water expression and consolidation do not influence contaminant behavior.

The underlying sediment concentration is assumed constant. In a real sediment capping system, as contaminants are transported from the former sediment-water interface to the clean cap material the concentrations in the underlying sediment would change. The

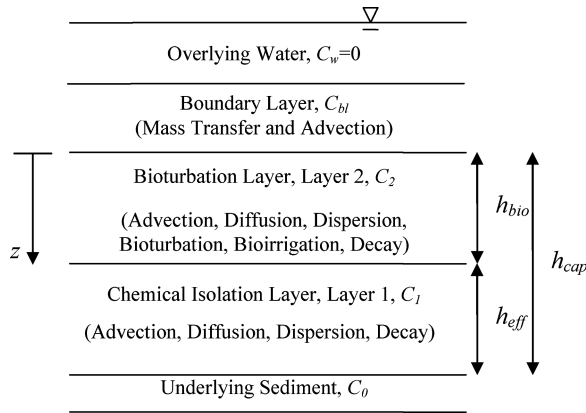


Figure 1. Sediment cap system and parameter definition.

concentration at the bottom of the cap would likely decrease with depletion of mass to the capping materials. However, as shown by Rabideau and Kandelwahl (1998), the most conservative boundary condition for the underlying contaminated material in a containment system is constant concentration. Any change in the actual concentration would likely be a decrease as mass is lost to the cap material, which provides further conservatism to this assumption. An alternative to constant concentration in the sediment would be to model the entire sediment layer; this approach is more robust but would require numerical simulation to describe behavior in the sediment column and capping layer.

The transport processes in the chemical isolation layer are advection, diffusion/dispersion, and decay. For the bioturbation layer, bioturbation-induced movement of particles and bioirrigation of pore water are also considered. Bioturbation-related processes are considered quasi-diffusive and hence are assumed to increase the effective diffusion/dispersion coefficient. Transport through the aqueous boundary layer is dictated by the benthic boundary layer mass transfer coefficient (Boudreau and Jorgensen, 2001). Benthic boundary layer mass transfer is controlled by the turbulence in the overlying water. For river systems, this process is controlled by parameters such as current and water depth. In lake systems, this coefficient is typically controlled by lake mixing processes. Imberger and Hamblin (1982) provide an excellent overview of mechanisms of mixing processes in lakes; mechanisms of lake mixing including wind, wave and buoyancy-driven circulation. Figure 1 shows the conceptual model of the sediment cap system along with the model coordinate system.

Due to the low solubility of most sediment contaminants, the bulk sediment loading, W (mass of contaminant on solid phase per mass of solid phase), is the parameter that is typically used for quantifying contaminant levels in sediments instead of the pore water (mobile phase) concentration. W depends upon the sorption properties of the sediment or cap layer, however, and is potentially discontinuous while the pore water concentration is both continuous across interfaces and directly represents the mobile phase contaminants. Under the assumption of linear partitioning, the bulk sediment loading can be related to the pore water concentration, C , through the following relationship, assuming local equilibrium:

$$W = K_d C \tag{1}$$

Where K_d represents the effective sediment-water partition coefficient in the cap material. It is generally reasonable to assume local equilibrium with the pore water at some effective (measured) partition coefficient due to the relatively slow contaminant migration rates within the sediment bed. Of critical importance to the rate of migration of contaminants in the cap material is the ratio of the total concentration (mass per unit volume) in the porous cap matrix to that of the mobile phase concentration, or the retardation factor, R_1 (defined in terms of model parameters subsequently).

For organic contaminants, the contaminant partition coefficient is often estimated as the product of the fraction organic carbon f_{oc} and the organic carbon partition coefficient, K_{oc} . This is likely a crude assumption in the underlying sediment that has been shown to exhibit a different relationship due to desorption resistance (McGroddy and Farrington, 1995) but may be a good assumption for the cap material and the new (clean) sediment. For typical sand, the organic carbon fraction tends to be less than 0.1%. At these low organic carbon contents, mineral sorption tends to become important even for organic compounds; so the assumption of 0.01–0.1% organic carbon is likely a lower bound to the effective sorption of organic contaminants on sandy cap materials (Schwarzenbach et al., 2003).

Due to the limited sorptive capacity of sand caps, permeable adsorptive caps, sometimes referred to as active caps, have been proposed (Reible et al., 2007; McDonough et al., 2007). These caps may contain organic sorbents such as activated carbon, organo-modified clays, coke, or metal sorbents such as apatite. These could be incorporated in the modeling approach herein by using the appropriate effective partition coefficient, although for sorbents exhibiting nonlinear sorption behavior, such as activated carbon, the model results are only approximate. Permeable reactive caps with enhanced degradation characteristics have also been proposed, although their long-term efficacy has not been demonstrated.

The approach presented here is developed using pore water concentrations, which represent the mobile contaminant phase in a stable cap and may be more closely related to the contaminants available for bioaccumulation (e.g. Lu et al., 2006; Beckles et al., 2007). Based on the assumptions listed above, the domain of the model for the cap system consists of two layers: the chemical isolation layer and the bioturbation layer. The underlying sediment, benthic layer, and overlying water are utilized to develop boundary conditions.

Transient Model and Containment Breakthrough Time

The governing transport equation for the chemical isolation layer (Layer 1) is:

$$R_1 \frac{\partial C_1}{\partial t} - U \frac{\partial C_1}{\partial z} = D_1 \frac{\partial^2 C_1}{\partial z^2} - \varepsilon_1 \lambda_1 C_1 \quad (2)$$

Where C_1 is the pore water concentration in the isolation layer, z is the depth downward from the cap-water interface, t is the time, λ_1 is the decay rate constant, R_1 is the retardation factor in the layer (defined here as the ratio of the total concentration to that in the mobile phase), U is the effective advective velocity (assumed to be directed upward although a negative value is still appropriate), and ε_1 is the porosity in the layer. The decay of the contaminant is assumed to be first-order and to occur only in the pore water. Thus seemingly large decay rate constants may have only a minimal impact on mass degradation rate since only a small fraction of the contaminants resides in the pore water. The strong sorptive nature of most sediment contaminants limits the rate of degradation due to limited bioavailability (Hyun et al., 2006; Beckles et al., 2007).

For an active capping system, the chemical isolation layer must be further subdivided into sand and active layer(s), which would require introduction of additional governing and appropriate boundary conditions (continuity of concentration and flux) for each layer. The transport equation for each layer would be essentially the same, with the primary difference arising from the retardation term. For sorbing cap materials such as organoclays and peats that obey linear partitioning relationships, the governing equations would differ only in the value of the retardation factor. For a nonlinear sorption model (such as activated carbon) the governing equations would be almost the same, although the retardation factor would no longer be constant but a function of concentration. Note that in either case at steady state the sorption term disappears and the steady state model developed herein still applies.

For the chemical isolation layer, the bottom boundary condition is assumed to be a first-type or Dirichlet boundary with a concentration of C_0 :

$$C_1(z = h_{cap}) = C_0 \quad (4)$$

For modeling during the transient period, i.e. before significant penetration of the overlying biologically active layer, the chemical isolation layer may be approximated as semi-infinite, which produces the second boundary condition:

$$\lim_{z \rightarrow -\infty} \frac{\partial C_1}{\partial z} = 0 \quad (5)$$

For an initially clean cap, the initial condition is:

$$C_1(t = 0) = 0 \quad (6)$$

The transient behavior can be estimated using an analytical solution to Equation (2) subject to the conditions in (4), (5), and (6). The solution to this problem was presented by van Genuchten (1981):

$$C(z, t) = \frac{C_0}{2} \left\{ \begin{array}{l} \exp \left[\frac{(U - u)(h_{cap} - z)}{2D_1} \right] \operatorname{erfc} \left[\frac{R_1(h_{cap} - z) - ut}{\sqrt{4D_1 R_1 t}} \right] + \\ \exp \left[\frac{(U + u)(h_{cap} - z)}{2D_1} \right] \operatorname{erfc} \left[\frac{R_1(h_{cap} - z) + ut}{\sqrt{4D_1 R_1 t}} \right] \end{array} \right\} \quad (7)$$

$$u = \sqrt{U^2 + 4\varepsilon\lambda_1 D_1}$$

The transient model (7) is appropriate until the time when the isolation layer is completely compromised by migration from below by the processes of advection, diffusion, and dispersion. For a diffusion-dominated problem with no decay, Equation (7) reduces to the well-known complementary error function solution:

$$C = C_0 \operatorname{erfc} \left(\frac{R_1^{0.5}(h_{cap} - z)}{\sqrt{4D_1 t}} \right) \quad (8)$$

This equation can be assumed valid while the concentration at the boundary of the containment and bioturbation layers is small; the complementary error function is equal to about 0.01 when the argument is about two (i.e. when the concentration predicted at the top of the cap layer is 1% of the underlying sediment concentration). Therefore, a conservative

estimate of penetration time for a diffusion-dominated system is:

$$t_{diff} = \frac{R_1 h_{eff}^2}{16D_1} \quad (9)$$

For an advection-dominated system with no decay, Equation (7) reduces to a front or step function with velocity U/R_1 ; hence an appropriate time for penetration is:

$$t_{adv} = \frac{R_1 h_{eff}}{U} \quad (10)$$

Because advection and diffusion/dispersion act together to compromise the chemical isolation layer, the time for penetration of the layer can be estimated by assuming the processes act in parallel. Thus, a time scale characteristic of the advective-diffusive migration through the isolation layer can be written:

$$t_{adv/diff} \approx \frac{1}{1/t_{diff} + 1/t_{adv}} \approx \frac{1}{16D_1/(R_1 h_{eff}^2) + U/(R_1 h_{eff})} \approx \frac{R_1 h_{eff}^2}{16D_1 + U h_{eff}} \quad (11)$$

For times long compared to $t_{adv/diff}$ a steady state model will describe concentrations and fluxes in the cap. The transient time through the biologically active layer is typically negligible compared to that in the chemical isolation layer due both to its small thickness (5–15 cm) and the rapid sediment reworking and contaminant migration rates in this layer. Thus for times long compared to $t_{adv/diff}$, a steady state model is applicable to both the chemical isolation layer and the overlying bioturbation layer.

To verify the applicability of the relatively simple approach in Equation (11), the time required to achieve a concentration at the top of the chemical isolation layer equal to 1% of the concentration at the sediment-cap interface ($C/C_0 = 0.01$) and the time required to achieve a flux at the top of the chemical isolation layer 1% of the flux at the sediment-cap interface, $F/F_0 = 0.01$, were calculated from a full advection-diffusion model and compared to the prediction of Equation (11). The ratio of the flux at the top of the chemical isolation layer to the flux at the sediment-cap interface was calculated by,

$$F/F_0 = \frac{F(z = h_{bio}, t)}{F(z = h_{cap}, t)} = \frac{UC(z = h_{bio}, t) + D_1 \frac{\partial C(z=h_{bio}, t)}{\partial z}}{UC(z = h_{cap}, t) + D_1 \frac{\partial C(z=h_{cap}, t)}{\partial z}} \quad (12)$$

The results were computed for dimensionless time, τ , in terms of the dimensionless Peclet number, Pe , which is defined as:

$$\tau = \frac{t D_1}{R_1 h_{eff}^2} \quad (13)$$

$$Pe = \frac{U h_{eff}}{D_1} \quad (14)$$

The times to concentration or flux equal to 1% of that at the bottom of the sediment were calculated for two solutions to Equation (2), a semi-infinite cap layer and a finite cap layer with a zero concentration at the cap-water interface ($z = 0$). The calculated times were identical for both boundary conditions, since the top boundary does not affect the solution until significant penetration of the complete chemical isolation layer has occurred. The results in Figure 2 show that the prediction of breakthrough based on Equation (11)

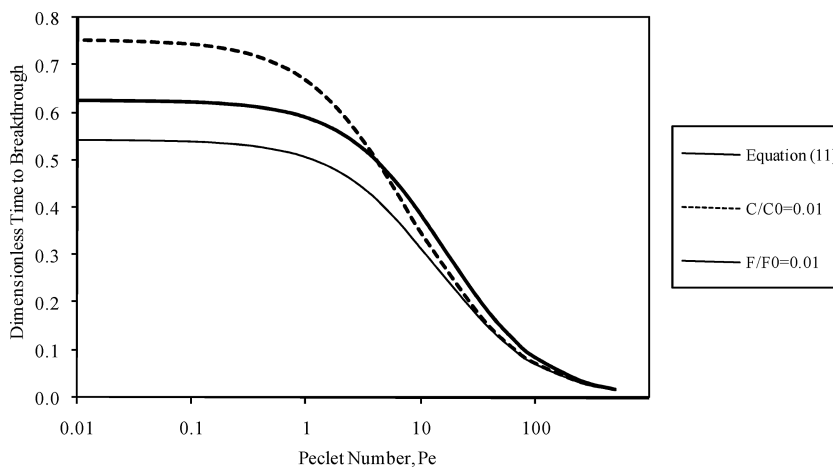


Figure 2. Comparison of breakthrough time approaches. Time required to achieve concentration (C) or flux (F) at top of the chemical isolation layer equal to 1% of the concentration (C_0) or flux (F_0) at the bottom of the layer from full solutions of Equation (2).

fall between those based on flux and concentration at low Pe , while at high Pe Equation (11) slightly over-predicts breakthrough for both cases. The maximum over prediction compared with an F/F_0 value of 0.01 basis was 23%. It appears that Equation (11) provides a reasonable estimate for penetration time for a non-reactive solute over the entire range of Pe and, in particular, provides a good estimate of the time before conditions in the biologically active layer will begin to influence concentration profiles within the cap. Any decay would retard the breakthrough time and as a result the predictions from Equation (11) would be conservative.

The Bioturbation Layer and the Sediment-Water Interface

The transport equation for the bioturbation layer has the same general form as the chemical isolation layer; however, the processes of bioturbation are assumed to increase the effective diffusion/dispersion coefficient. The decay rate and retardation factor in the bioturbation layer may also be different than those observed in the chemical isolation layer. The Darcy velocity U must be the same for water (assumed incompressible). The transport equation for the bioturbation layer (Layer 2) is:

$$R_2 \frac{\partial C_2}{\partial t} - U \frac{\partial C_2}{\partial z} = D_2 \frac{\partial^2 C_2}{\partial z^2} - \varepsilon_2 \lambda_2 C_2 \quad (15)$$

Where C_2 is the concentration in the bioturbation layer, R_2 is the retardation factor in the bioturbation layer, D_2 is the effective diffusion/dispersion coefficient for the bioturbation layer, λ_2 is the decay rate for the bioturbation layer, and ε_2 is the porosity in the layer.

At the interface between the chemical isolation layer and the bioturbation layer, the concentrations and fluxes in the two layers must be equal. Recognizing that the advective flux is the same in each layer, the following represent appropriate boundary conditions at the interface between the bioturbation and underlying containment layers (here C_{bio} is

defined as the concentration at the interface):

$$C_1(z = h_{bio}) = C_2(z = h_{bio}) = C_{bio} \quad (16)$$

$$-D_1 \frac{\partial C_1(z = h_{bio})}{\partial z} = -D_2 \frac{\partial C_2(z = h_{bio})}{\partial z} \quad (17)$$

The boundary condition at the cap-water interface is the most complex, as it essentially requires the effluent boundary condition from a porous medium, which has a long history and is the subject of many papers (Hulbert, 1944; Danckwerts, 1953; Wehner and Wilhelm, 1956). The concept of a benthic boundary layer mass transfer resistance composed of a laminar (diffusive) sublayer above the sediment-water interface has long been used for modeling mass transport from surficial sediments and is widely accepted in soil and marine science (see Boudreau, 1997). A complete mass balance on the interface results in the following expression (Boudreau and Jorgensen, 2001):

$$UC_2(z = 0^+) - D_2 \frac{\partial C_2(z = 0^+)}{\partial z} + R' = U_{bl}C_{bl}(z = 0^-) + k_{bl}(C_{bl} - C_w) \quad (18)$$

Where R' represents transport of contaminants from the exposed surficial sediment to the overlying water, and U_{bl} , k_{bl} , and $C_{bl}(z)$ represent the effective advective velocity, effective mass transfer coefficient, and concentration in the benthic boundary layer, respectively. The value of R' has been shown to be small relative to the other processes (Boudreau and Jorgensen, 2001). The effective mass transfer coefficient in the benthic boundary layer can also be thought of as a diffusion in a laminar sublayer of thickness, δ , separating the cap-water interface from the bulk overlying water of concentration, C_w :

$$k_{bl}(C_{bl} - C_w) = D_{bl} \frac{C_{bl} - C_w}{\delta} \quad (19)$$

The value in the overlying surface water is taken to be zero without loss of generality (all other concentrations are taken relative to this surface water concentration). Combining these assumptions results in the following boundary condition of the third kind (Boudreau and Jorgensen, 2001):

$$D_2 \frac{\partial C_2(z = 0^+)}{\partial z} = k_{bl}C_{bl}(z = 0^-) = k_{bl}C_2(z = 0^+) \quad (20)$$

Steady State Model

To evaluate the concentrations in the combined containment and bioturbation layers, the relative importance of the different transport mechanisms can be evaluated with the following dimensionless numbers, which are defined as:

$$Pe_1 = \text{Peclet number in chemical isolation layer} = \frac{U h_{eff}}{D_1} = \frac{\text{Rate of advection}}{\text{Rate of diffusion}} \quad (21)$$

$$Da_1 = \text{Damkohler number in chemical isolation layer} = \frac{\varepsilon_1 \lambda_1 h_{eff}^2}{D_1} = \frac{\text{Rate of decay}}{\text{Rate of diffusion}} \quad (22)$$

$$Pe_2 = \text{Peclet number in bioturbation layer} = \frac{U h_{bio}}{D_2} \tag{23}$$

$$Da_2 = \text{Damkohler number in bioturbation layer} = \frac{\varepsilon_2 \lambda_2 h_{bio}^2}{D_2} \tag{24}$$

$$Sh = \text{Sherwood number at cap-water interface} = \frac{k_{bl} h_{bio}}{D_2} = \frac{\text{Rate of mass transfer}}{\text{Rate of diffusion}} \tag{25}$$

Under steady state conditions the time derivatives in Equations (2) and (15) disappear. Equations (2) and (15) can be re-written in terms of the dimensionless parameters introduced above:

$$h_{eff}^2 \frac{\partial^2 C_1}{\partial z^2} + Pe_1 h_{eff} \frac{\partial C_1}{\partial z} - Da_1 C_1 = 0 \tag{26}$$

$$h_{bio}^2 \frac{\partial^2 C_2}{\partial z^2} + Pe_2 h_{bio} \frac{\partial C_2}{\partial z} - Da_2 C_2 = 0 \tag{27}$$

By assuming a solution of an exponential form, the general solution of (26) and (27) can be obtained. At steady state the concentrations at the boundaries of the domain are constant and assumed to have values of C_0 at the cap-sediment interface, C_{bio} at the boundary of the chemical isolation and bioturbation layers, and C_{bl} at the cap-water interface. The solutions to the governing ordinary differential equations are thus:

$$C_1 = \frac{C_{bio} e^{-\frac{Pe_1}{2}} - C_0 e^{-\beta}}{2 \sinh \beta} \exp \left[\left(\frac{Pe_1}{2} + \beta \right) \frac{h_{cap} - z}{h_{eff}} \right] + \frac{C_0 e^{\beta} - C_{bio} e^{-\frac{Pe_1}{2}}}{2 \sinh \beta} \times \exp \left[\left(\frac{Pe_1}{2} - \beta \right) \frac{h_{cap} - z}{h_{eff}} \right] \tag{28}$$

$$\beta = \sqrt{\frac{Pe_1^2}{4} + Da_1}$$

$$C_2 = \frac{C_{bl} e^{-\frac{Pe_2}{2}} - C_{bio} e^{-\gamma}}{2 \sinh \gamma} \exp \left[\left(\frac{Pe_2}{2} + \gamma \right) \frac{h_{bio} - z}{h_{bio}} \right] + \frac{C_{bio} e^{\gamma} - C_{bl} e^{-\frac{Pe_2}{2}}}{2 \sinh \gamma} \times \exp \left[\left(\frac{Pe_2}{2} - \gamma \right) \frac{h_{bio} - z}{h_{bio}} \right] \tag{29}$$

$$\gamma = \sqrt{\frac{Pe_2^2}{4} + Da_2}$$

The values of C_{bio} and C_{bl} can be determined by applying the boundary conditions (17) and (20) to Equations (28) and (29):

$$C_{bio} = \frac{C_0 \frac{Pe_2}{Pe_1} e^{\frac{Pe_1}{2}} \beta \sinh \gamma}{\frac{Pe_2}{Pe_1} \beta \cosh \beta \sinh \gamma + \gamma \sinh \beta \cosh \gamma - \frac{\gamma^2 \sinh \beta}{(Sh + \frac{Pe_2}{2}) \sinh \gamma + \gamma \cosh \gamma}} \tag{30}$$

$$C_{bl} = \frac{C_0 e^{\frac{Pe_1 + Pe_2}{2}}}{\left(\frac{Pe_1}{2} + \frac{Pe_1 Sh}{Pe_2}\right) \frac{\sinh \beta \cosh \gamma}{\beta} + \left(\frac{Pe_2}{2} + Sh\right) \frac{\cosh \beta \sinh \gamma}{\gamma} + \frac{Pe_1 \gamma \sinh \gamma \sinh \beta}{Pe_2 \beta} + \cosh \beta \cosh \gamma} \quad (31)$$

The concentration of contaminants in the bioturbation layer is of particular interest, as benthic organisms in the layer often provide the primary route of entry of contaminants into the food chain. Hence, another important parameter is the average concentration in the bioturbation layer. This concentration can be used to evaluate the potential long-term effectiveness of a sediment cap. Integrating Equation (29) over the bioturbation layer and dividing by the depth of the bioturbation layer provides the average value:

$$(C_{bio})_{avg} = \frac{C_{bl} e^{-\frac{Pe_2}{2}} - C_{bio} e^{-\gamma} e^{\frac{Pe_2}{2} + \gamma} - 1}{2 \sinh \gamma} \frac{\frac{Pe_2}{2} + \gamma}{\frac{Pe_2}{2} + \gamma} + \frac{C_{bl} e^{\gamma} - C_{bio} e^{-\frac{Pe_2}{2}} e^{\frac{Pe_2}{2} - \gamma} - 1}{2 \sinh \gamma} \frac{\frac{Pe_2}{2} - \gamma}{\frac{Pe_2}{2} - \gamma} \quad (32)$$

The average solids loading in the bioturbation layer, $(W_{bio})_{avg}$, can be determined from the partitioning relationship between the pore water and the sediment, where $(f_{oc})_{bio}$ is the expected fraction of organic carbon in the newly deposited sediment:

$$(W_{bio})_{avg} = (f_{oc})_{bio} K_{oc} (C_{bio})_{avg} \quad (33)$$

Additionally, the flux to the overlying water column, J , may be of interest. This can be evaluated by:

$$J = (k_{bl} + U) C_{bl} \quad (34)$$

Numerical Model Comparison

To check the validity of the analytical solutions for both the transient and steady state models, Equations (2) and (15) subject to boundary conditions (4), (16), (17), and (20) and initial condition (6) were solved independently by numerical analysis. A finite differencing scheme using the Crank-Nicolson method (Crank and Nicolson, 1947) with a forward difference for the advection term and central difference for the diffusion term was employed for the analysis. Reasonable estimates for the parameters were assumed for two cases using the methods described above. Simulations were performed for low and high values of Pe_1 . Figure 3 shows that results of the simulations and the analytical solutions (7) and (28–31) are equivalent. Thus the analytical solutions can be used to predict concentrations within the chemical isolation layer during the transient period and to predict the steady state behavior. For estimation of cap behavior in the transition time between $\tau_{adv/diff}$ and steady state, a numerical model must be employed to approximate the solution to the governing equations.

Characterization of Transport Parameters

The factors R_1 and R_2 as defined here are the ratios of the total concentration in an elementary sediment volume (stationary phase) to that in the pore water (mobile phase) for the containment and bioturbation layers, respectively. A significant proportion of the total concentration in the pore water may be present in colloidal organic matter (Baker et al., 1985; Chin and Gschwend, 1992; Schlautman and Morgan, 1993). Chin and

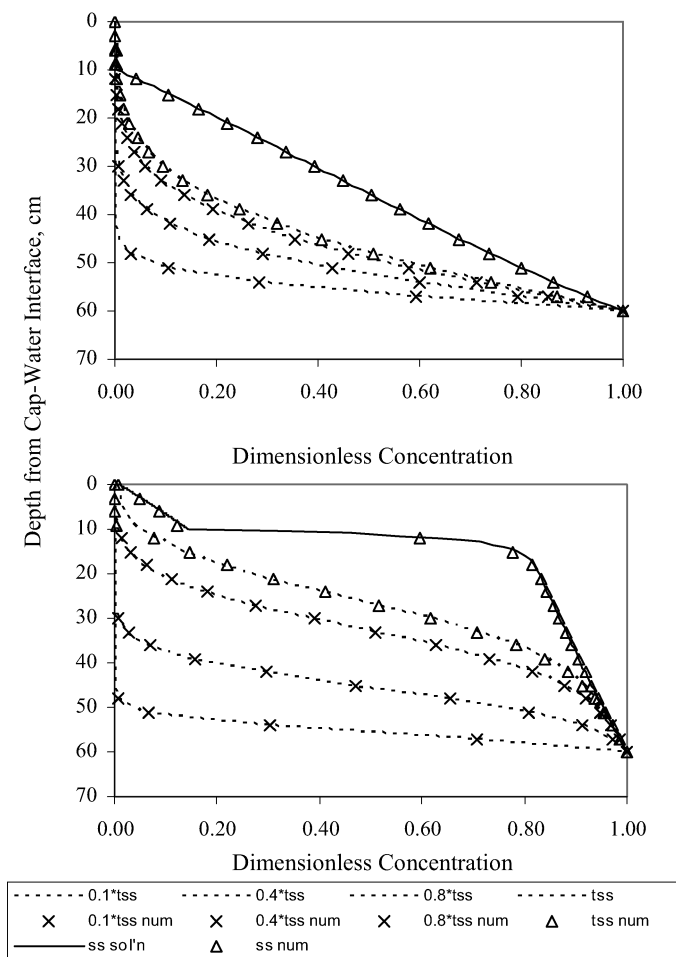


Figure 3. Transient and steady state concentration profiles throughout cap: comparison of analytical with numerical solution. Top: low flow ($Pe_1 = 0.66$); Bottom: high flow ($Pe_1 = 32.8$).

Gschwend (1992) found this relationship to be linear. Thus partitioning onto the total organic carbon in the pore water, ρ_{DOC} , with a colloidal organic carbon partition coefficient, K_{DOC} , serves to increase the effective solubility of the compounds. Coupling this assumption with the linear partitioning onto the cap material, and recognizing that the fractional organic carbon in the bioturbation layer, $(f_{oc})_{bio}$ will over time be different from that in the containment layer, $(f_{oc})_{eff}$, produces the following relationships for R_1 and R_2 in terms of ρ_{oc} , K_{DOC} , ε , the particle density ρ_P , and K_{oc} :

$$R_1 = \frac{\varepsilon_1 + \varepsilon_1 \rho_{DOC} K_{DOC} + (1 - \varepsilon_1) \rho_P (f_{oc})_{eff} K_{oc}}{1 + \rho_{DOC} K_{DOC}} \quad (35)$$

$$R_2 = \frac{\varepsilon_2 + \varepsilon_2 \rho_{DOC} K_{DOC} + (1 - \varepsilon_2) \rho_P (f_{oc})_{bio} K_{oc}}{1 + \rho_{DOC} K_{DOC}} \quad (36)$$

The Darcy velocity, U , here accounts for both groundwater upwelling and the effect of erosion/deposition. In a coordinate system fixed relative to the cap-water interface,

deposition or erosion changes the net advective flux. Because particle deposition effectively buries both pore water and solid associated contaminants, the effective advective flux also encompasses both. The effective advective velocity associated with both the Darcy pore water upwelling, V , the velocity of sediment deposition, V_{dep} , and the retardation factor applicable to the cap-sediment layer, R , is:

$$U = V - RV_{dep} \quad (37)$$

Note that although new sediment is typically deposited at the cap-water interface, the mixing in this region is rapid and governed by bioturbation, or particle mixing processes that are not subject to retardation by pore water transport. Transient migration in the underlying cap containment layer is delayed by burial with new sediment and the apparent shifting of the sediment interface. For estimation of the time delay associated with burial, R in Equation (37) can be conservatively estimated by R_1 (the retardation in the underlying sand), despite the fact that typically more sorbing sediment is deposited at the cap-water interface (characterized by R_2). In the event of net erosion rather than deposition the value of V_{dep} is negative. For the purposes of conservative estimates and due to uncertainties over future deposition rates, it is often assumed that the deposition of new sediment is negligible despite the fact that contaminated sediments have typically accumulated in net depositional areas.

The advective flow is perhaps the most important parameter in this analysis, as it will dominate in many natural systems. The flow may be upward or downward, in which case the value is negative. In the absence of direct measurements, the flow may be modeled using Darcy's Law. This approach requires an understanding of the hydrogeology of the area, including the effective hydraulic conductivity of the sediment/groundwater system and the local groundwater elevation levels driving the flow rate. For direct measurement of groundwater flux, seepage meters such as the one described by Lee (1977) may be used to measure the groundwater seepage rate. Alternatively, Cook et al. (2003) describe methods for estimating flux using different kinds of tracers. The local effective hydraulic conductivity for the sediment-cap system is dictated by the layer with the lowest hydraulic conductivity. The hydraulic conductivity of the system is generally unaffected by the presence of a cap (since it is often composed of relatively coarse granular media) although the cap could be constructed to control permeability or may cause consolidation in the underlying sediment, reducing its permeability.

The value of D_1 is the sum of the diffusion and dispersion coefficients. Diffusion through granular porous media is often characterized by an effective diffusion coefficient D_{diff} given by the molecular diffusivity D_w times the porosity (the available diffusion area) and divided by a hindrance parameter (the lengthening of the diffusion path by the media). The model of Millington and Quirk (1961), where the hindrance parameter is taken to be the porosity to the negative one-third power, is widely used for diffusion in granular porous media such as a typical sand cap:

$$D_{diff} = \varepsilon_1^{\frac{4}{3}} D_w \quad (38)$$

Boudreau (1997) suggests an alternative that may be more applicable for fine-grained sediments:

$$D_{diff} = \frac{\varepsilon_1 D_w}{1 - \ln \varepsilon_1^2} \quad (39)$$

The molecular diffusivity is a function of temperature and molecular weight and can be estimated from the literature (e.g. Lyman et al., 1990). Mechanical dispersion characterized by D_{disp} of the contaminant through the cap can be modeled as the product of the velocity through the cap and some length scale defined as the dispersivity, α :

$$D_{disp} = \alpha U \quad (40)$$

Thus, the effective diffusion/dispersion coefficient in the containment layer can be determined by:

$$D_1 = \varepsilon_1^{\frac{4}{3}} D_w + \alpha U \quad (41)$$

After placement of a sediment cap, new sediment is deposited at the cap surface. As this deposition occurs, the top of the sediment cap is re-colonized by benthic organisms (worms and other macro invertebrates). These organisms blend the sediments at the top of cap, resulting in relatively rapid transport of contaminants from the bottom of the layer to the overlying water. Provided that the movement of particles and pore water by these organisms is essentially random, the length scale of the movement of the particles is smaller than that being studied (i.e. the cap thickness), and time scale between mixing events is smaller relative to other processes, the transport processes can be taken as quasi-diffusive (Boudreau, 1986). The diffusion-like mixing of particles is known as bioturbation, while the diffusion-like mixing of pore water is bioirrigation. These processes increase diffusion/dispersion coefficient from the containment layer, D_1 , to that in the bioturbation layer, D_2 . The flux of a chemical species, J_{bio}^p , associated with the diffusion of these particles associated with a bioturbation coefficient of D_{bio}^p and a solid-phase concentration (mass of chemical species per unit volume sediment particle) of M is:

$$J_{bio}^p = -D_{bio}^p \frac{\partial M}{\partial z} \quad (42)$$

If the time for movement of the sediment particles plus the time between particle movement events is large compared with that of desorption of contaminants, local equilibrium can be assumed, and the value of M can be re-written in terms of pore water concentration (noting that ε , ρ_p , $(f_{oc})_{bio}$, and K_{oc} are independent of depth):

$$J_{bio}^p = -D_{bio}^p (1 - \varepsilon) \rho_p (f_{oc})_{bio} K_{oc} \frac{\partial C_2}{\partial z} \quad (43)$$

In addition to particle mixing, organisms also irrigate the surficial sediments through direct pore water exchange from the underlying sediments to the overlying water. The transport of contaminants associated with this process can be modeled by:

$$J_{bio}^{pw} = -D_{bio}^{pw} \frac{\partial C}{\partial z} \quad (44)$$

Thus the processes of bioturbation and bioirrigation serve to increase the effective diffusion/dispersion coefficient. The values of D_{bio}^p and D_{bio}^{pw} can be measured using radioactive tracers, such as described by McCaffree et al. (1980). Thoms et al. (1995) provide an extensive review of measured biodiffusion coefficients at different locations in the United States. The effective diffusion coefficient for the bioturbation layer, D_2 , can be determined

from the following:

$$D_2 = D_1 + D_{bio}^{pw} + D_{bio}^p(1 - \varepsilon)\rho_P(f_{oc})_{bio}K_{oc} \quad (45)$$

The decay rates λ_1 and λ_2 are highly compound and site specific. The model taken here is based on first-order kinetics, which may not be appropriate as the degradation may depend on many factors other than the contaminant concentration but provides a relatively simple way of incorporating this important mechanism into a mathematical model. In the absence of a site-specific study, the literature may be used to estimate a degradation rates.

Transport at the cap-water interface is dictated by the benthic boundary layer mass transfer coefficient, which is a function of the turbulence and shear of the overlying water column. Boudreau and Jorgensen (2001) and Thibodeaux (1996) present empirical correlations for k_{bl} based on mixing conditions in the overlying water. The value of k_{bl} should be conservatively estimated, as its value directly affects the surficial sediment concentrations.

Steady State Model Behavior

The steady state model presented in (28–31) is a function of only the five parameters (21–25) and the depth of the two layers. To illustrate the behavior of the solution, consider a one-foot (30 cm) thick sand cap with an expected bioturbation depth of 10 cm. For Case I, consider a conservative ($Da_1 = Da_2 = 0$) contaminant, with $Sh = 10$ (minimal mass transfer limitations) and $D_2 = 10D_1$ ($Pe_2 = 0.05Pe_1$). Figure 4 shows the dimensionless concentration profiles for $0.1 < Pe_1 < 200$. For low Pe_1 , the solution approaches a straight line in each layer, which is the expected result of a diffusion-dominated steady state profile. The increased diffusivity in the bioturbation layer results in lower concentrations in that layer. This behavior makes sense physically because the increased mixing rate in the layer reduces the concentrations there (contaminants are transported more rapidly in the bioturbation layer). If advection dominates (high Pe_1), the concentration profile approaches unity; again this is the expected result for an advection problem at steady state. The deviation near the boundary layer is a result of the simplifying assumptions made in the formulation of the top boundary condition. For high advection a more appropriate boundary condition would be a zero gradient. However, the profiles still approach the expected result and provide a reasonable estimation of cap performance even under these conditions. Clearly, at steady state in a high upwelling velocity system a cap will have limited effectiveness.

Now consider a system with degradation (Case II). For simplicity, the Damkohler number in the chemical isolation layer is assumed to be four. The value of D_2 was again taken as $10D_1$, and again it is assumed that $Sh = 10$. The decay rate in the bioturbation layer is taken as ten times that in the chemical isolation layer, a reasonable assumption due to higher levels of nutrients, organic matter, and electron acceptors. These assumptions result in $Pe_2 = 0.05Pe_1$ and $Da_2 = 0.25Da_1 = 1$. Figure 4 shows the dimensionless concentration profiles for $0.1 < Pe_1 < 200$. When compared with the no decay situation, the concentration profiles are lower, as expected. In general, the graphs perform as anticipated mathematically. The concentrations in the bioturbation layer are significantly decreased versus the underlying sediment concentrations. Hence, if it can be proven that a contaminant will decay in a cap, capping is an extremely attractive alternative for remediation.

To evaluate the effects of mass transfer resistance on model output, consider the systems presented in Cases I and II with $Sh = 0.1$ rather than 10 (Cases III and IV). Figure 4 also shows the results for these parameters. For Case III, the concentrations in the cap are minimally reduced even when diffusion-dominated (low Pe_1). The performance

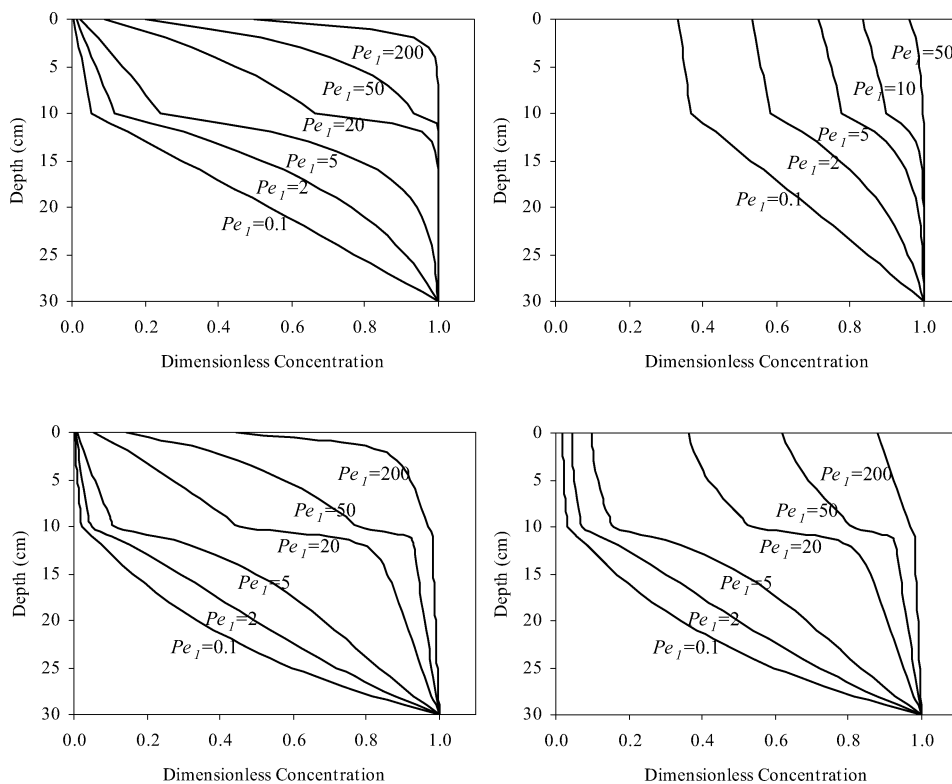


Figure 4. Steady state model behavior. Top left, Case I ($Da_1 = Da_2 = 0, Sh = 10$). Bottom left, Case II ($Da_1 = 4, Da_2 = 1, Sh = 10$). Top right, Case III ($Da_1 = Da_2 = 0, Sh = 0.1$). Bottom right, Case IV ($Da_1 = 4, Da_2 = 1, Sh = 0.1$). The dashed lines represent the interface between the chemical isolation and the bioturbation layers.

is as expected theoretically, with a linear profile in the containment layers at low Pe_1 , which approaches a uniform profile for high values of Pe_1 . In Case IV, the importance of decay on long term capping success is demonstrated. For a diffusion-dominated system, the bioturbation layer concentrations are drastically reduced over pre-cap levels, even with mass transfer resistance at moderately high advection ($Pe_1 = 5$). Again, as the upwelling velocity is increased, the cap performance is limited.

It is important to note that the model presents steady state concentrations, which may not be realized for many years. Capping may still be a viable option in a case where the transient migration through the containment layer is sufficiently long that natural attenuation processes not included in the models are expected to render the contaminants inconsequential. Steady state predictions beyond this time frame may not be considered important.

These results show the importance of the ground water upwelling velocity in the effectiveness of a cap. The upwelling velocity is a critical parameter in a transient analysis as well as it often controls the steady state flux. Upwelling velocities of the order of cm/day or more may be high enough to effectively negate the effectiveness of a cap even for moderately sorbing contaminants. In addition, the local equilibrium assumption may fail under the influence of extremely high upwelling. So, if capping is under consideration

for management of contaminated sediments, it is important for the designer to measure or make a good estimate of the upwelling velocity before making a final decision. Due to the inherent heterogeneity in this parameter, it is also important to evaluate a range of values of upwelling velocity for predicting concentrations that will be used in design and decision making.

The traditional material used for capping sediment is clean sand. However, as demonstrated by these modeling results, a passive sand cap may not be an effective long-term approach for contaminated sediment management for high seepage/low degradation systems. For this reason, one current research focus (Reible et al., 2007; McDonough et al., 2007) is on active capping; that is, capping with materials that may enhance sequestration/degradation in situ or decrease the seepage flow rates through a sediment cap.

Conclusions

In this article, the key processes controlling chemical migration in a cap isolation layer and in the overlying biologically active layer have been highlighted. A simple means for incorporating these processes into an analytical modeling approach has been developed. The approach is subject to a number of limitations. First, several of the models for individual processes are simplistic (e.g. deposition, linear pore water partitioning, first-order decay). The underlying sediment is assumed to maintain a constant concentration. A more robust approach to assessing the concentration in the sediment would be to model fate and transport within the layer based on an initial concentration profile. However, this approach would normally require a numerical simulation in the full-advection diffusion case. Finally, the model is based on two homogeneous layers. Predicting transient concentration profiles in more complex sediment caps with more than two homogeneous layers or with nonlinear sorption would require a more robust approach. The steady state model presented here, however, would still be valid provided the values of diffusion/dispersion coefficients and decay rates were the same. For predicting transient performance of a cap under these scenarios, a numerical solution to the governing equations would be required. The exact solutions presented here represent an important check for future models of this kind.

The model presented here allows calculation of the steady state concentration profile and flux in a sediment cap. When coupled with a transient model of advection, diffusion, and reaction in the chemical isolation layer, this approach forms a relatively simple means of evaluating sediment caps. If the steady state condition is sufficient for achieving remediation objectives, there is no need for a more complicated transient approach. A spreadsheet that computes the analytical model output is available at <http://www.cae.utexas.edu/reiblegroup/downloads.html> for interested parties.

References

- Azcue, J.M., Zeman, A.J., Mudroch, A., Rosa, F., and Patterson, T. 1998. Assessment of sediment and porewater after one year of subaqueous capping of contaminated sediments. *Water Sci. Technol.* **37**, 323–329.
- Baker, J.E., Capel, P.D., Eisenreich, S.J. 1985. Influence of colloids on sediment-water partition coefficients of polychlorobiphenyl congeners in natural waters. *Environ. Sci. Technol.* **20**, 1136–1143.
- Bear, J. 1972. *Dynamics of Fluids in Porous Media*. Elsevier, New York.
- Beckles, D., Chen, W., Hughes, J. 2007. Bioavailability of polycyclic aromatic hydrocarbons sequestered in sediment: microbial study and model prediction. *Environ. Toxicol. Chem.* **26**, 878–883.

- Boudreau, B. 1986. Mathematics of tracer mixing in sediments, I. Spatially-dependent, diffusive mixing. *Am. J. Sci.* **286**, 161–198.
- Boudreau, B. 1997. *Diagenetic Models and Their Implementation: Modeling Transport Reactions in Aquatic Sediments*. Springer-Verlag, New York.
- Boudreau, B., and Jorgensen, B. 2001. *The Benthic Boundary Layer*. Oxford University Press, New York.
- Chin, Y.P., Gschwend, P.M. 1992. Partitioning of polycyclic aromatic hydrocarbons to marine pore water organic colloids. *Environ. Sci. Technol.* **26**, 1621–1626.
- Cook, P.G., Favreau, G., Dighton, J.C., Tickell, S. 2003. Determining natural groundwater influx to a tropical river using radon, chlorofluorocarbons, and ionic environmental tracers. *J. Hydrol.* **277**, 74–88.
- Crank, J., and Nicolson, P. 1947. A practical method for numerical evaluation of solutions of partial differential equations of the heat conduction type. *Proc. Camb. Phil. Soc.* **43**, 50–64.
- Dankwerts, P.V. 1953. Continuous flow systems. *Chem. Eng. Sci.* **2**, 1–13.
- Hulburt, H.M. 1944. Chemical processes in continuous-flow systems: reaction kinetics. *Ind. Eng. Chem.* **36**, 1012–1017.
- Hyun, S., Jafvert, C., Lee, L., and Rao, P. 2006. Laboratory studies to characterize the efficacy of sand capping a coal tar-contaminated sediment. *Chemosphere* **63**, 1621–1631.
- Imberger, J., and Hamblin, P. 1982. Dynamics of lakes, reservoirs, and cooling ponds. *Annu. Rev. Fluid Mech.* **14**, 153–187.
- Lee, D.R. 1977. A device for measuring seepage fluxes in lakes and estuaries. *Limnol. Oceanogr.* **22**, 140–147.
- Lu, X., Reible, D.D., and Fleeger, J.W. 2006. Bioavailability of polycyclic aromatic hydrocarbons in field-contaminated Anacostia River (Washington, DC) sediment. *Environ. Toxicol. Chem.* **25**, 2869–2874.
- Lyman, W.J., Reehl, W.F. and Rosenblatt, D.H. 1990. *Handbook of Chemical Property Estimation Methods: Environmental Behavior of Organic Compounds*. American Chemical Society, Washington, DC.
- Malusis, M., and Shackelford, C. 2002. Theory for reactive solute transport through clay membrane barriers. *J. Contam. Hydrol.* **59**, 291–316.
- McCaffree, R.J., Myers, A.C., Davey, E., Morrison, G., Bender, M., Luedtke, N., Cullen, D., Froelich, P., and Klinkhammer, G. 1980. The relation between pore water chemistry and benthic fluxes of nutrients and manganese in Narragansett Bay, Rhode Island. *Limnol. Oceanogr.* **25**, 31–44.
- McDonough, K., Murphy, P., Olsta, J., Zhu, Y., Reible, D., and Lowry, G. 2007. Development of a sorbent-amended thin layer sediment cap in the Anacostia River. *Soil Sed. Contam.* **16**, 313–322.
- McGroddy, S.E., and Farrington, J.W. 1995. Sediment porewater partitioning of polycyclic aromatic hydrocarbons in three cores from Boston Harbor, Massachusetts. *Environ. Sci. Technol.* **29**, 1542–1550.
- Millington, R.J., and Quirk, J.M. 1961. Permeability of porous solids. *Trans. Far. Soc.* **57**, 1200–1207.
- Murphy, P., Marquette, A., Reible, D. and Lowry, G.V. 2006. Predicting the performance of activated carbon-, coke-, and soil-amended thin layer sediment caps. *J. Environ. Eng.* **132**, 787–794.
- Palermo, M., Maynard, S., Miller, J. and Reible, D. 1998. *Guidance Document for In Situ Subaqueous Capping of Contaminated Sediments*, EPA 905-B96-004.
- Parametrix. 1998. St. Paul Waterway Area Remedial Action and Habitat Restoration Project. Final 1998 Monitoring Report.
- Rabideau, A., and Khandelwal, A. 1998. Boundary conditions for modeling transport in vertical barriers. *J. Environ. Eng.* **124**, 1135–1139.
- Reible, D.D., Lampert, D.J., Constant, D., Mutch, R., and Zhu, Y. 2007. Active capping demonstration in the Anacostia River in Washington, DC. *Remed. J.* **17**, 39–53.
- Rowe, P.K., and Booker, J.R. 1985. 1-D pollutant migration in soils of finite depth. *J. Geotech. Eng.* **111**, 479–499.
- Rubin, H., and Rabideau, A. 2000. Approximate evaluation of contaminant transport through vertical barriers. *J. Contam. Hydrol.* **40**, 311–333.

- Schlautman, M.A., and Morgan, J.J. 1993. Effects of aqueous chemistry on the binding of polycyclic aromatic hydrocarbons by dissolved humic materials. *Environ. Sci. Technol.* **27**, 961–969.
- Schwarzenbach, R., Gshwend, P., and Imboden, D. 2003. Chapter 9, Sorption I: Introduction and sorption processes involving organic matter and Chapter 11: Sorption III: Sorption processes involving inorganic surfaces. *Environmental Organic Chemistry*, 2nd ed., pp. 275–330 and 387–458. Wiley & Sons, Hoboken, New Jersey.
- Simpson, S., Pryor, I., Mewburn, B., Batley, G., and Jolley, D. 2002. Considerations for capping metal-contaminated sediments in dynamic estuarine environments. *Environ. Sci. Technol.* **36**, 3772–3778.
- Thibodeaux, L.J. 1996. Chapter 5: Chemical exchange between water and adjoining earthen material. *Environmental Chemodynamics*, pp. 255–368. John Wiley, New York.
- Thoma, G., Reible, D., Valsaraj, K., and Thibodeaux, L. 1991. Efficiency of capping contaminated bed sediments in situ. 1. Laboratory-scale experiments on diffusion-adsorption in the capping layer. *Environ. Sci. Technol.* **25**, 1578–1584.
- Thoms, S.R., Matisoff, G., McCall, P.L., and Wang, X. 1995. *Models for Alteration of Sediments by Benthic Organisms*, Project 92-NPS-2, Water Environment Research Foundation, Alexandria Virginia.
- Van Genuchten, M. 1981. Analytical solutions for chemical transport with simultaneous adsorption, zero order production and first order decay. *J. Hydrol.* **49**, 213–233.
- Wehner, J., and Wilhelm, R. 1956. Boundary conditions of flow reactor. *Chem. Eng. Sci.* **6** 89–93.
- Zeman, A., and Patterson, T. 1997. Preliminary results of demonstration capping project in Hamilton Harbour. *Water Qual. Res. J. Can.* **32**, 439–452.



Memorandum

Date: November 23, 2010
From: Charles Andrews
To: Caryn Kiehl-Simpson
Subject: **Active Capping Transport Model – Version 2.0**

The Active Capping Transport Model is a computer program developed by David Lampert and Danny Reible at the University of Texas. The model calculates one-dimensional vertical transport of a contaminant through a sediment cap considering the processes of advection, diffusion, dispersion, reaction, bioturbation, deposition, consolidation, and retardation with local equilibrium between sediment, pore water, and dissolved organic matter. Excellent background documents that describe the processes simulated with the model are “*Guidance for In-Situ Subaqueous Capping of Contaminated Sediments: Appendix B: Model for Chemical Containment by a Cap*” (Palermo and others 1996) and a paper published in *Soil and Sediment Contamination* by Lampert and Reible (2009). I highly recommend that all users of Active Capping Transport Model read and familiarize themselves with these background documents.

The Active Capping Transport Model was developed as a MATLAB program and is run within the MATLAB environment. I have reviewed several versions of the Active Capping Transport Model and described the results of my reviews in memoranda dated January 6, 2009 and November 5, 2010. In my reviews, I noted several coding issues in the Active Capping Transport Model. These coding issues have all been addressed.

The Active Capping Transport Model Version 2.0 was developed to simulate contaminant transport in a six layer system; model parameters can vary from layer to layer. The governing equation in the Active Capping Transport Model is:

$$R \frac{\partial C}{\partial t} = -U \frac{\partial C}{\partial x} + D \frac{\partial^2 C}{\partial x^2} - n\lambda C \quad (1)$$

where: C = concentration;
U = Darcy velocity;
D = effective diffusion/dispersion coefficient (sum of diffusion and dispersive coefficients);
R = retardation factor for compound of interest; and
 λ = first-order degradation rate.

The governing equation is solved using a two-point upstream centered finite-difference scheme in space with the Crank-Nicolson method. The model automatically creates a finite-difference grid with sufficiently fine-vertical spacing to minimize numerical dispersion; for typical problems a vertical spacing



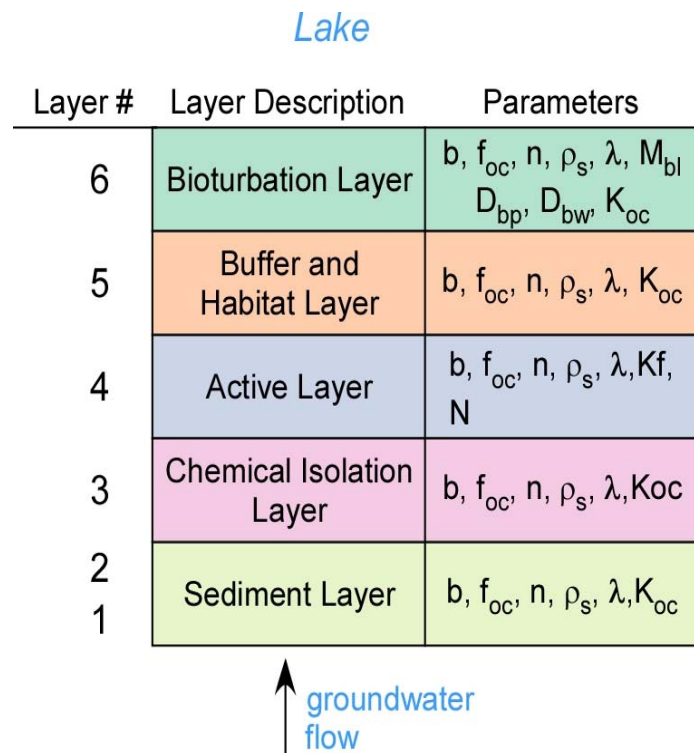
To: Caryn Kiehl-Simpson
Date: November 23, 2010
Page: 2

of 0.5 centimeters is specified. The time step size is increased with time from start of simulation for computational efficiency.

A schematic of the 6-layer system simulated with the Active Capping Transport Model is shown to the right. The bottom two layers represent the underlying sediment. These layers can be specified at a constant concentration, can be specified with a finite thickness with depth varying concentrations to simulate a depleting source with time, and can be specified with a constant concentration at base of sediment layer.

Overlying the sediment layer is the chemical isolation layer, which in turn is overlain by an active layer – a layer containing activated carbon.

Overlying the active layer is the buffer and habitat layer, which in turn is overlain by a bioturbation layer. In the real world, the bioturbation zone develops in the upper part of the buffer and habitat layer. In the model the bioturbation zone is treated as a separate layer with properties that differ from those in the underlying layer. At the top of the bioturbation layer, a mass transfer coefficient (M_{bl}) specifies the rate of contaminant transfer to the overlying lake water.



The model parameters that are specified for the layers are shown on the schematic above and are defined as follows (note that parameters must be specified in units listed below):

b = layer thickness (cm)
 n = porosity
 λ = first order decay rate (1/yr)
 N = Freundlich coefficient
 ρ_s = particle density (g/cm^3)
 M_{bl} = mass transfer coef. (cm/hr)

f_{oc} = fraction organic carbon content
 Kf = Freundlich coefficient (ug/kg)(L/ug) ^{N}
 D_{bw} = water biodiffusion coefficient (cm^2/yr)
 D_{bp} = particle biodiffusion coefficient (cm^2/yr)
 K_{oc} = organic carbon partition coefficient for specific contaminant (specified for sediment, sand and bioturbation layers separately, L/kg).



Note that the Freundlich coefficients (Kf and N), which are contaminant specific, are specified only in the active layer, and the particle biodiffusion coefficient and the water biodiffusion coefficient are only specified in the bioturbation layer.

In addition to the model parameters that are layer specific are the following parameters:

- Kdoc = colloidal partition coefficient for a specific contaminant (L/kg);
- Dw = diffusion coefficient for specific contaminant in water (cm²/sec);
- U = Darcy velocity (cm/yr);
- Uss = steady-state Darcy velocity (cm/year),
- Uc = Darcy velocity due to consolidation (cm/year),
- α = dispersion length (cm); and
- Coc = colloidal matter concentration (mg/L).

It is important to note that the governing equation (1) has only four parameters – U, R, D and λ. One of these parameters, the first-order decay rate (λ) is specified directly. The other three parameters are derived from the parameters described above. The derivation of the parameters R, D, and U in the governing equation are described below.

The retardation factor is defined for all layers, except for the active layer, as:

$$R = \frac{n + (1 - n)\rho_s K_{oc} f_{oc} + nC_{oc} K_{doc}}{1 + C_{oc} K_{doc}} \quad (2)$$

For the active layer, the retardation factor is defined as follows with sorption described by the Freundlich isotherm:

$$R = \frac{n + (1 - n)\rho_s K_f N C^{(N-1)} + nC_{oc} K_{doc}}{1 + C_{oc} K_{doc}} \quad (3)$$

The effective diffusion/dispersion coefficient (D) is defined for all layers except the sediment layer and the bioturbation layer as follows:

$$D = n^{(4/3)} D_w + \alpha |U| \quad (4)$$



To: Caryn Kiehl-Simpson
Date: November 23, 2010
Page: 4

For the sediment layer the effective diffusion/dispersion coefficient (D) is defined as:

$$D = \frac{nD_w}{1 - \ln(n^2)} + \alpha |U| \quad (5)$$

This definition uses a relationship developed by Boudreau (1996) to adjust the water diffusion coefficient for the tortuosity of a porous sediment. This relationship better defines the tortuosity relationship in natural sediments than the term used in equation 4 that is based on a relationship developed by Millington (1959). The Millington relationship works best for relatively uniform sands.

For the bioturbation layer the effective diffusion/dispersion coefficient is defined as:

$$D = n^{(4/3)}D_w + \alpha |U| + D_{bp}\rho_s(1-n)K_{OC}f_{OC} + D_{bw} \quad (6)$$

The Darcy velocity in the Active Transport Model consists of two components: a steady-state groundwater velocity and a velocity component due to consolidation as

$$U = U_{ss} + U_c \quad (7)$$

The velocity component due to consolidation is defined on the basis of two parameters (*a* and *b*) as follows:

$$U_c = 30.48 * a * b * t^{(b-1)} \quad (8)$$

where *a* and *b* are coefficients, and *t* is time in years since placement of the cap.

It is important for the user of Active Capping Transport Model to note that the retardation parameter and the effective diffusion/dispersion parameter as defined by equation 1 are not equivalent to those commonly used in the groundwater literature. The retardation parameter commonly used in the groundwater literature (R') is equal to the retardation parameter defined above divided by the porosity ($R = R'/n$); and equivalently $D = D'/n$ where D' is the effective diffusion/dispersion coefficient commonly used in the groundwater literature.



To: Caryn Kiehl-Simpson
Date: November 23, 2010
Page: 5

Review and Verification

I checked the accuracy of the calculated concentrations from the Active Capping Transport Model by simulating eight test cases with this computer code and with other computer codes. The other computer codes I used were MT3D (Zheng, 2006), the most-widely used groundwater transport model that has been extensively verified, and an analytical solution to equation 1 (Neville, 2005). The analytical solution was only used for test case 1 as it requires uniform properties. In using MT3D, the test cases were set up in a similar fashion to that used in the Active Capping Transport Model; a finite-difference grid with a vertical spacing of 0.5 centimeters. The TVD solution method was used in MT3D. Consolidation in MT3D was simulated by adjusting the velocity at each time step.

The input parameter values for the eight verification test cases are listed on Table 1. The various test cases were designed to test the model with various combinations of model parameters and boundary conditions. In five of the test cases, a Darcy velocity of 2 cm/year was used. When this velocity is specified, the contaminant transport is dominated by diffusive processes. The other three test cases used velocities of 10 and 20 cm/year. Only one of the test cases, test case 8, considers consolidation. The results from the test cases are presented on Figure 1 which is a series of plots of concentrations with depth as calculated with the models at various times after placement of the cap.

In test case 1, the calculated concentrations from all three models were nearly identical at all times (Figure 1). This indicates that for a media with uniform properties, that both MT3D and the Active Capping Transport Model correctly solve equation 1. This provides a level of confidence that MT3D is an appropriate code to use for verification of the Active Capping Transport Model.

The calculated concentrations from MT3D and the Active Capping Transport Model for tests cases 2 through 8 at various times since placement of the cap are also shown on Figure 1. For each of the test cases, nearly identical concentrations were calculated by MT3D and the Active Capping Transport Model. This provides confidence that the Active Capping Transport Model correctly solves the governing equation.

Conclusions

The Active Capping Transport Model is an appropriate model to use for the evaluation and design of sediment caps for Onondaga Lake. Based on the evaluations described in this memorandum, the computer model accurately solves the governing equation. The computer code for the model is concisely written and is relatively easy to understand. The model is very efficient which makes it feasible to easily conduct Monte Carlo type simulations.



To: Caryn Kiehl-Simpson
Date: November 23, 2010
Page: 6

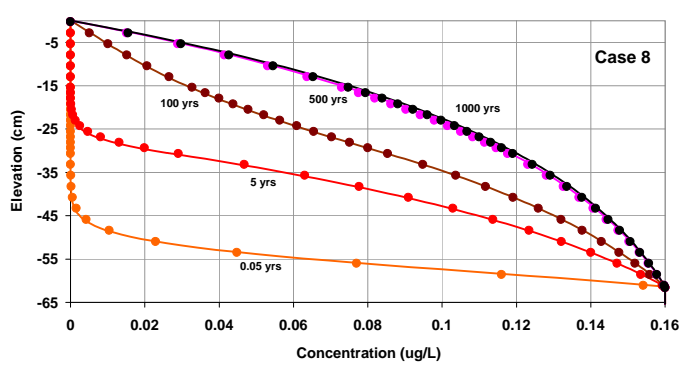
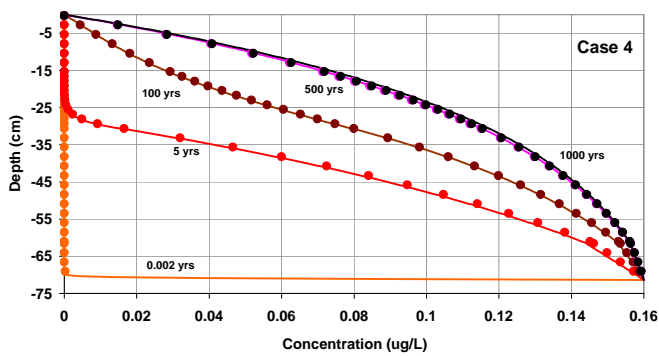
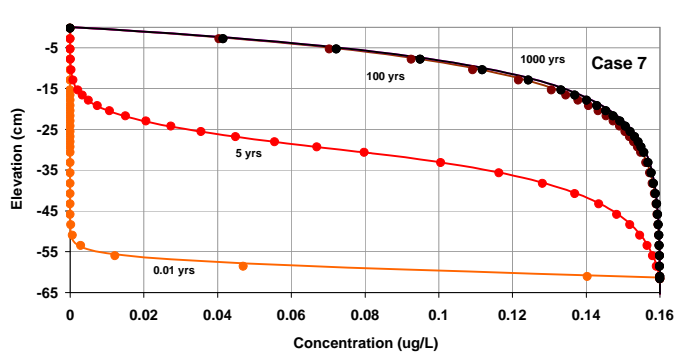
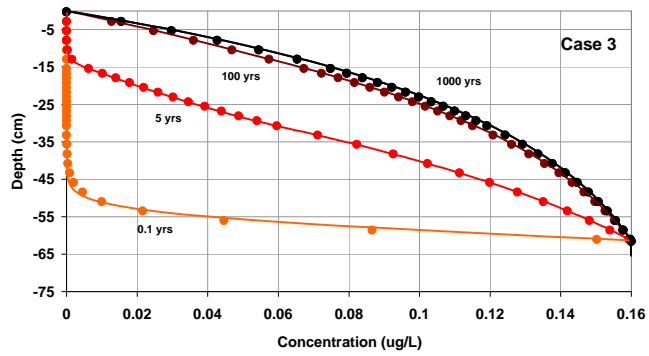
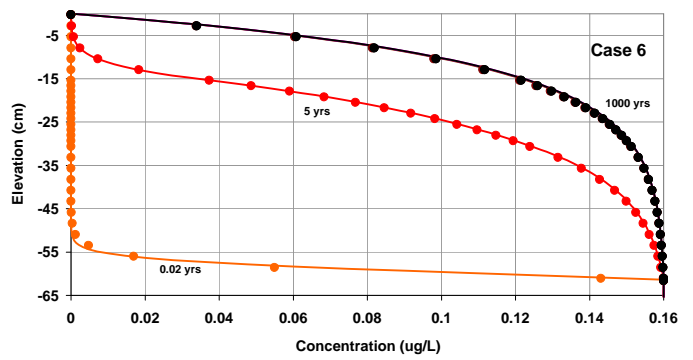
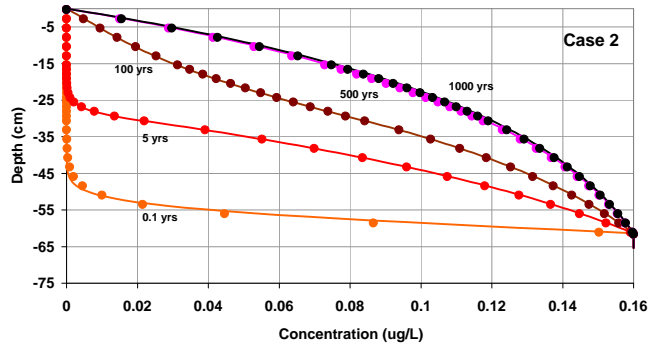
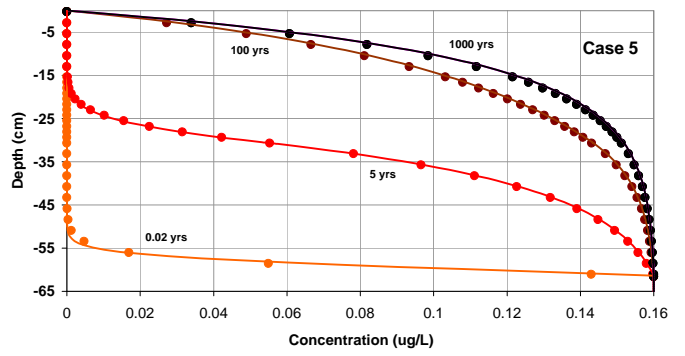
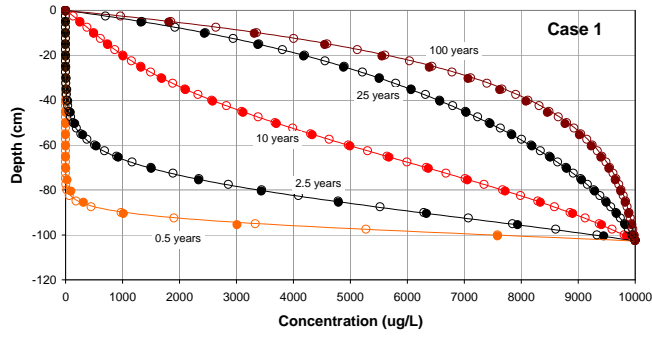
References

- Boudreau, B. 1996. The Diffusive Tortuosity of Fine-Grained Unlithified Sediments: *Geochimica et Cosmochimica Acta* 60, no. 16: 3139-3142.
- Lambert, D. and D. Reible, 2009. An Analytical Approach for Evaluation of Capping of Contaminated Sediments. *Soil and Sediment Contamination*. 18:470-488.
- Millington, R.J., 1959. Gas diffusion in porous media. *Science*, Vol. 130:100-102.
- Neville, C., 2005. ADFL Analytical Solution – Version 4, User’s Guide. S.S. Papadopoulos & Associates, Inc. Bethesda, MD.
- Palermo, M.R., S. Maynard, J. Miller, and D. Reible, 1996. Guidance for in-situ subaqueous capping of contaminated sediments. Environmental Protection Agency, EPA 905-B96-004, Great Lakes National Program Office, Chicago, IL. Available at <http://www.epa.gov/grtlakes/sediment/iscmain/appndb.pdf>.
- Zheng, C. 2006. MT3DMS v5.2, A modular three-dimensional multispecies transport model for simulation of advection, dispersion and chemical reactions of contaminants in groundwater systems. Supplemental User’s Guide. U.S. Army Corps of Engineers Technical Report, October 2006.

Table 1
Input Parameter Values for Test Cases

Parameter	Case 1	Case 2	Case 3	Case 4	Case 5	Case 6	Case 7	Case 8
Contaminant Properties (Contaminant Specific)								
Contaminant	Toluene	Mercury						
log Koc	2.35	2.35	2.35	2.35	2.35	2.35	2.35	2.35
log literature Koc - for sand layers	0	2.35	1.00	2.35	2.35	1.00	2.35	2.35
log Kdoc	0	0	0	0	0	0	0	0
Dw	5.2E-06	4.7E-06						
Flow and System Properties (Site Specific)								
Darcy Velocity	2	2	2	2	10	10	20	2
depositional velocity	0	0	0	0	0	0	0	0
hydrodynamic dispersivity	0.42	6.13	6.13	6.13	6.13	6.13	6.13	6.13
boundary layer mass transfer coeff.	0.33	0.36	0.36	0.36	0.36	0.36	0.36	0.36
colloidal matter concentration	0	0	0	0	0	0	0	0
Sediment Properties (Site Specific)								
sediment porosity	0.4	0.79	0.79	0.79	0.79	0.79	0.79	0.79
sediment particle density	2.6	2.62	2.62	2.62	2.62	2.62	2.62	2.62
sediment foc	0.001	0.1	0.1	0.01	0.1	0.1	0.1	0.1
sediment initial decay rate	0	0	0	0	0	0	0	0
duration for initial decay rate	0	1000	1000	1000	1000	1000	1000	1000
sediment final decay rate	0	0	0	0	0	0	0	0
Chemical Isolation Layer Properties (Design Parameters)								
layer thickness	30	30.48	30.48	30.48	30.48	30.48	30.48	30.48
layer porosity	0.4	0.4	0.4	0.4	0.4	0.4	0.4	0.4
layer particle density	2.6	2.6	2.6	2.6	2.6	2.6	2.6	2.6
layer foc	0.001	1E-07						
layer initial decay rate	0	2.1E-09						
layer final decay rate	0	2.1E-09						
Active Layer Properties (Design Parameters)								
active layer thickness (sand plus AC)	17.0	0.3846	0.3846	0.3846	0.3846	0.3846	0.3846	0.3846
active layer porosity	0.4	0.35	0.35	0.35	0.35	0.35	0.35	0.35
active layer particle density (calculated)	2.6	0.80	0.80	0.80	0.80	0.80	0.80	0.80
active layer Freundlich Kf	0.22	22.36	22.36	22.36	22.36	22.36	22.36	22.36
active layer Freundlich 1/n	1	1	1	1	1	1	1	1
active layer initial decay rate	0	2.1E-09						
active layer final decay rate	0	2.1E-09						
Buffer and Habitat Restoration Layer Properties (Design Parameters)								
Habitat Restoration Layer thickness	55.7	30.48	30.48	30.48	30.48	30.48	30.48	30.48
Buffer Layer thickness	0	0	0	0	0	0	0	0
layers porosity	0.4	0.4	0.4	0.4	0.4	0.4	0.4	0.4
layers particle density	2.6	2.6	2.6	2.6	2.6	2.6	2.6	2.6
layers foc (Cl and non-bio HR)	0.001	0.1	0.1	0.1	0.1	0.1	0.1	0.1
layers initial decay rate	0	2.1E-09						
layers final decay rate	0	2.1E-09						
Bioturbation Layer Properties (Site Specific)								
bioturbation depth	5.5	15.24	15.24	15.24	15.24	15.24	15.24	15.24
bioturbation layer porosity	0.4	0.4	0.4	0.4	0.4	0.4	0.4	0.4
bioturbation layer particle density	2.6	2.6	2.6	2.6	2.6	2.6	2.6	2.6
bioturbation layer foc	0.001	0.1	0.1	0.1	0.1	0.1	0.1	0.1
bioturbation layer initial decay rate	0	2.1E-09						
bioturbation layer final decay rate	0	2.1E-09						
Pore Water Biodiffusion Coefficient	0	4.7E-06						
Particle Biodiffusion Coefficient	0	0	0	0	0	0	0	0
Bioturbation Layer logKoc	0	2.35	2.35	2.35	2.35	2.35	2.35	2.35
Consolidation Data								
parameter a	0	0	0	0	0	0	0	0.211
parameter b	0	0.235	0.235	0.235	0.235	0.235	0.235	0.235
total time for consolidation (years)	0	30	30	30	30	30	30	30
Simulation Parameters								
Simulation length (years)	100	1,000	1,000	1,000	1,000	1,000	1,000	1,000
Minimum number of grid points	150	150	150	150	150	150	150	150
Minimum number of time steps	400	400	400	400	400	400	400	400
Answer 1 for yes and 0 for no								
Infinite source?	1	1	1	0	1	1	1	1
Infinite source at sediment bottom?	1	1	1	1	1	1	1	1

Note: Shaded cells indicate parameters changed relative to Test Case 2.



MT3D results plotted as solid dots, Active Capping Transport Model results plotted as solid lines and in Case 1 AFLD results plotted as open circles.

Figure 1 Comparison of Calculated Concentrations for Test Cases 1 through 8



Memorandum

Date: January 6, 2009
From: Charles Andrews
To: Files
Subject: **Active Capping Transport Model – Version 2.0**

Introduction

Active Capping Transport Model is a computer program developed by David Lampert and Danny Reible at the University of Texas. The model calculates one-dimensional vertical transport of a contaminant through a sediment cap considering the processes of advection, diffusion, dispersion, reaction, bioturbation, deposition and retardation with local equilibrium between sediment, pore water, and dissolved organic matter. An excellent background document that describes the processes simulated with the model is “Guidance for In-Situ Subaqueous Capping of Contaminated Sediments: Appendix B: Model for Chemical Containment by a Cap” (Palermo and others 1996). I highly recommend that all users of Active Capping Transport Model read and familiarize themselves with this background document.

I reviewed Version 2.0 of the Active Capping Transport Model dated December 10, 2008. The model was developed as a MATLAB program and is run within the MATLAB environment. I used MATHLAB Version 7.7 to run the program. The model reads input data from an Excel spreadsheet and writes model outputs to an Excel spreadsheet. The model will not run on earlier versions of MATLAB that do not support reading and writing from Excel files.

Active Capping Transport Model Version 2.0 was developed to simulate contaminant transport in a five layer system; model parameters can vary from layer to layer. The governing equation in the Active Capping Transport Model is:

$$R \frac{\partial C}{\partial t} = -U \frac{\partial C}{\partial x} + D \frac{\partial^2 C}{\partial x^2} - n\lambda C \quad (1)$$

where: C = concentration;
U = Darcy velocity;
D = effective diffusion coefficient (sum of diffusion and dispersive coefficients);
R = retardation factor for compound of interest; and
 λ = first-order degradation rate.



To: File
Date: January 6, 2009
Page: 2

The governing equation is solved using a two-point upwind centered finite-difference scheme in space with the Crank-Nicolson method. The model automatically creates a finite-difference grid with sufficiently fine-vertical spacing to minimize numerical dispersion; for typical problems a vertical spacing of 0.5 centimeters is specified. The time step size is increased with time from start of simulation for computational efficiency.

A schematic of the 5-layer system simulated with the Active Capping Transport Model is shown to the right.

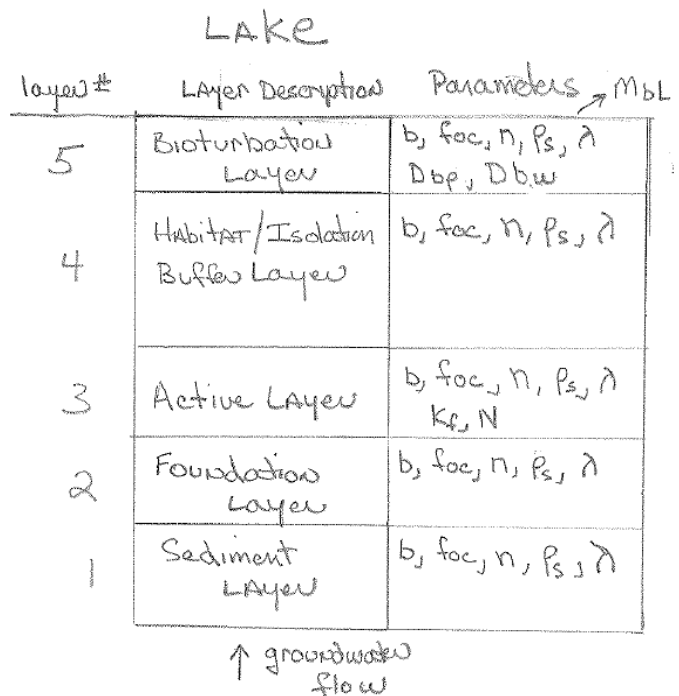
The bottom layer is the sediment layer. This layer can be specified at a constant concentration or it can be specified with a finite thickness with depth varying concentrations to simulate a depleting source with time.

Overlying the sediment layer is the cap foundation layer, which in turn is overlain by an active layer – a layer containing activated carbon.

Overlying the active layer is the habitat/isolation/buffer layer, which in turn is overlain by a bioturbation layer. In the real world, the bioturbation zone develops in the upper part of the habitat/isolation/buffer layer. In the model the bioturbation zone is treated as a separate layer with properties that differ from those in the underlying layer. At the top of the bioturbation layer, a mass transfer coefficient (M_{bl}) specifies the rate of contaminant transfer to the overlying lake water.

The model parameters that are specified for each layer are shown on the schematic above and are defined as follows (note that parameters must be specified in units listed below):

- | | |
|-------------------------------------------|------------------------------------------------------------|
| b = layer thickness (cm) | foc = fraction organic carbon content |
| n = porosity | ρ_s = particle density (g/cm^3) |
| λ = first order decay rate (1/yr) | Kf = Freundlich coefficient ($(ug/kg)(L/ug)^N$) |
| N = Freundlich coefficient | D_{bp} = particle biodiffusion coefficient (cm^2/yr) |
| | D_{bw} = water biodiffusion coefficient (cm^2/yr) |





To: File
Date: January 6, 2009
Page: 3

Note that the Freundlich coefficients (K_f and N), which are contaminant specific, are specified only in the active layer, and the particle biodiffusion coefficient and the water biodiffusion coefficient are only specified in the bioturbation layer.

In addition to the model parameters that are layer specific are the following parameters:

K_{oc} = organic carbon partition coefficient for a specific contaminant (L/kg);
 K_{doc} = colloidal partition coefficient for a specific contaminant (L/kg);
 D_w = diffusion coefficient for specific contaminant in water (cm²/sec);
 U = Darcy velocity (cm/yr);
 α = dispersion length (cm);
 C_{oc} = colloidal matter concentration (mg/L); and
 M_{bl} = upper layer mass transfer coefficient (cm/hr).

It is important to note that the governing equation (1) has only four parameters – U , R , D and λ . Two of these parameters, the Darcy velocity (U) and the first-order decay rate (λ) are specified directly. The other two parameters are derived from the parameters described above. The derivation of the parameters R and D in the governing equation are described below.

The retardation factor is defined for all layers, except for the active layer, as:

$$R = \frac{n + (1-n)\rho_s K_{oc} f_{oc} + nC_{oc} K_{doc}}{1 + C_{oc} K_{doc}} \quad (2)$$

For the active layer, the retardation factor is defined as follows with sorption described by the Freundlich isotherm:

$$R = \frac{n + (1-n)\rho_s K_f N C^{(N-1)} + nC_{oc} K_{doc}}{1 + C_{oc} K_{doc}} \quad (3)$$

The effective diffusion coefficient (D) is defined for all layers except the sediment layer and the bioturbation layer as follows:

$$D = n^{(4/3)} D_w + \alpha |U| \quad (4)$$



To: File
Date: January 6, 2009
Page: 4

For the sediment layer the effective diffusion coefficient (D) is defined as:

$$D = \frac{nD_w}{1 - \ln(n^2)} + \alpha |U| \quad (5)$$

This definition uses a relationship developed by Boudreau (1996) to adjust the water diffusion coefficient for the tortuosity of a porous sediment. This relationship better defines the tortuosity relationship in natural sediments than the term used in equation 4 that is based on a relationship developed by Millington (1959). The Millington relationship works best for relatively uniform sands.

For the bioturbation layer the effective diffusion coefficient is defined as:

$$D = n^{(4/3)}D_w + \alpha |U| + D_{bp}\rho_s(1-n)K_{OC}f_{OC} + D_{bw} \quad (6)$$

It is important for the user of Active Capping Transport Model to note that the retardation parameter and the effective diffusion parameter as defined by equation 1 are not equivalent to those commonly used in the groundwater literature. The retardation parameter commonly used in the groundwater literature (R') is equal to the retardation parameter defined above divided by the porosity ($R = R'/n$); and equivalently $D = D'/n$ where D' is the effective diffusion coefficient commonly used in the groundwater literature.

Review and Verification

I checked the computer code for Active Capping Transport Model (parsons.m) to verify that the model input parameters specified for model layers were correctly converted into the parameters used in the governing equation. These conversions are made on lines 99-199 and 329 to 330 of the model code. In the latest version of the code that I reviewed, these conversions were correct except for the calculation of the retardation coefficient with a Freundlich isotherm (equation 3). I modified the code to correctly calculate the retardation coefficient using equation 3 (in the version of the code I reviewed, the term “n+” in the numerator on the right hand side was missing).

I checked the accuracy of the calculated concentrations from the Active Capping Transport Model by simulating four test problems with this computer code and with other computer codes. The other computer codes I used were MT3D (Zheng and Wang, 1998), the most-widely used groundwater transport model that has been extensively verified, and an analytical solution to equation 1 (Neville, 2005). In the first three test cases, a Darcy velocity of 2 cm/year was used. When this velocity is specified, the contaminant transport is dominated by diffusive processes. The fourth test case used a Darcy velocity of 10 cm/year.



To: File
Date: January 6, 2009
Page: 5

The four test problems consisted of the following: 1) problem with uniform properties in the five model layers, 2) problem with uniform properties except for porosity which was varied from layer to layer, 3) problem with sorption in active layer simulated with Freundlich isotherm (in other test problems the Freundlich coefficient N was specified as 1 to simulate linear sorption), and 4) identical to test problem 3 except that Darcy velocity increased from 2 cm/year to 10 cm/year. The model parameters specified for the Active Capping Transport Model for the four test problems are listed below in the format that they appear in the Excel spreadsheet used for model input.

Input Parameter Values for Test Problems					
	Test Problem 1	Test Problem 2	Test Problem 3	Test Problem 4	
<u>Contaminant Properties (Contaminant Specific)</u>					
log Koc	2.34947	2.34947	2.34947	2.34947	log L/kg
log Kdoc	0	0	0	0	log L/kg
Dw	5.2187E-06	5.2187E-06	5.2187E-06	4.8541E-06	cm ² /s
<u>Flow and System Properties (Site Specific)</u>					
Darcy Velocity	2	2	2	10	cm/yr
depositional velocity	0	0	0	0	cm/yr
hydrodynamic dispersivity	0.42361	0.42361	0.42361	0.42361	cm
boundary layer mass transfer coeff.	0.328	0.328	0.328	0.328	cm/hr
colloidal matter concentration	0	0	0	0	mg/L
<u>Sediment Properties (Site Specific)</u>					
sediment porosity	0.4	0.4	0.4	0.4	
sediment particle density	2.6	2.6	2.6	2.6	g/cm ³
sediment foc	0.001	0.001	0.001	0.001	
sediment decay rate	0	0	0	0	yr ⁻¹
<u>Foundation Layer Properties (Design Parameters)</u>					
foundation layer thickness	30	30	30	30	cm
foundation layer porosity	0.4	0.5	0.4	0.4	
foundation layer particle density	2.6	2	2.6	2.6	g/cm ³
foundation layer foc	0.001	0.001	0.001	0.001	
foundation layer decay rate	0	0	0	0	yr ⁻¹
<u>Active Layer Properties (Design Parameters)</u>					
active layer thickness	17.0	17.0	17.0	17.0	cm
active layer porosity	0.4	0.8	0.35	0.35	
active layer particle density	2.6	0.8	0.8	0.8	g/cm ³
active layer Freundlich Kf	0.22	0.22	5,000.00	5,000.00	ug/kg*(ug/L) ⁻ⁿ
active layer Freundlich n	1	1	0.44	0.44	
active layer decay rate	0	0	0	0	yr ⁻¹
<u>Isolation, Buffer, and Habitat Restoration Layer Properties (Design Parameters)</u>					
Habitat Restoration Layer thickness	40.48	40.48	40.48	40.48	cm
Chemical Isolation Layer thickness	15.24	15.24	15.24	15.24	cm
Buffer Layer thickness	0	0	0	0	cm
isolation layers porosity	0.4	0.3	0.4	0.4	
isolation layers particle density	2.6	2.2286	2.6	2.6	g/cm ³
isolation layer foc	0.001	0.001	0.001	0.001	
isolation layer decay rate	0	0	0	0	yr ⁻¹
<u>Bioturbation Layer Properties (Site Specific)</u>					
bioturbation depth	5.5	5.5	5.5	5.5	cm
bioturbation layer porosity	0.4	0.4	0.4	0.4	
bioturbation layer particle density	2.6	2.6	2.6	2.6	g/cm ³
bioturbation layer foc	0.001	0.001	0.001	0.001	
bioturbation layer decay rate	0	0	0	0	yr ⁻¹
Pore Water Biodiffusion Coefficient	0	0	0	0	cm ² /yr
Particle Biodiffusion Coefficient	0.00	0.00	0.00	0.00	cm ² /yr



To: File
Date: January 6, 2009
Page: 6

The results from the test simulations are shown on the following pages. The analytical solution was only used for test problem 1 as it requires uniform properties. In using MT3D, the problem were set up in a similar fashion to that used in the Active Capping Transport Model; a finite-difference grid with a vertical spacing of 0.5 centimeters was used and the TVD solution method.

In test problem 1 the calculated concentrations from all three models were nearly identical (Figure 1). For the second test problem, the solutions from MT3D and the Active Capping Transport Model compared well (Figure 2). For the third test problem, the solutions from MT3D and the Active Capping Transport Model did not compare well (Figure 3). In the MT3D simulation, based on results for 100 years, it appears that the effective retardation coefficient in the active layer is higher than in the Active Capping Transport Model. Another simulation was made in which the Freundlich coefficient (K_f) in MT3D was reduced by 15.5% to check if the differences between the models were related to specification of retardation coefficient. The results from this MT3D simulation compared very well with the results from the Active Capping Model for test problem 3.

It was determined that the discrepancy between the MT3D solution and the Active Capping Transport Model solution was the result of differences in time-step sizes. The Active Capping Transport Model was rerun for test problem 3 with each time step reduced by a factor of 32 and the solution compared well with the MT3D solution (Figure 4). Test problem 4 was also run with a reduced time step size and the comparison between the MT3D solution and the Active Capping Transport Model solution is good.

The reduction factor of 32 was chosen arbitrarily. Initially chose a factor of 8 and this did not produce acceptable results, the factor was then increased to 32 and the results were acceptable.

Conclusions

The Active Capping Transport Model is an appropriate model to use for the evaluation and design of a sediment cap for Onondaga Lake. Based on our evaluations that computer model accurately solves the governing equation. In addition, note that the computer code for the model is concisely written and is relatively easy to understand. The model is very efficient which makes it feasible to easily conduct Monte Carlo type simulations.



To: File
Date: January 6, 2009
Page: 7

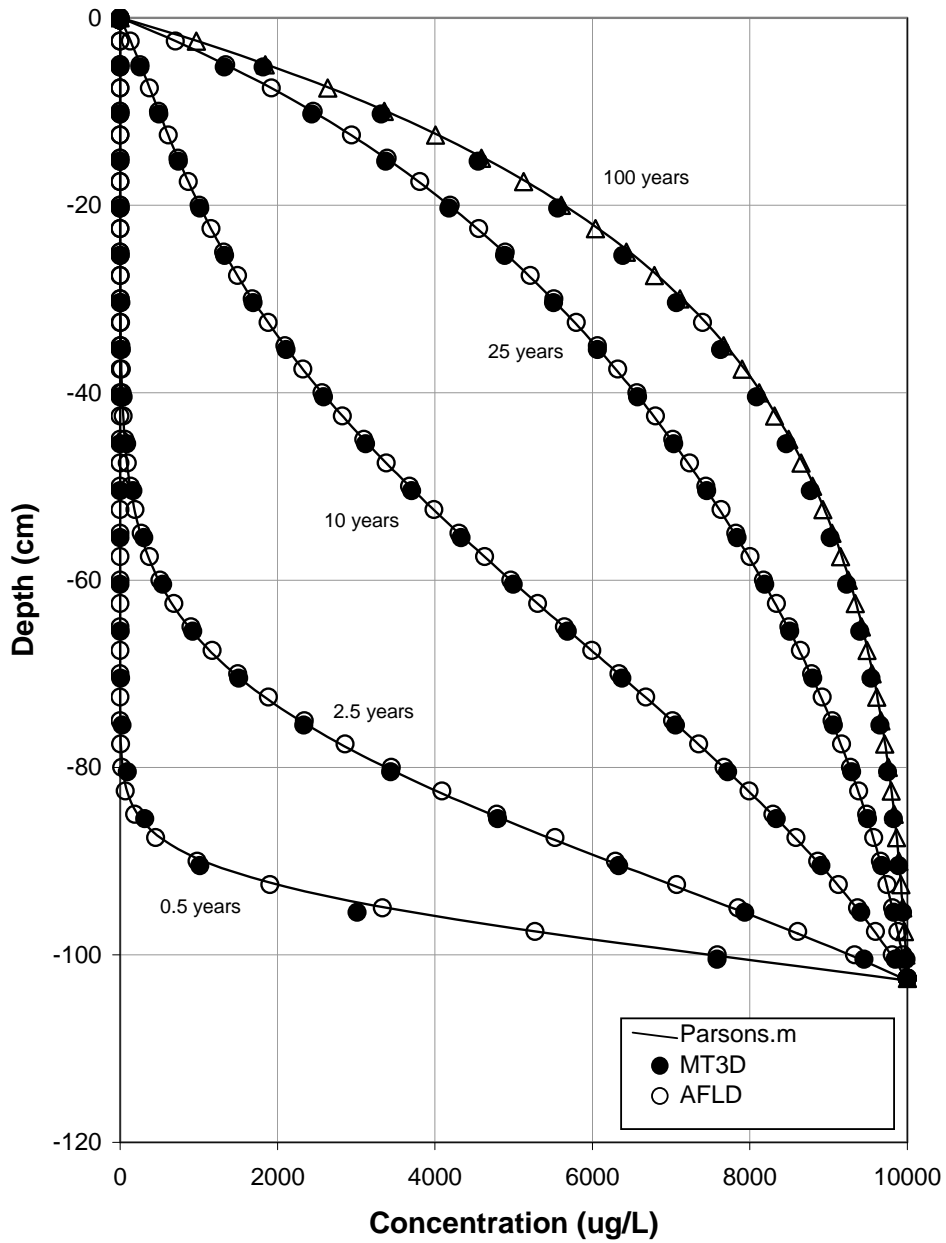


Figure 1 Test Problem 1 Uniform Properties



To: File
Date: January 6, 2009
Page: 8

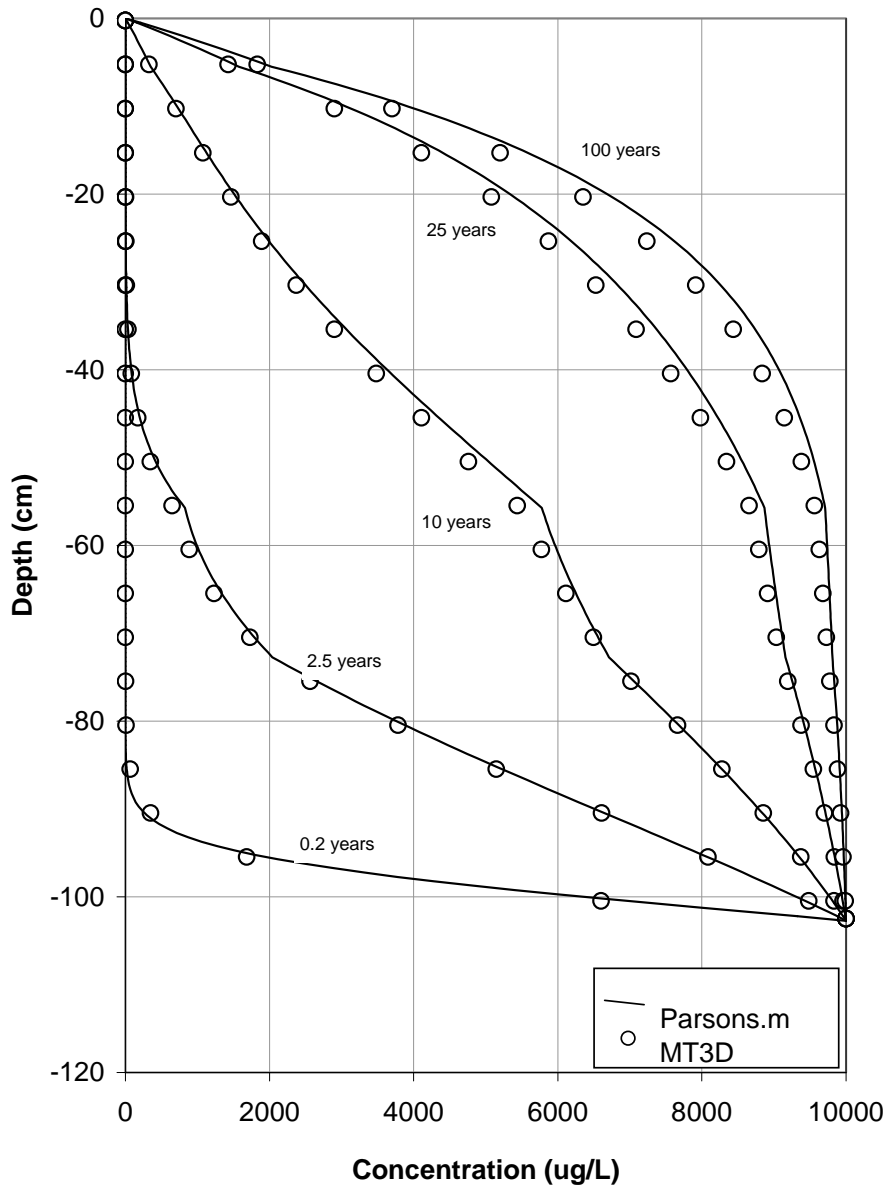


Figure 2 Test Problem 2 -- Non-Uniform Properties (porosity varies among five layers)



To: File
Date: January 6, 2009
Page: 9

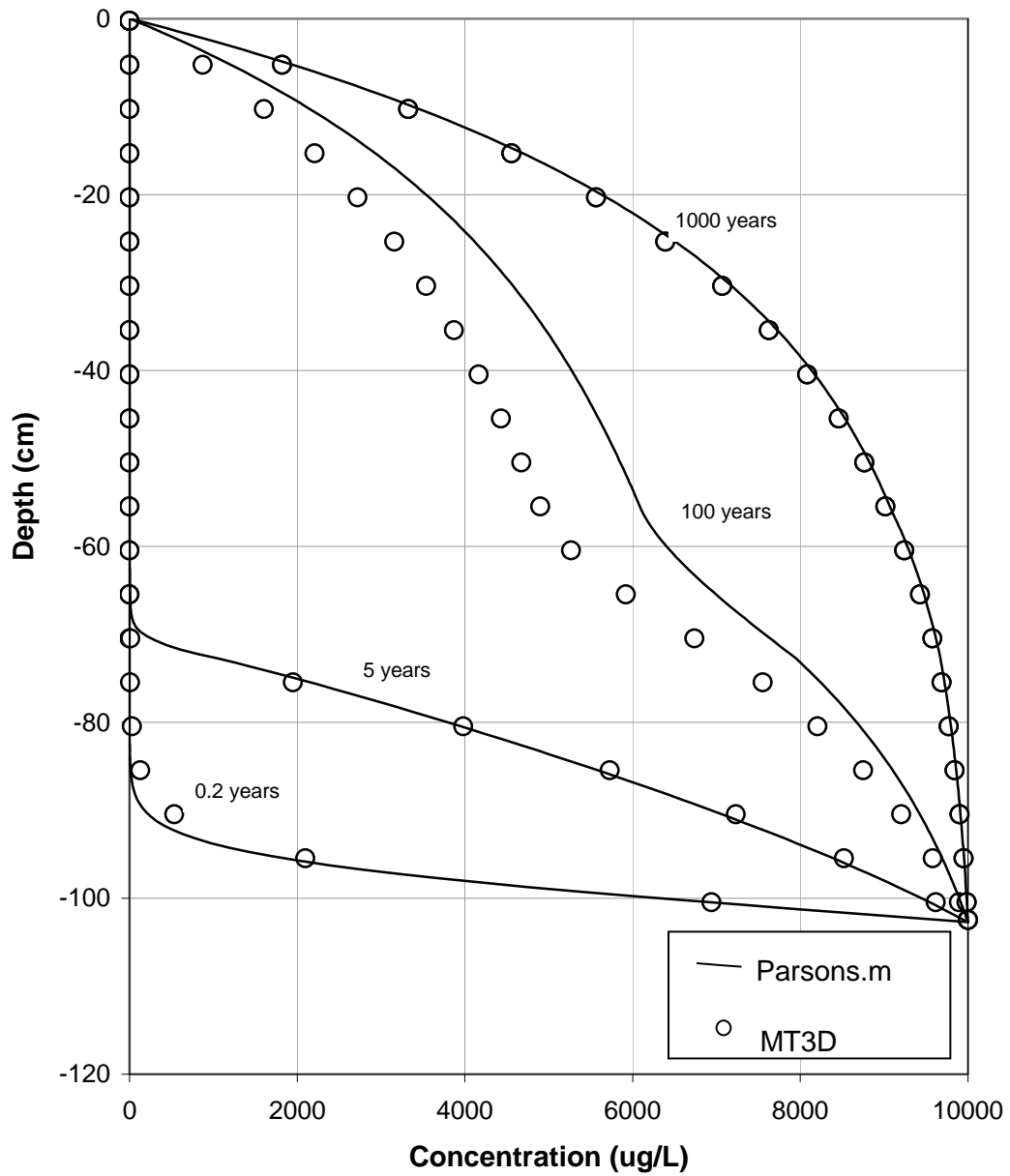


Figure 3 Test Problem 3



To: File
Date: January 6, 2009
Page: 10

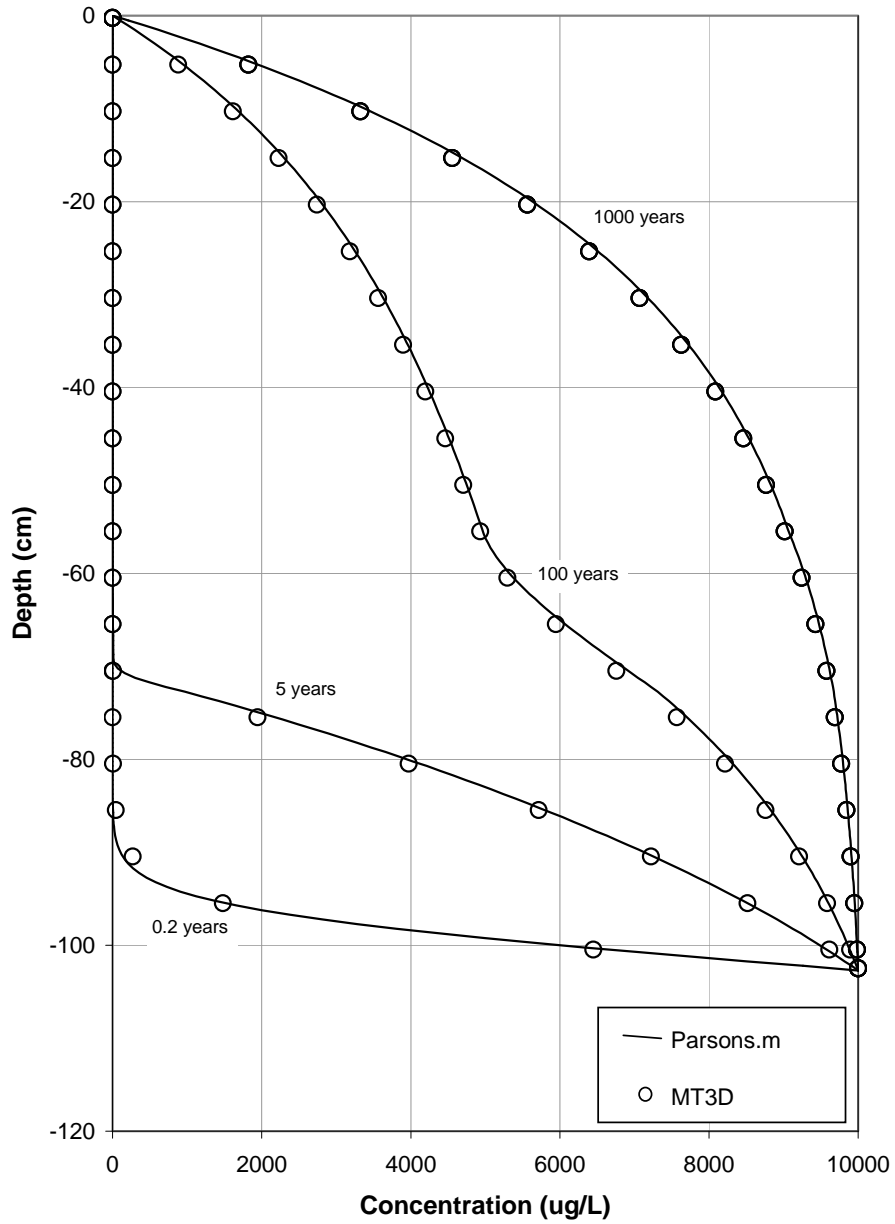


Figure 4 Test Problem 3 (decreased time step size in Parsons.m)



To: File
Date: January 6, 2009
Page: 11

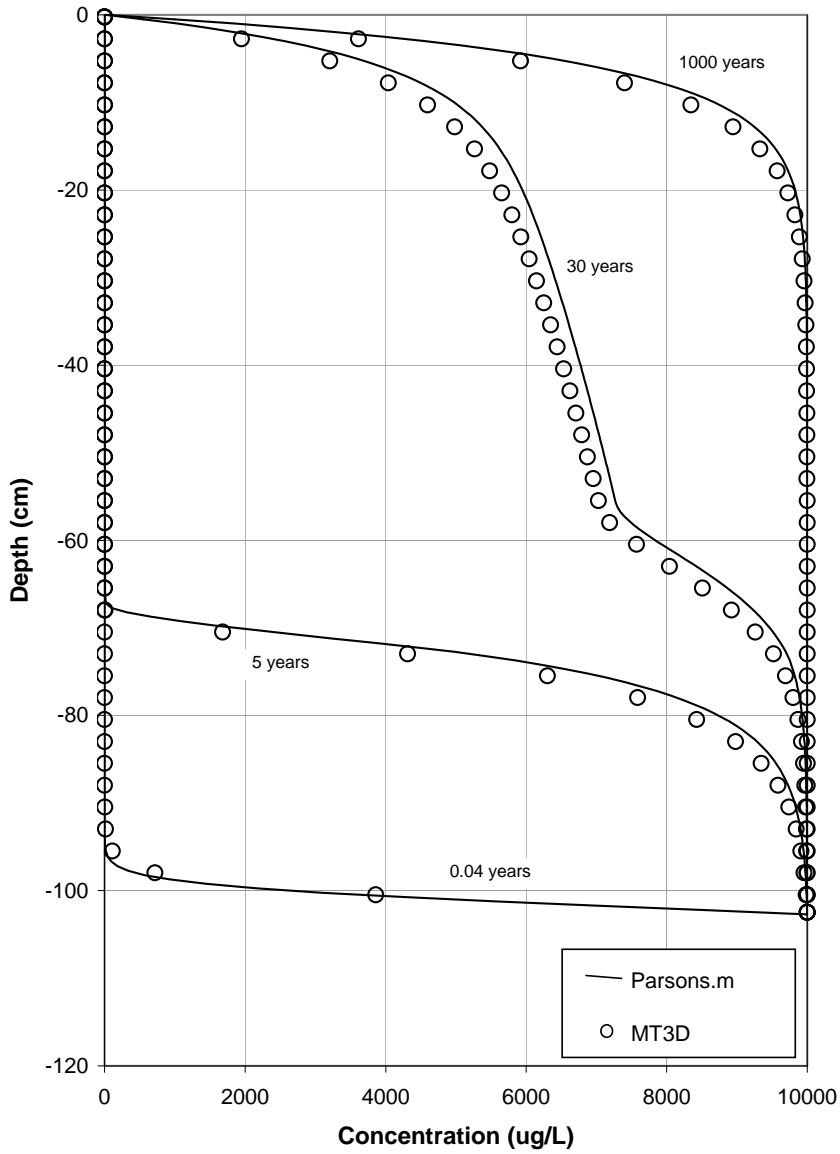


Figure 5 Test Problem 4 (decreased time step size in Parsons.m)



To: File
Date: January 6, 2009
Page: 12

References

- Boudreau, B. 1996. The Diffusive Tortuosity of Fine-Grained Unlithified Sediments: *Geochimica et Cosmochimica Acta* 60, no. 16: 3139-3142.
- Millington, R.J., 1959. Gas diffusion in porous media. *Science*, Vol. 130:100-102.
- Neville, C., 2005. ADFL Analytical Solution – Version 4, User’s Guide. S.S. Papadopoulos & Associates, Inc. Bethesda, MD.
- Palermo, M.R., S. Maynard, J. Miller, and D. Reible, 1996. Guidance for in-situ subaqueous capping of contaminated sediments. Environmental Protection Agency, EPA 905-B96-004, Great Lakes National Program Office, Chicago, IL. Available at <http://www.epa.gov/grtlakes/sediment/iscmain/appndb.pdf>.
- Zheng, C. and P. Wang, 1998. MT3DMS, A modular three-dimensional multispecies transport model for simulation of advection, dispersion and chemical reactions of contaminants in groundwater systems. Documentation and User’s Guide. U.S. Army Corps of Engineers Technical Report, June 1998.

MEMORANDUM

To: Caryn Kiehl-Simpson, Parsons
Ed Glaza, Parsons
Date: March 1, 2012

From: Deirdre Reidy, Kevin Russell, and Peter Song,
Anchor QEA
Project: 090139-01.20

Re: Summary of changes to the numerical cap model code

This memorandum summarizes changes and updates to the Onondaga Lake numerical cap model (Matlab) code made by Anchor QEA, LLC (Anchor QEA) between May 2011 and February 2012 (i.e., subsequent to the versions of the model code that were included with the Intermediate Design). All changes to the code made by Anchor QEA were reviewed by the original authors (i.e., Danny Reible and Dave Lampert at the University of Texas) and the code has been thoroughly tested to make sure all modifications performed as intended. The code changes described in this memorandum are grouped into three categories: 1) added functionality for site-specific modeling; 2) improvements to numerical methods/computational efficiency; and 3) corrections of minor errors.

CODE MODIFICATIONS TO INCREASE FUNCTIONALITY

- Specification of biodegradation rates for each cap layer in the probabilistic (Monte Carlo) version of the code (May 2011): The early versions of the probabilistic model input file and model code (e.g., prior to and including the Intermediate Design) allowed the user to specify “initial” and “final” biodegradation rates for the model using two sets of input parameters: one set to specify the “initial” and “final” biodegradation rates for the bioturbation zone and one set of inputs for the remaining layers, the latter of which was specified by the parameter “below bioturbation layer.” The input file was updated along with the model code to allow separate “initial” and “final” degradation rates to be specified for each unique layer simulated by the model (i.e., foundation layer, [active] isolation layer, habitat restoration layer, and bioturbation zone). These changes were made to allow biodegradation and lag times to be properly represented in the model.
-

-
- Specification of a uniform distribution for bioturbation zone TOC in the Monte Carlo version of the code (August 2011): The probabilistic code was modified to allow for sampling from a uniform distribution for bioturbation zone TOC. Allowing the user to specify the type of distribution was necessary because a uniform TOC distribution was used in the modeling of the wetlands (WB1-8, WBB-West, WBB-Center, and WBB-East) and Remediation Area A, whereas a lognormal distribution was used for all other model areas. This modification also required a slight change to the model input file, which now contains a flag to indicate the distribution used: lognormal or uniform (Cells I24-I39 of the chemical-specific tabs).
 - Development of a version of the code that includes an additional model layer for simulating wetland areas (September 2011 to February 2012): In the approach used for the Final Design of modeling wetland areas, the Onondaga Lake cap model code was modified to include an additional model layer that lies between the habitat restoration layer and the chemical isolation layer. This new version of the model was developed by making the following changes:
 - Three unique layers above the chemical isolation layer are needed for the wetland areas: 1) the “Bioturbation Zone,” which is upper portion of the high TOC habitat layer, within which mixing occurs (i.e., 6 inches); 2) a layer of high TOC material that has no bioturbation, which is referred to in the model as the “Upper Habitat Restoration Layer”; and 3) a layer of low TOC material, which is referred to in the model as the “Lower Habitat Restoration Layer.” Most of the changes made to the code were based on the indexing of the boundary points for the “active” layer and in a couple of places, the code was changed to properly reference the new layer number for the Upper Habitat Restoration Layer. This new seventh layer also required a change to the location of various inputs within the Excel input file (A45 to C52) as well as an increase in the number of elements in the variable arrays within the deterministic and Monte Carlo versions of the code. Indexing of the variables affected indices 5, 6, and 7, which refer to the Lower Habitat Restoration, Upper Habitat Restoration, and Bioturbation Zone layers, respectively. Indexing of the inputs from the Excel input file (variable name “Inputs”) affected indices 46 through 71 of the deterministic code.
-

- When modeling the wetlands in the Final Design, a higher TOC value was simulated in the upper 8 inches of the cap—that is, the Bioturbation Zone (6 inches) and the Upper Habitat Restoration Layer (the next 2 inches), as described above. During the probabilistic modeling of the wetlands, the TOC value for the bioturbation zone was selected from a uniform distribution. The TOC value in the upper habitat layer should vary the same way; however, a separate distribution could not be specified for each because the values would then vary independently for each probabilistic realization. The model input files were, therefore, updated to include a flag indicating whether to use the same TOC values as in the Bioturbation Zone, or to use the static value specified for the Upper Habitat Restoration Layer. The code was then updated to check this flag and use the appropriate values (i.e., either the realization values generated for the bioturbation zone [sampled from a uniform distribution ranging over 5 to 15%] or the static value set in the input file for the Upper Habitat Restoration Layer).

CODE CHANGES TO IMPROVE NUMERICAL METHODS/COMPUTATIONAL EFFICIENCY

- Model timeframe to be as long as the user-specified “Simulation length” (July 2011): In the Intermediate Design versions of the model code, the timeframe for certain model simulations was found to be less than the “Simulation length” specified in the model input file. In order to assess compliance with the design criteria over a set timeframe (1,000 years was used for the Final Design), the model code was updated to ensure that the model runs for at least the length specified in the input file.
 - Time domain division to ensure complete simulation length (August 2011): Changes were made to also ensure that the conversions to and from the dimensionless time used in the solution of the governing equation are based on a constant value for the characteristic diffusion time, which was used to specify dimensionless time steps and simulation length.
-

CODE CORRECTIONS

- User-specified lag time for biodegradation (May 2011): A lag period during which no biological decay would occur was specified in the model to allow adequate time for a biological community to establish in the cap material. This lag period is simulated by specifying two decay rates: an “initial” rate (which was set to zero to simulate no biodegradation) and a “final” rate, the latter of which is used after a user-specified duration (i.e., the lag time). While reviewing results from model tests conducted during development of the Draft Final Design (which was the first time this feature was used for the Onondaga Lake cap design), it was discovered that the final rate was not being applied at the user-specified time, but several years later. Time stepping in the code is performed on two levels—a large-scale time step and finer-scale time step. The code that initiates the “final” decay rate was located within the larger time step and, therefore, the first time step after the lag period specified by the user was several years later. To correct this inconsistency, the code that handles the start of the “final” decay rate was moved inside the second level time loop, which is on a finer scale, so that the “final” decay rate begins at the user-specified time.
 - Discrepancy between model output to the screen versus the model output to the *.CSV file (June 2011): As noted in NYSDEC’s comments to the Intermediate Design Report, the concentrations at the bottom of the Bioturbation Zone (Wbio) and the bottom of the Habitat Restoration Layer (Whr) printed to the screen did not match those reported in the output file (*.CSV). Throughout the code, the “active” layer (i.e., that which contains a sorptive amendment that is characterized by non-linear [Freundlich] partitioning) is handled separately from the remaining layers. After the model finishes simulating porewater concentrations within a given time step, it calculates the sorbed-phase concentrations using partitioning relationships. At this point in the code, modifications were made to correctly handle the indexing of the “active” layer so that there is no inconsistency in the reported outputs.
 - Calculation of retardation factor in probabilistic code (February 2012): The calculation of the retardation factor in the “active” layer at early times was referencing the incorrect porewater concentration from the model input file, using the static value reserved for deterministic runs rather than the probabilistic
-

value from a given realization. The model code was updated in two places to correct this issue.

ATTACHMENT 4

MODEL FILES

ATTACHMENT 5

NINE MILE CREEK SPITS EVALUATION

ATTACHMENT 5

NINE MILE CREEK SPITS EVALUATION

The Nine Mile Creek spits have been incorporated into the cap design in Remediation Area A. The cap effectiveness criteria within the spits are established in the Ninemile Creek ROD, and differ slightly from those defined in the lake ROD. The Ninemile Creek ROD established criteria for the COCs in Ninemile Creek, which included hexachlorobenzene, benzo(a)pyrene, phenol, total PAHs, lead, arsenic and mercury. Soil concentrations for the locations on the spits were compared to the Ninemile Creek ROD criteria. Results and conclusions from this evaluation are as follows:

- There are no exceedences of the Ninemile Creek criteria in the spits soil data for hexachlorobenzene, benzo(a)pyrene, total PAHs, or lead. Therefore the cap will be protective for these contaminants and modeling of these contaminants was not required.
- There was one exceedence of the Ninemile Creek ROD criterion for phenol; a concentration of 79.32 g/g OC was measured compared with the criterion of 25 ug/g OC. As shown in Table A5-1 below, the phenol concentrations in the spits are lower than those measured in Model Area A2. The performance criterion for phenol is the same for Ninemile Creek and the lake, in that both are based on the NYSDEC SSC. Therefore the cap design in Model Area A2 (including the specified GAC application rate) is conservative for the spits with regard to phenol and no additional modeling is required.
- There were two minor exceedences for both arsenic and PCBs. For PCBs, concentrations of 22.045 and 22.189 ug/g OC were measured compared with the criterion of 19.3 ug/g OC, and two samples of arsenic where concentrations of 34.4 and 34.8 mg/kg were measured compared with the criterion of 33 mg/kg. These exceedences are sporadic and only marginally above the Ninemile Creek criteria; therefore the cap will be protective with regard to these contaminants and modeling of these contaminants was not required.
- Exceedences for the Ninemile Creek mercury criterion of 0.15 mg/kg were present in the spits. Therefore, cap performance with respect to mercury was modeled for the spits (using Model Area A2 inputs), recognizing that the mercury criterion in the spits is 0.15 mg/kg compared with the lake criterion of 2.2 mg/kg. The approach taken and the results are as follows:
 - As shown in Table A5-1 below, mercury concentrations in the spits are similar to those in Model Area A2. Therefore, the mercury concentrations used in Model Areas A2 are applicable to the spits.
 - In addition, groundwater upwelling in the spits is predicted to be consistent with the upwelling in Model Area A2. As stated in Appendix C: No pore-water or sediment-conductivity data were collected along the spits at the mouth of Ninemile Creek. Under existing conditions, the upwelling velocities on the spits are likely downward because of recharge that occurs on the spits. Following

construction of the wetlands, upwelling velocities will be consistent with those observed in adjacent areas in Model Area A2. Therefore, for cap design purposes, the upwelling velocities in the proposed wetland area were assumed to be the same as those in Model Area A2.

- The Model Area A2 model was therefore used to simulate mercury in the spits, comparing the results against the Ninemile Creek performance criteria of 0.15 mg/kg. Results from this modeling are included in Attachment 4. The results show that at the 95th percentile porewater concentration, an isolation layer thickness between 9 and 10 inches would meet the mercury criterion of 0.15 mg/kg for over 1,000 years. Given that the actual thickness of the isolation layer would be 12” and that the modeling does not represent the effects of siderite or GAC on limiting mercury transport, and taking into consideration the other model conservatisms described in Section 3.3 of Appendix B, these model results indicate that the cap specified for Model Area A2 would be also protective for the spits, in that it would meet the Ninemile Creek mercury criterion for 1,000 years.

**Table A5-1
Nine Mile Creek Spits Soil and Model Area A-2 Sediment Concentrations**

<u>Ninemile Creek Spits Area Soil Locations</u> Concentration* Statistics				<u>Model Area A2 Sediment Concentration*</u> Statistics			
	Maximum	Average	95 th Percentile		Maximum	Average	95 th Percentile
Mercury (mg/kg)	169	23	112	Mercury (mg/kg)	189	30	110
Phenol (ug/kg)	656	58	104	Phenol (ug/kg)	5,900	215	1,435

Notes

* - Non-detects are at half value.

ATTACHMENT 6

ADDITIONAL SENSITIVITY EVALUATIONS

ATTACHMENT 6

ADDITIONAL SENSITIVITY EVALUATIONS

Underlying Sediment Thickness

Model sensitivity evaluations were conducted to evaluate the effect of the specified thickness of the underlying sediment layer on GAC performance. As discussed in Section 3.2 of Appendix B, the model assumes an underlying thickness of 250 cm. To evaluate the sensitivity of the model results to this parameter, thicknesses of 200 and 100 cm were evaluated. This evaluation consisted of repeating the deterministic numerical simulations in which the model was iteratively used to determine the GAC application rate required to meet design criteria (i.e., the approach described in Section 7.2 of Appendix B) for each of these two alternate sediment thicknesses. These simulations were conducted for Model Areas D-West and E3, and the results are listed in the table below:

Sediment Thickness (cm)	Model Area D-West Carbon Application Rate (lb/sf)	Model Area E3 Carbon Application Rate (lb/sf)
250	1.33	0.008
200	1.33	0.008
100	1.33	0.008

The results shown above, which are consistent with those from sensitivity tests conducted in other model areas during previous stages of the design, indicate that the GAC application rates determined with the model are not sensitive to the thickness of underlying sediment included in the model.

Remediation Area D Consolidation Parameters

Model sensitivity analyses were conducted to evaluate the effect of parameters associated with consolidation of the underlying sediment resulting from cap placement Remediation Area D on GAC performance. As described in Attachment 1, conservative values were specified in the base modeling of consolidation in all model areas; in Remediation Area D, the base consolidation curve results in 0.67 ft of porewater flux over 30 years. To evaluate the sensitivity of this parameter, an alternate set of upper bound parameters for Remediation Area D, in which the total porewater flux was 0.81 ft, was evaluated. The basis for this upper bound estimate of porewater flux is provided in Appendix E of the Final Design. This evaluation consisted of repeating the deterministic numerical simulations in which the model was iteratively used to determine the GAC application rate required to meet design criteria (i.e., the approach described in Section 7.2 of Appendix B) for all four subareas of Remediation Area D for the alternate consolidation parameters. The results of these sensitivity analyses are provided in the table below.

Model Area	Base RA-D Consolidation (0.67 ft)		Alternate Upper Bound RA-D Consolidation (0.81 ft)	
	Controlling Chemical	Carbon Application Rate (lb/sf)	Controlling Chemical	Carbon Application Rate (lb/sf)
D-SMU2	Naphthalene	0.044	Naphthalene	0.045
D-West	Phenol	1.33	Phenol	1.34
D-Center	Xylenes	0.93	Xylenes	0.93
D-East	Naphthalene	0.44	Chlorobenzenes	0.44

The results shown above indicate that the GAC application rates determined with the model are not sensitive to the alternate upper bound consolidation parameters for Remediation Area D.

Remediation Area D Shoreline Planting Area

The in-lake planting area within Remediation Area D, which covers a 25-ft strip along the shoreline adjacent to Model Areas D-East, D-Center, and D-West are being designed to contain higher total organic carbon (TOC) in the cap’s habitat layer as compared to the remainder of Remediation Area D. To evaluate the higher habitat layer TOC specific to these areas, sensitivity analyses were conducted to evaluate the impacts on carbon amendments. The sensitivity analyses conducted for these three ILWD model areas consisted of deterministic numerical modeling using the same methods as described in Section 7.2, except that a higher TOC value (10% vs. 4.56%; see Attachment 1) was specified within the upper portion of the habitat layer. The results from these sensitivity analyses are shown in the table below.

Area	Controlling Chemical(s)	Carbon Application Rate (lb/sf)	
		TOC = 4.56%	TOC = 10%
D-West Shoreline	Phenol	1.33	1.33
D-Center Shoreline	Xylenes	0.93	1.02
D-East Shoreline	Chlorobenzene	0.44	0.53

These results indicate that the higher TOC in the planting areas would require GAC application rates that are equal to or only slightly higher than those required in the larger model areas.